THE RECEPTOR-LIKE KINASES *GSO1, GSO2*, *RPK1* AND *TOAD2* MEDIATE ARABIDOPSIS ROOT PATTERNING AND GROWTH

by

Adriana Racolta

A Dissertation Submitted to the Faculty of the

DEPARTMENT OF MOLECULAR AND CELLULAR BIOLOGY

In Partial Fulfillment of the Requirements

For the Degree of

DOCTOR OF PHILOSOPHY

In the Graduate College

THE UNIVERSITY OF ARIZONA

2013

THE UNIVERSITY OF ARIZONA

GRADUATE COLLEGE

As members of the Dissertation Committee, we certify that we have read the dissertation prepared by Adriana Racolta, titled Receptor-Like Kinases *GSO1*, *GSO2*, *RPK1* And *TOAD2* Mediate Arabidopsis Root Patterning And Growth and recommend that it be accepted as fulfilling the dissertation requirement for the Degree of Doctor of Philosophy.

_____Date: 12/11/2013
Hanna Fares

_____Date: 12/11/2013
Karen Schumaker

_____Date: 12/11/2013
Daniela Zarnescu

Final approval and acceptance of this dissertation is contingent upon the candidate's submission of the final copies of the dissertation to the Graduate College.

I hereby certify that I have read this dissertation prepared under my direction and recommend that it be accepted as fulfilling the dissertation requirement.

_____Date: 12/11/2013

Dissertation Director: Frans Tax

STATEMENT BY AUTHOR

This dissertation has been submitted in partial fulfillment of the requirements for an advanced degree at the University of Arizona and is deposited in the University Library to be made available to borrowers under rules of the Library.

SIGNED: Adriana Racolta

Acknowledgements:

I am very grateful to Dr. Frans Tax for his endless patience and dedication in providing the guidance and support I needed to reach this stage of my doctoral program. I am very thankful to all the generous people I meet along the way that provided support and shared their knowledge with me, especially Amanda, Tony and Mike. I am also grateful to my thesis committee: Dr. Karen Schumaker for her advice and helping me think more critically about my work, Dr. Ravi Palanivelu, Dr. Daniela Zarnescu and Dr. Hanna Fares for their continuous advice and support. I am very thankful to my family, here and far away, for believing in me.

Dedication:

To Bogdan, as an inspiration to always try your best.

TABLE OF CONTENTS

LIST OF FIGURES

ABSTRACT

During *Arabidopsis* embryogenesis, cell-cell signaling plays an essential role in establishing an organized body plan centered around two major axes of development: apical-basal and radial. Two topics of great interest are how the layered structure is initiated and maintained during and after embryogenesis and how communication between layers is achieved to allow for coordinated development. Recent research involving Receptor-Like Kinases (RLKs) in plants suggests that their roles in integrating various signals are important in many aspects of development, including embryonic and post-embryonic patterning. The research presented here describes the roles of two pairs of RLKs with independent roles in two different signaling environments. The first RLK pair, GSO1 and GSO2, function in root development at the transition to photoautotrophic nutrition to integrate sugar signals and regulate root growth. GSO1 and GSO2 regulate root epidermal cell identity by controlling the pattern of cell division of stem cells. The second pair of RLKs, RPK1 and TOAD2, function to control root development by regulation of meristem proliferation and a coordinated response to signaling molecules of the CLE family. The response of wild-type roots to treatment with CLE peptides (A-type) is meristem growth arrest, resulting in short roots. *toad2* mutants are insensitive to the effect of CLE peptides in reducing meristem size and TOAD2 also regulates RPK1 upon CLE stimulation. Although responding to different signals, the two pairs of RLK share a common output of regulating cell proliferation in and around the root meristem, especially in the epidermis of the root.

CHAPTER 1: INTRODUCTION

Embryo patterning as a framework for plant development

Early embryonic development in Arabidopsis starts with an asymmetric cell division of the fertilized egg cell, producing a smaller apical and a larger basal cell, a signature of an already established apical-basal axis of development. Subsequent cell divisions of the apical daughter cell create a spherical embryo with an outer, protodermal layer and an inner mass of cells at the dermatogen stage. From this stage on, a radial patterning axis is superimposed on the apical-basal axis serving as a framework for further pattern elaboration. For example, to reach the next stage of embryo development (the globular stage) the cells from the inner mass have to divide such that an inner, provascular layer and a middle, ground tissue layer arise. Thus, at the late globular stage, the three embryonic tissue layers: protoderm, ground tissue initials and provascular have distinctive morphology (Mansfield, 1991) and specific activity of transcriptional programs (Lu et al., 1996; Wysocka-Diller et al., 2000; Friml et al., 2003; Haecker et al., 2004).

Embryonic pattern formation is of special importance for establishing a basic framework for constructing the future tissues and organs of the plant. Studies of Arabidopsis embryogenesis, facilitated by the nearly invariant cell division pattern in the early embryo and the availability of well characterized molecular markers advanced our understanding of how a superimposition of apical-basal and radial symmetry with

ordered cell division pattern leads to cell fate determination. While complex networks of transcription factors and the involvement of the growth hormone auxin have a role in apical-basal patterning (Liu et al., 1993; Haecker et al., 2004) there is little information about signaling besides the classical phytohormone paradigm in radial pattern formation. This might be due to the difficulty of discerning radial patterning mutants from mutants affecting general metabolism, both of which might lead to loss of primary tissue types and embryo development arrest.

To date, the mechanisms by which radial patterning occurs in differentiating cells of the embryo or mature organs are not well understood, but the available experimental data suggests cell-cell signaling is often required for proper patterning. In the *Arabidopsis thaliana* genome, 610 genes have been annotated as members of the Receptor-Like Kinases (RLKs) family including at least 125 Receptor-Like Cytoplasmic Kinases (RLCKs) and over 400 membrane bound RLKs (Shiu and Bleecker, 2001; Shiu et al., 2004). The RLK family contains proteins with a predicted extracellular domain, a single-pass transmembrane domain and a cytoplasmic serine/threonine/tyrosine kinase domain. The sheer number of receptor kinases in *Arabidopsis*, *Oryza* and other plant species suggests that signaling through receptor proteins plays a fundamental role in plant growth and development. Over the past fifteen years, functional analysis of RLKs in model plants has revealed that they have important roles in various aspects of development and cell fate specification during patterning of organs.

Patterning of the outermost, epidermal cell layer of the embryo (protoderm) emerges as a key regulatory prerequisite for normal embryo development. The first RLK

reported to function in epidermal development, affecting not only in the embryo but also the mature plant, is CRINKLY LEAF-4 (CR4). Embryos of maize *cr4* mutants have seed endosperm defects in the epidermal-like aleurone layer (Becraft et al., 1996). The Arabidopsis genome encodes five CR4-related genes, the closest homolog being designated Arabidopsis CR4 (ACR4) (Tanaka et al., 2002). *acr4* mutants have similar embryonic and mature organ epidermal defects as the maize *cr4* mutant, including crinkly leaf surfaces, fusions between organs, abnormal outer layer morphology of ovules, and altered cuticle development (Becraft et al., 1996; Watanabe et al., 2004). ACR4 expression in the protoderm indicates it may function to maintain embryo epidermal identity, although the arrested growth phenotypes of *acr4* mutant embryos could be attributed in part to the seed integument defects. Embryos expressing ACR4 anti-sense RNA showed more severe abnormal embryonic morphological defects, possibly due to downregulation of other closely related ACR4-like genes (Tanaka et al., 2002). These data suggest that ACR4 may act redundantly with other ACR-related genes in the maintenance of the protodermal cell fate. Genetic and biochemical analyses have revealed that the ABNORMAL LEAF SHAPE 2 (ALE2) RLK inteacts with ACR4 during embryo development (Tanaka et al., 2007). Mutant phenotypes of *acr4 ale2* mutants that resemble *ale2* defects, as well as their biochemical interaction, indicate that ACR4 and ALE2 act in the same pathway. Additional genetic interactions, as revealed by mutant combinations of *ale2* or *acr4* with mutants of the subtilisin-like protease, ABNORMAL LEAF-SHAPE1 (ALE1), show earlier embryo defects that are not apparent in *acr4* or *ale2* single mutants. *ale1*; *acr4* and *ale1*; *ale2* double mutants cause

embryo lethality at the heart stage of embryo development and a loss of expression of

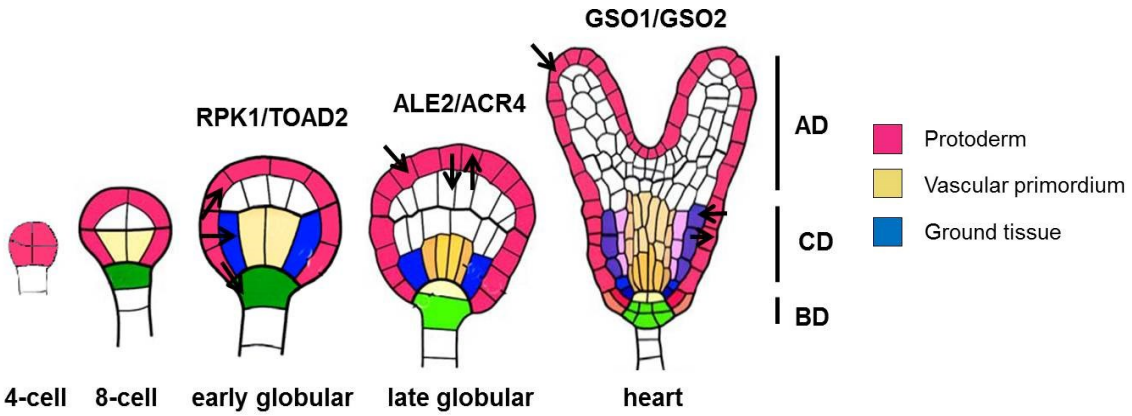

protodermal markers. Due to a redundant requirement between ALE1 and either ALE2 or ACR4 for maintenance of protoderm identity and embryo growth, these genes may be essential for coordinating growth of the entire embryo through regulation of protoderm specification (Figure 1).

Figure 2. RLKs with known function during embryogenesis. Illustrations of embryos at the 4-cell stage through the heart stages are shown. Arrows represent proposed directional signaling. RPK1 and TOAD2 maintain protodermal cell fate identity in the central domain during the early globular stage. ACR4and ALE2 promote protoderm cell fate maintenance, particularly in the apical domain. GSO1and GSO2 control maintenance of the epidermis beginning at the heart stage. AD-apical domain, CD-central domain, BD- basal domain.

Two other RLKs containing leucine-rich repeats (LRRs) in their extracellular domains (LRR-RLKs) are redundantly required for embryonic pattern formation (Nodine et al., 2007). These two genes, named RECEPTOR PROTEIN KINASE1 (RPK1) and TOADSTOOL2/ RECEPTOR PROTEIN KINASE2 (TOAD2/RPK2) show partially

overlapping expression patterns in embryos and mature plant organs (stems, anthers, pedicels, roots, and floral organs). Their role in patterning and cell fate specification is suggested by studies of mutants in embryos (Nodine et al., 2007) where they are redundantly required for maintenance of specific tissue layers along the radial axis (Figure 1). Mutations in both genes cause lethality at an early stage of embryo development (the Toadstool phenotype, a mushroom-shaped embryo) and the production of brown, shrunken seeds containing the developmentally arrested embryo. At the dermatogen stage, the *rpk1*;*toad2* double mutants embryos establish a normal protoderm identity, which is then lost in subsequent stages. This was identified by the loss of protodermal fate markers in the outer cell layer and their replacement by internal tissue type markers, resulting in an embryo lacking proper concentric layering of differentiated cell types. The fact that about half of the *rpk1*;*toad2*+/- embryos also show embryonic arrest is an indication that RPK1 and TOAD2 share overlapping function in a signaling event (or events) that depends on a critical threshold. The mechanism underlying this threshold is not known but the ratio of surviving embryos could be perturbed by additional effects on the signaling pathways and therefore provides a sensitized genetic tool to identify other genes involved in signaling via RPK1 and TOAD2.

The finding that *rpk1*;*toad2* fail to maintain protoderm identity beyond the dermatogen stage indicates a role for RPK1 and TOAD2 in earlier signaling in embryo development compared to other kinases. These two receptors are likely to also share

conserved downstream targets in radially patterned tissues not restricted to the embryo, based on their overlapping expression domains in mature organs of the plant.

There is evidence that two additional LRR RLKs, GASSHO1 (GSO1) and GASSHO2 (GSO2) are required together for epidermal identity by the late heart stage of embryogenesis and during early seedling development (Figure 1). The *gso1*; *gso2* double mutants display morphological defects during embryogenesis, including adherence of the embryo to the inner seed integument, loss of cuticle formation and abnormal cell divisions in early seedling stages, resulting in seedling lethality soon after germination (Tsuwamoto et al., 2008). Additional evidence for a role in embryo development for GSO1 and GSO2 is provided by genetic interaction analyses with the secreted protease ALE1 (Xing et al., 2013). The defects of embryonic cuticle formation and adherence to the seed endosperm of *gso1*; *gso2* double mutants are similar to, but more severe than those of *ale1* mutants. In addition, in the *gso1*; *gso2*; *ale1* triple mutants, the seed and seedling phenotypes were indistinguishable from *gso1*; *gso2* double mutants, indicating these genes act in the same pathway. This contrasts with the synergistic interaction observed between ALE1 and ACR4 or ALE2, suggesting that GSO1/GSO2 and ALE2/ACR4 function in two major pathways involved in regulation of epidermal development during *Arabidopsis* embryogenesis.

The summary presented here indicates that several receptor kinases (RPK1, TOAD2, ALE2, ACR4, GSO1, and GSO2) are required for the maintenance of epidermal cell fate during embryo development, and also exert postembryonic functions. A survey of RLKs expressed in the embryos suggests that numerous other RLKs are

likely to play an important signaling role in the embryo (Nodine et al., 2011). Of special interest to elucidate the mode of action of these RLKs is to uncover whether parallel ligand/ receptor pathways or complex physical interactions between RLKs drives the mechanisms controlling epidermal specification.

RLKs in postembryonic regulation of meristems function

The postembryonic life of an *Arabidopsis* plant starts upon seed germination by growth and elongation of embryonic organs and activation of groups of stem cells that will generate adult tissues and organs. The stem cells are clustered in confined domains, called meristems, that proliferate and control the growth of the plant at the tip of the shoot and root, the development of vasculature as well as the generation of new organs. As they grow, plants have to adapt their development to numerous internal and external factors that impinge on the balance between cell proliferation and cell differentiation. The plasticity of meristems therefore becomes essential in developmental decisions that affect how a plant will continue to grow, or how a patterned tissue is maintained.

To keep it all together, plants have evolved signaling mechanisms that facilitate intercellular communication for a coordinated response and allocation of resources. Recent studies have uncovered a common signaling feature in the shoot and root meristems involving RLKs and small peptide ligands of the CLAVATA3/ENDOSPERM SURROUNDING REGION-LIKE (CLV3/ESR, CLE) family, that act often redundantly in

both meristems. The CLE genes encode small proteins which share a conserved C-terminal amino acid sequence, the CLE motif. The CLE proteins are proteolytically processed to generate a 12 to 14 amino acid long extracellular signaling peptide corresponding to the CLE motif (Cock and McCormick, 2001; Oelkers et al., 2008). Several studies on the founding member of this group, CLAVATA3 (CLV3), show that the CLE motif is the only functional region of the CLV3 protein (Fiers et al., 2005; Fiers et al., 2006; Ni and Clark, 2006). Furthermore, exogenous application of synthetic CLV3 or other CLE peptides triggers a similar response as the overexpression of these proteins in plants (Fiers et al., 2005; Fiers et al., 2006; Kinoshita et al., 2007; Meng and Feldman, 2010). In addition, further posttranslational modifications such as arabinosylation and hydroxylation of proline residues was reported (Kondo et al., 2008; Ohyama et al., 2009; Ni et al., 2011; Tamaki et al., 2013). Besides the spatial regulation of CLE gene expression, the proteolytic processing and the modifications of CLE peptides possibly represent an added layer of regulation for functional specificity.

Signaling modules containing CLEs and putative receptors of the RLK family have been described. One such module, containing the LRR-RLK CLAVATA1 (CLV1), the receptor protein kinase CORYNE (CRN) and the receptor-like protein CLAVATA2 (CLV2) functions to control the size of the shoot apical meristem (SAM). Binding of the CLV3 ligand to these receptors (Ogawa et al., 2008), triggers a signaling cascade that ultimately restricts the expression of the homeodomain transcription factor WUSCHEL(WUS) to a small group of cells. WUS expression is required in these cells to maintain a stem cell fate (Schoof et al., 2000). The common phenotypic read-outs of

defects in the CLV pathway are marked by an enlarged SAM and supernumerary floral and fruit organs (Clark et al., 1997; Schoof et al., 2000; Durbak and Tax, 2011). The current model established that a negative feedback mechanism maintains a constant stem cell population. After a burst of cell division, an increase in stem cell number results in an increase in CLV3 signaling that acts through CLV1 to repress WUS, which in turn will allow cells at the periphery of the stem cell zone to differentiate. As a result, the population of stem cells decreases and therefore less CLV3 ligand is produced. A reduced CLV1 signaling may then allow for WUS upregulation, which will result in an increase stem cell activity. Such regulation by negative feedback was supported by mathematical models that show that meristem homeostasis can be maintain by these simple networks when they act over a short distance (Hohm and Zitzler, 2010).

Additional genetic screens for mutants that are insensitive to exogenous application of CLE peptides revealed that TOAD2 can also transmit the CLV3 signal. The shoot phenotypes of *toad2* appear less severe when compared to those of *clv1*, *clv2*, *crn* or *clv3* (Kinoshita et al., 2010), although synergistic interactions were observed in which double mutants present stronger phenotypes. In addition, overexpression of TOAD2 resembles the phenotypes of CLV3 overexpression and the *wus* mutant phenotype in which the size of the SAM is reduced (Kinoshita et al., 2010). These observations suggest TOAD2 could mediate additional signaling pathways acting in parallel to CLV1 and CLV2/CRN.

Conserved signaling modules and mechanisms of regulation are often reused in different spatial contexts by the plant. One example is the coordination of root apical

meristem maintenance by the CLV1/ACR4 signaling module. ACR4, which plays a key role in embryo patterning, is also required to perceive signals for specifying and maintaining cell fates in the root meristem (Stahl et al., 2009). The signaling module comprising the putative ligand, CLE40, the receptors CLV1/ACR4 and a downstream transcription factor, WUS-RELATED HOMEOBOX 5 (WOX5) controls distal meristem proliferation and differentiation. In this root regulatory network, *acr4* mutants, similar to *cle40* and *clv1* mutants, show expanded expression of WOX5 and the formation of extra

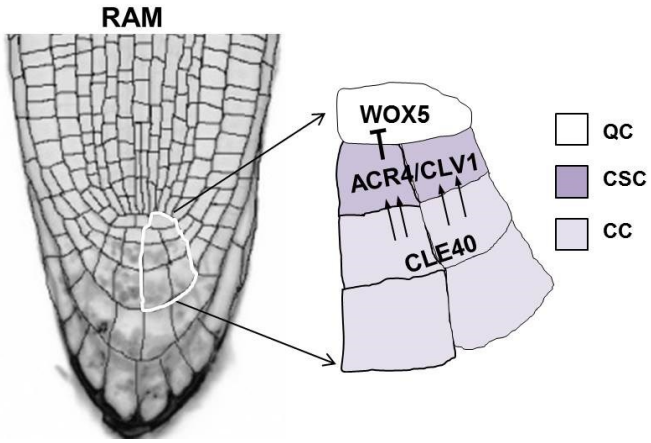

columella stem cells (CSC, Figure 2) (De Smet et al., 2008; Stahl et al., 2009; Stahl et al., 2013). As ACR4 has a different extracellular domain (containing a unique β-propeller structure) (Gifford et al., 2005) compared to other CLE interacting LRR-RLKs, and a biochemical interaction between CLE40 and ACR4 has not been validated, it was proposed that ACR4 may be a part of a regulatory complex including other kinases. Indeed, a direct biochemical interaction was reported between CLV1 and ACR4*, in planta* (Stahl et al., 2013).Similar to the distinctive expression domains occupied by ligand and receptors in the shoot meristem, CLE40 is expressed in the root in the CCs, ACR4 and CLV1 in the CCs and CIs and WOX5 in the QC (Figure 2).

Figure 2. Root apical meristem (RAM) morphology. Image of a five-day old Arabidopsis root and diagram representing the expression domains of CLE40, ACR4, CLV1 and WOX5 in the distal (towards the tip) root meristem. CLE40 signals through ACR4/CLV1 (arrows) to negatively regulate WOX5 (bar).QC- quiescent center; CSC-columella stem cells; CC-columella cells.

ACR4 is transcriptionally upregulated in roots treated with exogenous CLE40 peptide, suggesting a regulatory model in which CLE40 signaling originating from differentiated CCs regulates the activity of stem cells. Interestingly, ACR4 also undergoes rapid endocytosis upon ligand binding, providing an additional level of control to diminish signaling. The interaction between CLV1 and ACR4 is very complex, as CLV1 is downregulated in the absence of ACR4 and to a lesser extent in the absence of CLE40. In the absence of CLV1, the plants are even more sensitive to the CLE40 treatment suggesting that additional components could trigger the sensitive response.

The implications raised by observations such as the increased sensitivity of *clv1* mutants to CLE40 treatment and the synergistic interactions of *toad2* with *clv1* and *clv2* are that additional CLE-mediated signaling modules function in the meristem for providing a complex and redundant environment that regulates meristem activity.

Signaling from the outside radial layers as a mechanism for meristem maintenance

In addition to the pathways regulated by CLE signaling, root apical meristem growth also responds to different regulatory pathways mediated by other RLKs. Spatiotemporal regulation of the activity of these RLKs contributes to additional coordination of plant growth and development. The LRR-RLK BRASSINOSTEROID INSENSITIVE1 (BRI1), functions in brassinosteroid (BR) hormone perception, and mutations in BRI1 cause a dwarf phenotype (Li and Chory, 1997; Clouse and Sasse, 1998). The main roles of BRs are to promote growth by increasing the rate of cell division and cell expansion, in addition to signaling through different RLKs (BRI1-Like, BRL) to modulate patterning of vascular tissues (Caño-Delgado et al., 2004). Mutations in the signaling constituents or in the BR biosynthetic pathway components result in a dwarf phenotype (Clouse and Sasse, 1998), including smaller root meristems and shorter roots (Gonzalez-Garcia et al., 2011) due to reduced proliferative activity. However, no patterning defects were reported to be associated with the short root phenotype of *bri1* mutants (Gonzalez-Garcia et al., 2011). The growth defects of *bri1* mutants, but not vascular tissue defects, are rescued by the expression of a functional BRI1 receptor from the *Arabidopsis thaliana* MERISTEM LAYER 1 (AtmL1) promoter that has a restricted expression domain within the epidermis (Savaldi-Goldstein et al., 2007). This suggests that signaling in the epidermis is sufficient to restore cell-cell communication with inner layers in order to coordinate the growth of the entire plant.

Expression from the inner layers has less effect in rescuing the growth (Savaldi-Goldstein et al., 2007). Additional experiments in which BRI1 expression is restricted to specific radial layers shows that signaling in the outer layer has the most significant effect on regulating root meristem size and QC identity (Hacham et al., 2011). These data suggest that signaling mechanisms taking place in the outer layers drive plant growth, although there is also evidence of “inside-out” signaling (Gallagher et al., 2004; Cui et al., 2007; Yadav et al., 2008).

The LRR-RLK PHYTOSULFOKINE RECEPTORS (PSKRs) perceive the ligand phytosulfokine (PSK), a secreted disulfated pentapeptide (Matsubayashi et al., 2002). There is evidence that PSK controls root and shoot growth, since *pskr1; pskr3* double mutants have shorter roots that wild-type plants (Song et al., 2013). Similar to the BRI1 activity from the epidermis, PSKR1 expression under the control of an epidermal specific promoter, or a promoter specific for only a subtype of epidermal cells, restores normal root morphology in the double mutants (Song et al., 2013). This suggests not only that PSK signaling acts non-cell autonomously, but also that epidermis can regulate the PSK-dependent growth of the entire root from the epidermis.

Although the significance of epidermal control of inner tissue growth and the nature of the signal responsible for communication between a signal-receptive epidermis and the rest of the non-receptive inner tissues are still issues of debate, it is clear from these examples that the epidermis can act as an “organizing” center of root growth (Kutschera, 2008b). The idea of the outer layer acting as the “pacemaker” of plant growth (Kutschera, 2008a) is illustrated by findings that once the epidermis is

removed, the cells of inner layers expand rapidly. This suggests that epidermis imposes constraints on the growth and elongation of inner layers due to limited growth of the stiff cell walls. As the epidermis grows, the underlying tissues experience less mechanical compression and expand as well; under this hypothesis, the changes in tissue tension may be translated as a mechanical signal at the plasma membrane or at the cell wall of inner cells. Indeed, coupling of mechanical sensing with microtubules cytoskeleton arrangements was proposed to control patterning in the shoot apical meristem (Hamant et al., 2008).

An explanation of the dissertation format

I present my dissertation in two chapters and two appendices. Chapter 1 provides an explanation of the problem and its context, as well as a review of the literature. Chapter 2 summarizes the methods, results and conclusions of the research, as well as future directions and how this research contributes to my field of study. The three appendices include a published manuscript (Appendix A) and a manuscript that is in preparation for submission (Appendix B) and, per my committee's request, a chapter discussing global perspectives (Apendix C).

An explanation of the student contribution

For the manuscript included in Appendix A, for which I am a first co-author, I performed the experiments, analyzed the data and interpreted the results summarized in Figures 1(B,D), Figure 2(H,I,K,L), Figure 3, Figure 4(K), Figure 5, Figure 6, Figure 7, Figure 8(B-E,H-K) and Figure 9. I also designed the experiments described in Figures 1(B,D), Figure 2(K,L), Figures 3,6,7 and Figure 8(B-E) and I wrote the majority of the manuscript.

For the manuscript included in the Appendix B, for which I am the first author, I designed the majority of the experiments, except for the promoter swap experiments (M.N.) and the CLE treatment experiment (collaboration with M.N., S.R. and F.E.T). I performed all the experiments, collected the data, analyzed the results and wrote the manuscript.

CHAPTER 2: PRESENT STUDY

The methods, results and conclusions of the present study are described in the manuscripts appended to this dissertation. The following is a summary of the most important findings of this study.

The receptor-like kinases GSO1 and GSO2 together regulate root growth of *Arabidopsis* through control of cell division and cell fate specification

Racolta, A., Bryan, A.C., and Tax, F.E. (2013).Dev Dyn. 2013 Oct 3. doi: 10.1002/dvdy.24066. [Epub ahead of print]

Previous research established that two *Arabidopsis* receptor-like kinases GASSHO1 (GSO1) and GSO2 are important regulators of embryo development by controlling the formation of epidermal layer. Postembryonically, these defects in the outer layer obstruct normal cuticle layer formation and affect patterning of cells on the surface of the cotyledons. Our research analyzed the role of GSO1 and GSO2 in the roots of young seedling. We employed mutant analysis, molecular marker expression, histological preparation, staining and microscopy to show that *gso1; gso2* seedlings also have root growth and patterning defects. We identified aberrant root morphology and arrested growth that correlates with a reduced number of cells in the longitudinal files comprising the meristem of double mutants. In the radial dimension, we identified

aberrant cell division planes, extra cells and missexpression of epidermal differentiation markers. The *gso1; gso2* root growth defects, but not the patterning phenotypes, are rescued by growth on media containing metabolizable sugars. We concluded that GSO1 and GSO2 function together in intercellular signaling to positively regulate cell proliferation, differentiation of root cell types, and stem cell identity. In addition, GSO1 and GSO2 act to modulate sucrose-induced cell cycle reactivation, but they also function in sucrose-independent signaling regulating development of seedling root tissues.

CLE-mediated regulation of root growth requires signaling through the receptor kinases TOAD2 and RPK1

Racolta, A., Nodine, D.M., Rowe, S., and Tax, F.E.

Two closely related LRR-RLKs TOAD2 and RPK1 show a genetic interaction in the process of embryo formation where they coordinate central domain protoderm patterning during the late globular stage of embryogenesis (Nodine et al., 2007). Double homozygous *rpk1; toad2* mutants are embryo lethal and arrest their development during early stages of embryogenesis and lack the normal radial specification of cell types. The research presented here made use of the sensitized genetic background of *rpk1; toad2/+* to analyzed the roles of these two RLKs in patterning of the root. The most important findings are that *rpk1* and *rpk1; toad2/+* mutants show a low penetrance short root phenotype. The affected roots have a disorganized RAM caused by misoriented

cell divisions in the lateral root cap, epidermis, cortex and the QC. *toad2* mutants do not have short roots, and also they continue to grow after treatment with CLE peptides while wild-type plants cease their growth. Our interpretation is that TOAD2 may function to perceive endogenous CLE signals. Exogenous CLE peptide treatment of wild type and mutants induces an increased proliferation of QC cells but also stops the separation of other stem cells (cortical endodermal stem cells) into tissue specific initials, indicating a loss of control of progression to differentiation. The most significant difference between plants insensitive and sensitive to CLE treatment is that the latter have a much reduced frequency of amplifying cell divisions in the proximal meristem. CLE treatment induces downregulation of RPK1, but only in the absence of TOAD2, indicating a requirement for signaling from TOAD2 through RPK1 in modulation of the CLE response. We conclude that RPK1/TOAD2 function together in a pathway that controls root growth by integrating CLE signaling and modulating cell division patterns in the root.

Future directions

Future analysis for identification and functional characterization of the molecules involved in the signaling pathway mediated by RPK1 and TOAD2 will increase our understanding of the mechanisms that regulate development. To this end, I took several approaches targeted at identifying potential interactors of RPK1 and TOAD2.

Using a Yeast-two-hybrid screen I identified a putative cytoplasmic adenylate kinase (*ADENYLATE MONOPHOSPHATE KINASE 4*, *AMK4*) that interacts with the

cytoplasmic domain of TOAD2, but not with RPK1 or several other known RLKs. AMK4 has not yet been characterized in *Arabidopsis* or other plants and belongs to a family of 10 kinases, most of which are located in the mitochondria or plastids. Adenylate kinases have roles in cellular energetics, catalyzing the reversible formation of ADP by the transfer of one phosphate group from ATP to AMP. Further analysis of truncated versions of the AMK4 kinase into its two predicted subdomains revealed that the interaction with TOAD2 occurs only with an almost full length version of AMK4, indicating a requirement for both subdomains. Mutant analysis of *amk4* did not revealed the presence of obvious phenotypes, maybe due to the presence of a highly close homolog, for which insertional mutants are not available. A kinase assay to detect possible phosphorylation of AMK4 by TOAD2 uncovered that AMK4 is able to autophosphorylate, but a cross-phosphorylation between the two kinases was not detected under our experimental conditions.

In a second yeast-two-hybrid screen, using a candidate gene approach, I tested the interaction of cytoplasmic domains of RPK1 and TOAD2 with several known kinases that are expressed in same domains as RPK1 and TOAD2. The outcome of this screen was the finding that BRI1 interacts with both RPK1 and TOAD2. These results were followed up with genetic interaction tests. The method for screening made use of the sensitized genetic background of *rpk1; toad2/+* in which about 50% of the embryos are dead and the seeds containing these embryos appear shriveled and dark brown (the brow shrunken seeds, BSS). Also, this phenotype is observed with a low frequency in the *rpk1* mutants (3%) or in the *rpk1/+; toad2/+* mutants (15 %). A genetic interaction

was discovered between BRI1 and RPK1 in which mutants *bri1-301; rpk1-1* and *bri1-5; rpk1-1* have an increased frequency of BSS (approximately 15%). No *bri1; rpk1;toad2/+* plants were recovered for any of the alleles tested.

These preliminary studies suggest that RPK1 and TOAD2 may interact with a well-known signaling pathway that controls growth through response to hormone signaling (BR pathway). Also, future analysis of the interaction with downstream components, such as AMK4, could uncover if signaling from TOAD2 couples the energetics of cells, and therefore the allocation of resources for growth, with other hormone signaling or with patterning regulation by CLE peptides.

REFERENCES

Becraft, P.W., Stinard, P.S., and McCarty, D.R. (1996). CRINKLY4: A TNFR-like receptor kinase involved in maize epidermal differentiation. Science **273,** 1406-1409.

Caño-Delgado, A., Yin, Y., Yu, C., Vafeados, D., Mora-García, S., Cheng, J.C., Nam, K.H., Li, J., and Chory, J. (2004). BRL1 and BRL3 are novel brassinosteroid receptors that function in vascular differentiation in Arabidopsis. Development **131,** 5341-5351.

Clark, S.E., Williams, R.W., and Meyerowitz, E.M. (1997). The CLAVATA1 gene encodes a putative receptor kinase that controls shoot and floral meristem size in Arabidopsis. Cell **89,** 575-585.

Clouse, S.D., and Sasse, J.M. (1998). BRASSINOSTEROIDS: Essential Regulators of Plant Growth and Development. Annu Rev Plant Physiol Plant Mol Biol **49,** 427-451.

Cock, J.M., and McCormick, S. (2001). A large family of genes that share homology with CLAVATA3. Plant Physiol **126,** 939-942.

Cui, H., Levesque, M.P., Vernoux, T., Jung, J.W., Paquette, A.J., Gallagher, K.L., Wang, J.Y., Blilou, I., Scheres, B., and Benfey, P.N. (2007). An evolutionarily conserved mechanism delimiting SHR movement defines a single layer of endodermis in plants. Science **316**, 421-425.

De Smet, I., Vassileva, V., De Rybel, B., Levesque, M.P., Grunewald, W., Van Damme, D., Van Noorden, G., Naudts, M., Van Isterdael, G., De Clercq, R., Wang, J.Y., Meuli, N., Vanneste, S., Friml, J., Hilson, P., Jürgens, G., Ingram, G.C., Inzé, D., Benfey, P.N., and Beeckman, T. (2008). Receptor-like kinase ACR4 restricts formative cell divisions in the Arabidopsis root. Science **322**, 594-597.

Durbak, A.R., and Tax, F.E. (2011). CLAVATA signaling pathway receptors of Arabidopsis regulate cell proliferation in fruit organ formation as well as in meristems. Genetics **189,** 177-194.

Fiers, M., Golemiec, E., Xu, J., van der Geest, L., Heidstra, R., Stiekema, W., and Liu, C.M. (2005). The 14-amino acid CLV3, CLE19, and CLE40 peptides trigger consumption of the root meristem in Arabidopsis through a CLAVATA2-dependent pathway. Plant Cell **17,** 2542-2553.

Fiers, M., Golemiec, E., van der Schors, R., van der Geest, L., Li, K.W., Stiekema, W.J., and Liu, C.M. (2006). The CLAVATA3/ESR motif of CLAVATA3 is functionally independent from the nonconserved flanking sequences. Plant Physiol **141,** 1284-1292.

Friml, J., Vieten, A., Sauer, M., Weijers, D., Schwarz, H., Hamann, T., Offringa, R., and Jurgens, G. (2003). Efflux-dependent auxin gradients establish the apical-basal axis of Arabidopsis. Nature **426**, 147-153.

Gallagher, K.L., Paquette, A.J., Nakajima, K., and Benfey, P.N. (2004). Mechanisms regulating SHORT-ROOT intercellular movement. Curr Biol **14,** 1847-1851.

Gifford, M.L., Robertson, F.C., Soares, D.C., and Ingram, G.C. (2005). ARABIDOPSIS CRINKLY4 function, internalization, and turnover are dependent on the extracellular crinkly repeat domain. Plant Cell **17,** 1154-1166.

Gonzalez-Garcia, M.P., Vilarrasa-Blasi, J., Zhiponova, M., Divol, F., Mora-Garcia, S., Russinova, E., and Cano-Delgado, A.I. (2011). Brassinosteroids control meristem size by promoting cell cycle progression in Arabidopsis roots. Development **138**, 849-859.

Hacham, Y., Holland, N., Butterfield, C., Ubeda-Tomas, S., Bennett, M.J., Chory, J., and Savaldi-Goldstein, S. (2011). Brassinosteroid perception in the epidermis controls root meristem size. Development **138**, 839-848.

Haecker, A., Gross-Hardt, R., Geiges, B., Sarkar, A., Breuninger, H., Herrmann, M., and Laux, T. (2004). Expression dynamics of WOX genes mark cell fate decisions during early embryonic patterning in Arabidopsis thaliana. Development **131,** 657-668.

Hamant, O., Heisler, M.G., Jönsson, H., Krupinski, P., Uyttewaal, M., Bokov, P., Corson, F., Sahlin, P., Boudaoud, A., Meyerowitz, E.M., Couder, Y., and Traas, J. (2008). Developmental patterning by mechanical signals in Arabidopsis. Science **322**, 1650-1655.

Hohm, T., and Zitzler, E. (2010). A hierarchical approach to model parameter optimization for developmental systems. Biosystems **102,** 157-167.

Jun, J., Fiume, E., Roeder, A.H., Meng, L., Sharma, V.K., Osmont, K.S., Baker, C., Ha, C.M., Meyerowitz, E.M., Feldman, L.J., and Fletcher, J.C. (2010). Comprehensive analysis of CLE polypeptide signaling gene expression and overexpression activity in Arabidopsis. Plant Physiol **154**, 1721-1736.

Kinoshita, A., Nakamura, Y., Sasaki, E., Kyozuka, J., Fukuda, H., and Sawa, S. (2007). Gain-of-function phenotypes of chemically synthetic CLAVATA3/ESR-related (CLE) peptides in Arabidopsis thaliana and Oryza sativa. Plant Cell Physiol **48,** 1821-1825.

Kinoshita, A., Betsuyaku, S., Osakabe, Y., Mizuno, S., Nagawa, S., Stahl, Y., Simon, R., Yamaguchi-Shinozaki, K., Fukuda, H., and Sawa, S. (2010). RPK2 is an essential receptor-like kinase that transmits the CLV3 signal in Arabidopsis. Development **137**, 3911-3920.

Kondo, T., Nakamura, T., Yokomine, K., and Sakagami, Y. (2008). Dual assay for MCLV3 activity reveals structure-activity relationship of CLE peptides. Biochem Biophys Res Commun **377,** 312-316.

Kutschera, U. (2008a). The pacemaker of plant growth. Trends Plant Sci **13,** 105-107.

Kutschera, U. (2008b). The growing outer epidermal wall: design and physiological role of a composite structure. Ann Bot **101,** 615-621.

Li, J., and Chory, J. (1997). A putative leucine-rich repeat receptor kinase involved in brassinosteroid signal transduction. Cell **90,** 929-938.

Liu, C., Xu, Z., and Chua, N.H. (1993). Auxin Polar Transport Is Essential for the Establishment of Bilateral Symmetry during Early Plant Embryogenesis. Plant Cell **5,** 621-630.

Lu, P., Porat, R., Nadeau, J.A., and O'Neill, S.D. (1996). Identification of a meristem L1 layer-specific gene in Arabidopsis that is expressed during embryonic pattern formation and defines a new class of homeobox genes. Plant Cell **8,** 2155-2168.

Mansfield, S.G., Briarty, L.G. . (1991). Early embryogenesis in Arabidopsis thaliana. II. The developing embryo. . Can. J. Bot. **69,** 461-467.

Matsubayashi, Y., Ogawa, M., Morita, A., and Sakagami, Y. (2002). An LRR receptor kinase involved in perception of a peptide plant hormone, phytosulfokine. In Science (United States), pp. 1470-1472.

Meng, L., and Feldman, L.J. (2010). CLE14/CLE20 peptides may interact with CLAVATA2/CORYNE receptor-like kinases to irreversibly inhibit cell division in the root meristem of Arabidopsis. Planta **232,** 1061-1074.

Ni, J., and Clark, S.E. (2006). Evidence for functional conservation, sufficiency, and proteolytic processing of the CLAVATA3 CLE domain. Plant Physiol **140,** 726-733.

Ni, J., Guo, Y., Jin, H., Hartsell, J., and Clark, S.E. (2011). Characterization of a CLE processing activity. Plant Mol Biol **75,** 67-75.

Nodine, M.D., Yadegari, R., and Tax, F.E. (2007). RPK1 and TOAD2 are two receptor-like kinases redundantly required for arabidopsis embryonic pattern formation. Dev Cell **12,** 943-956.

Oelkers, K., Goffard, N., Weiller, G.F., Gresshoff, P.M., Mathesius, U., and Frickey, T. (2008). Bioinformatic analysis of the CLE signaling peptide family. BMC Plant Biol **8**, 1.

Ogawa, M., Shinohara, H., Sakagami, Y., and Matsubayashi, Y. (2008). Arabidopsis CLV3 peptide directly binds CLV1 ectodomain. Science **319,** 294.

Ohyama, K., Shinohara, H., Ogawa-Ohnishi, M., and Matsubayashi, Y. (2009). A glycopeptide regulating stem cell fate in Arabidopsis thaliana. Nat Chem Biol **5,** 578-580.

Savaldi-Goldstein, S., Peto, C., and Chory, J. (2007). The epidermis both drives and restricts plant shoot growth. Nature **446,** 199-202.

Schoof, H., Lenhard, M., Haecker, A., Mayer, K.F., Jürgens, G., and Laux, T. (2000). The stem cell population of Arabidopsis shoot meristems in maintained by a regulatory loop between the CLAVATA and WUSCHEL genes. Cell **100,** 635-644.

Shiu, S.H., and Bleecker, A.B. (2001). Receptor-like kinases from Arabidopsis form a monophyletic gene family related to animal receptor kinases. Proc Natl Acad Sci U S A **98,** 10763-10768.

Shiu, S.H., Karlowski, W.M., Pan, R., Tzeng, Y.H., Mayer, K.F., and Li, W.H. (2004). Comparative analysis of the receptor-like kinase family in Arabidopsis and rice. Plant Cell **16,** 1220-1234.

Song, X.F., Guo, P., Ren, S.C., Xu, T.T., and Liu, C.M. (2013). Antagonistic peptide technology for functional dissection of CLV3/ESR genes in Arabidopsis. Plant Physiol **161,** 1076-1085.

Stahl, Y., Wink, R.H., Ingram, G.C., and Simon, R. (2009). A signaling module controlling the stem cell niche in Arabidopsis root meristems. Curr Biol **19,** 909-914.

Stahl, Y., Grabowski, S., Bleckmann, A., Kühnemuth, R., Weidtkamp-Peters, S., Pinto, K.G., Kirschner, G.K., Schmid, J.B., Wink, R.H., Hülsewede, A., Felekyan,

S., Seidel, C.A., and Simon, R. (2013). Moderation of Arabidopsis root stemness by CLAVATA1 and ARABIDOPSIS CRINKLY4 receptor kinase Complexes. Curr Biol **23**, 362-371.

Tamaki, T., Betsuyaku, S., Fujiwara, M., Fukao, Y., Fukuda, H., and Sawa, S. (2013). Suppressor of llp1 1-mediated c-terminal processing is critical for cle19 peptide activity. Plant J.

Tanaka, H., Watanabe, M., Watanabe, D., Tanaka, T., Machida, C., and Machida, Y. (2002). ACR4, a putative receptor kinase gene of Arabidopsis thaliana, that is expressed in the outer cell layers of embryos and plants, is involved in proper embryogenesis. Plant Cell Physiol **43,** 419-428.

Tanaka, H., Watanabe, M., Sasabe, M., Hiroe, T., Tanaka, T., Tsukaya, H., Ikezaki, M., Machida, C., and Machida, Y. (2007). Novel receptor-like kinase ALE2 controls shoot development by specifying epidermis in Arabidopsis. Development **134,** 1643-1652.

Tsuwamoto, R., Fukuoka, H., and Takahata, Y. (2008). GASSHO1 and GASSHO2 encoding a putative leucine-rich repeat transmembrane-type receptor kinase are essential for the normal development of the epidermal surface in Arabidopsis embryos. The Plant Journal **54,** 30-42.

Watanabe, M., Tanaka, H., Watanabe, D., Machida, C., and Machida, Y. (2004). The ACR4 receptor-like kinase is required for surface formation of epidermis-related tissues in Arabidopsis thaliana. Plant J **39,** 298-308.

Wysocka-Diller, J.W., Helariutta, Y., Fukaki, H., Malamy, J.E., and Benfey, P.N. (2000). Molecular analysis of SCARECROW function reveals a radial patterning mechanism common to root and shoot. Development **127,** 595-603.

Xing, Q., Creff, A., Waters, A., Tanaka, H., Goodrich, J., and Ingram, G.C. (2013). ZHOUPI controls embryonic cuticle formation via a signalling pathway involving the subtilisin protease ABNORMAL LEAF-SHAPE1 and the receptor kinases GASSHO1 and GASSHO2. Development **140,** 770-779.

Yadav, R.K., Fulton, L., Batoux, M., and Schneitz, K. (2008). The Arabidopsis receptor-like kinase STRUBBELIG mediates inter-cell-layer signaling during floral development. Dev Biol **323,** 261-270.

APPENDICES

APPENDIX A: THE RECEPTOR-LIKE KINASES *GSO1* AND *GSO2* TOGETHER REGULATE ROOT GROWTH OF *ARABIDOPSIS* THROUGH CONTROL OF CELL DIVISION AND CELL FATE SPECIFICATION

Racolta, A., Bryan, A.C., and Tax, F.E. Developmental Dynamics. 13 Nov 2013 doi: 10.1002/dvdy.24066 [Epub ahead of print]

The receptor-like kinases GSO1 and GSO2 together regulate root growth of Arabidopsis through control of cell division and cell fate specification

Adriana Racolta[1,*], Anthony C. Bryan[1,3,*] and Frans E. Tax[1,2]

[1]Department of Molecular and Cellular Biology
[2]School of Plant Sciences
University of Arizona, Tucson, AZ 85721, USA
Phone: (520) 622-1186
Fax: (520) 621-3709
Corresponding author: Frans E. Tax (fetax@email.arizona.edu)
[*]Authors contributed equally
[3]Current address:
Biosciences Division
Oak Ridge National Laboratory
P.O. Box 2800
Oak Ridge, TN 37831

Running title: Roles of GSO1 and GSO2 in roots

Keywords: receptor-like kinase, epidermal differentiation, root apical meristem, seedling development, sugar signaling, stem cells

Key findings:

- *GSO1* and *GSO2* are necessary for root growth in *Arabidopsis* by maintaining proper proliferative activity of the proximal and distal root meristem.

- *GSO1* and *GSO2* regulate root epidermal cell identity by controlling the pattern of cell division of stem cells.
- Growth on metabolizable sugars rescues proliferation defects but not patterning defects of *gso1; gso2* double mutants.

Abstract

Background: The root apical meristem of *Arabidopsis* is established post-embryonically as the main source of root cells, and its activity is maintained by complex bidirectional signaling between stem cells and mature cells. The receptor-like kinases GASSHO1 (GSO1) and GSO2 have been shown to regulate aerial epidermal function and seedling growth in *Arabidopsis*.

Results: Here we show that *gso1; gso2* seedlings also have root growth and patterning defects. Analyses of mutant root morphology indicate abnormal numbers of cells in longitudinal files and radial cell layers, as well as aberrant stem cell division planes. *gso1; gso2* double mutants misexpress markers for stem cells and differentiated root cell types. Finally, *gso1; gso2* root growth defects, but not marker missexpression or patterning phenotypes, are rescued by growth on media containing metabolizable sugars.

Conclusions: We conclude that GSO1 and GSO2 function together in intercellular signaling to positively regulate cell proliferation, differentiation of root cell types, and

stem cell identity. In addition, GSO1 and GSO2 control seedling root growth by modulating sucrose response after germination.

Introduction

Plants generate new organs and achieve their final shape through patterned cell divisions and position-dependent cell fate specification, tightly coordinated via cell-cell communication. The shoot apical meristem (SAM) and root apical meristem (RAM), which are sources of many of the cells in the adult plant, require extrinsic signals as well as intrinsic factors in order to maintain their identity and activity (Aichinger et al., 2012). The nearly invariant organization of the *Arabidopsis* root (Dolan et al., 1993) provides a powerful developmental system to investigate the integration of genetic and environmental control of morphogenesis.

The *Arabidopsis* RAM comprises a niche of self-renewing stem cells that perform asymmetric (formative) cell divisions to generate daughter cells, which subsequently divide symmetrically within delineated longitudinal cell files. On the longitudinal axis of the root, the RAM is organized in morphologically and functionally distinct zones: a distal (towards the tip) and a proximal (towards the stem) meristematic zone (MZ), relative to the location of the stem cell niche. Cells in the proximal MZ undergo anticlinal cell divisions (both transverse and perpendicular to the longitudinal axis), increasing the pool of cells in the RAM. The stem cell niche contains two types of cells: the actively dividing stem cells, known as initials, which surround the centrally located quiescent

center (QC), a group of four cells that divide infrequently to renew the initial cells (Dolan et al., 1993). Normal root growth requires not only an adequate proliferative activity of the RAM, but also coordinated cell growth in the elongation zone (EZ) of the root, located proximally and delimited from the RAM by a small transition zone (TZ) in which cells stop dividing. Root cells, generated in the RAM, reach their final size and carry out their ultimate function in the uppermost region of the root, the differentiation zone. Unraveling signaling mechanisms that coordinate communication within and between different regions of the root is important in understanding the coordination of patterning and growth during morphogenesis.

The distal zone of the RAM contains the columella initials (CIs), a group of 4 central and 8 surrounding cells immediately distal to the QC (van den Berg et al., 1997) that undergo asymmetric divisions to generate the columella cells (CC) that accumulate starch granules upon their differentiation. Laterally and distal from the QC, a ring of 16 cells surrounding the CIs form the Epidermal/Lateral Root Cap (E/LRC) initials. E/LRC cells typically undergo a periclinal (parallel to the root surface) division to first generate a lateral root cap cell (LRC) towards the surface of the root and regenerate an E/LRC cell that then performs a second transverse anticlinal division to generate an epidermal cell daughter proximally, and regenerate the E/LRC initial. Subsequent transverse anticlinal divisions of these daughters will generate the epidermis, a single cell layer in *Arabidopsis,* and the LRC cells that form a three to four cell layer structure at the root tip. The division of the initials occurs infrequently and in an ordered pattern; the CIs and E/LRC initials divide less frequently (aprox. 0.13 divisions/hour) than the epidermal

daughter cells in the proximal meristem (aprox. 0.25 divisions/hour) (Wildwater et al., 2005; Campilho et al., 2006). The division of the E/LRC initials advances from the first dividing cell to the neighboring one, along the gyre of a spiral (Baum and Rost, 1996), but subsequent transverse anticlinal divisions of the daughter cells offset the spiral pattern, making it less apparent in the proximal meristem. Towards the EZ, where LRC cells are shed, the epidermis becomes the outermost layer of the main root.

In the RAM, the root epidermis contains two types of cells, organized in alternating longitudinal files: trichoblasts (T) which differentiate in hair-bearing cells (H), and atrichoblasts (A) which will develop into non-hair (N) cells. Specification of these two types of epidermal cells is dependent on their position: A cells are in contact with the outer periclinal wall of only one underlying cortical cell while T cells overlay the junction of two underlying cortical cells. In one week-old wild-type roots, there are 8 T and 10 to 14 A cell files (Baum et al., 2002). Additional A files form through anticlinal longitudinal divisions of T cells that generate T-clones in which one of the two clonal files adopts an A fate based on its position relative to the underlying cortical cells. The divisions that generate the T-clone occur much more frequently in the T cells (1 in 30 trichoblasts) than in the A cells (aprox. 20 times less) (Berger et al., 1998). The cell fate specification of the epidermal cell types is marked by *GLABRA2* (*GL2*), encoding a homeodomain transcription factor (Di Cristina et al., 1996) and *CAPRICE* (*CPC*), encoding a single repeat MYB protein (Wada et al., 1997); both are transcribed in the A cells of the wild-type root.

The Cortex (Co) and Endodermis (En) form the next internal cell layers of the root; each comprises a ring of eight cells that surround the pericycle and the stele. At the one week stage, eight Cortex/Endodermis initials (CEI) encircle the QC cells and generate both Co and En layers. Initial anticlinal formative cell divisions of CEIs generate a daughter cell which then divides periclinally to form the En stem cell towards the inside and the Co stem cell towards outside (Baum et al., 2002). In roots older than seven days, CEI cells stop dividing anticlinally and undergo a single periclinal division that generates an Endodermal Initial (EnI) and a Cortex Initial (CoI). These then undergo several symmetric (amplifying) transverse anticlinal divisions to generate cells in their respective files. The vascular initials situated above the QC generate the cells of the stele.

Several molecular networks controlling cell division, patterning and cell fate maintenance in the RAM comprise transcription factors, plant hormones and their receptors and other signaling molecules, including receptor-like kinases (RLKs). Two transcription factors of the GRAS family, SHORTROOT (SHR) and SCARECROW (SCR) play essential roles in regulating asymmetric cell divisions of CEIs, identity of the QC and the function of the stem cells surrounding the QC, thereby contributing to proper radial patterning of the root (Di Laurenzio et al., 1996; Helariutta et al., 2000; Sabatini et al., 2003). Interaction of SHR/SCR with two zinc finger proteins, JACKDAW (JKD) and MAGPIE (MGP) further refines their regulation of radial patterning and meristem activity (Welch et al., 2007; Ogasawara et al., 2011). In addition, JKD

relays positional signals that regulate patterning of epidermal cell subtypes (Hassan et al., 2010).

A link between cell division and cell fate regulation of the QC and stem cells by SCR/SHR could be CYCLIND6;1 (CYCD6;1), reported as one of the direct targets of SCR and SHR (Sozzani et al., 2010). SCR also has a role in integrating growth responses, as *scr* mutants arrest their root growth and accumulate high levels of sugars and starch in their cotyledons when plants are grown on sugar-containing media (Cui et al., 2012). These observations support the view that cells recruit conserved signaling modules that regulate cell patterning and specification to integrate intrinsic and extrinsic developmental signals.

Genetic and physical interaction of RETINOBLASTOMA RELATED (RBR), a plant homolog of the mammalian cell cycle regulator *RETINOBLASTOMA* (*pRB*) gene (Wildwater et al., 2005; Cruz-Ramirez et al., 2012) with SCR as well as the CYCLIND6;1 complex-dependent phosphorylation of RBR, further links cell cycle regulation with stem cell niche maintenance. In addition, RBR acts downstream of SCR to maintain the stem cell niche in *Arabidopsis* (Wildwater et al., 2005), to restrict cell divisions of the QC and columella stem cells, and to stimulate differentiation of columella stem cell daughters (Wachsman et al., 2011). Another homeodomain transcription factor acting downstream of SCR, WUS-RELATED HOMEOBOX 5 (WOX5), functions in the QC to maintain columella stem cell signaling (rather than QC identity) (Sarkar et al., 2007). An integrative role of RBR in metabolic and developmental control is illustrated by its activity to mediate sugar response at the

transition to photoautotrophic nutrition: seedlings with a reduced level of RBR arrest growth and retain their embryonic features (Gutzat et al., 2011). Exogenously applied sucrose causes a strong response in these seedlings by increasing ectopic cell divisions and the accumulation of starch, as well as upregulation of late-embryonic genes. One of the critical factors required for seedling transition from heterotrophic (utilizing seed storage) to photoautotrophic (photosynthesis-generated) nutrition depends on the accessibility of photosynthesis-derived sugars and is induced by dynamic transcriptional changes mediated by the Target of Rapamycin (TOR) pathway (Xiong et al., 2013).

Several RLKs and their putative signaling peptides have been implicated in the development of the RAM. *Arabidopsis CRINKLY4* (*ACR4*), an RLK of the *CRINKLY*4 family (Stahl et al., 2009) is required to perceive signals for specifying and maintaining cell fates in the RAM as well as maintaining epidermal cell fate in embryo and adult development. Root phenotypes caused by *ACR4* mutations, similarly to mutations in the signaling peptide *CLAVATA3/ENDOSPERM SURROUNDING REGION-LIKE40* (*CLE40*) result in the expanded expression of WOX5 and the formation of extra columella initials (De Smet et al., 2008; Stahl et al., 2009). While *CLE40* is expressed in the CCs, *ACR4* is expressed in CCs and CIs and is up-regulated in roots treated with exogenous CLE40 peptide, suggesting a regulatory model in which CLE40 signaling originating from differentiated CCs regulates the activity of stem cells. ACR4 also forms plasma membrane-localized heterodimers with another Leucine-rich repeat (LRR) RLK, CLAVATA1 (CLV1), an essential stem cell maintenance factor in the

SAM (Stahl et al., 2013) and that ACR4 and CLV1 together regulate the maintenance of RAM distal stem cells. This interaction and the potential of CLV1 to directly bind CLE40 (Guo et al., 2010), illustrates the importance of signaling complexes containing multiple RLKs to regulate RAM homeostasis.

Additional RLKs have been found to regulate the size and identity of the RAM cells. During seedling development, the LRR-RLK SCRAMBLED (SCM) is required for perceiving positional signals for directing the differentiation of epidermal cells into N and H cells in the root epidermis (Kwak et al., 2005). *SCM* is proposed to regulate position-dependent signaling between the epidermis and the inner cortex through its effects on downstream transcription factors responsible for the differentiation of H and N cell types (Kwak and Schiefelbein, 2007; Kwak and Schiefelbein, 2008).

Epidermal cell differentiation in roots is also regulated by additional signals, including the plant hormone brassinosteroids (BRs) (Kuppusamy et al., 2009). Loss of function of the BR receptor BRASSINOSTEROID INSENSITIVE1 (BRI1), another LRR-RLK, results in epidermal cells with ectopic expression of GL2 in cells that would normally become H cells, a phenotype similar to that of *scm* mutants (Kuppusamy et al., 2009). BRs and the perception of BRs in the epidermis also regulate meristematic activity. A RAM of reduced size, accompanied by a decrease in mitotic activity, is detected in both loss- and gain-of-function mutants in BR signaling genes, suggesting the balance of BRs is important for the regulation of meristem size (Gonzalez-Garcia et al., 2011). Perception of BRs in the epidermal layer is sufficient to regulate RAM size and activity (Hacham et al., 2011). These results substantiate not only the roles of BRs

and *BRI1* in the maintenance and differentiation of the epidermal layer, but also the importance of communication between cell layers to coordinate growth.

Here we describe a role for two paralogous LRR RLKs, *GASSHO1* (*GSO1*) and *GSO2*, in regulating root growth and the response to exogenous sucrose at the transition to photoautotrophic nutrition. Previously *GSO1* and *2* were demonstrated to be required together for seedling growth and aerial epidermal surface formation and patterning (Tsuwamoto et al., 2008); concurrent mutation of both RLKs results in seedling lethality. Our analysis of the expression patterns of GSO1 and 2 coupled with phenotypic analysis of double mutants reveals that these two RLKs are developmentally regulated in the root at the transition from embryonic to seedling stage and are required for stem cell proliferation and cell specification in the RAM. GSO1 and 2 act as positive regulators of cell division plane orientation and couple the timing of cell division with the differentiation of RAM cells. We propose that GSO1 and 2 function together in the root to integrate signaling from mature/aerial organs with signaling from the stem cell niche for proper patterning of root epidermis and maintenance of RAM activity.

Results

GSO1 and GSO2 control primary root growth in Arabidopsis

Defects in embryonic growth and aerial epidermal patterning caused by *gso1-1*; *gso2-1* insertion mutants were previously described (Tsuwamoto et al 2008). To further analyze developmental roles of GSO1 and 2, we isolated two new alleles from the

SALK T-DNA collection (Alonso et al 2003), *gso1-2* (SALK_043539) and *gso2-2* (SALK_147249); both are exonic T-DNA insertions in the extracellular domains (Fig. 1A). Consistent with previous phenotypic analyses of the *gso1-1; gso2-1* null alleles, (Tsuwamoto et al 2008), *gso1-2; gso2-1* and *gso1-1; gso2-2* seedlings produce shorter hypocotyls and concave cotyledons (Fig. 1B,D) whereas these defects were not observed in any of the single mutants (Fig. 1B). In addition, roots of plants containing any of the double mutant combination of alleles above fail to elongate on Murashige and Skoog (MS) media without added sucrose (Fig. 1B,C), a phenotype not previously reported. While germination rates of double mutants (100%, n=74) are similar to those of wild-type seeds (100%, n=82), double mutant roots do not elongate to the extent of wild-type roots at three days after germination (DAG) and show significantly reduced elongation by five DAG ($P < 0.001$) (Fig. 1B,C). Mutant roots also have a shorter growth zone as evident from the emergence of root hairs closer to the root tip, indicating that the RAM and the EZ are shortened: in three DAG *gso1-2; gso2-1* mutants, the root hairs have emerged at 0.44 mm±.08 from the tip compared to 0.94 mm±0.16 in wild-type roots (n=15) (Fig. 1D). Although a small percentage (18%) of mutant roots elongate, similarly to wild-type roots, most seedlings (82%, n=219) completely arrest their growth by five DAG on MS media without added sucrose. In contrast, all double mutant seedlings elongate their roots similarly to wild type when grown on MS media with 1% sucrose (n=50 for each allelic combination: *gso1-1; gso2-1*, *gso1-2; gso2-1* and *gso1-1; gso2-2*). All allelic combinations also show the previously reported aerial

phenotype of adherent cotyledons (Tsuwamoto et al., 2008) when grown in presence of sucrose (Fig. 1B,D).

gso1 and *2* mutants misspecify root epidermal cell fates

Although defects in the aerial epidermal layer have been described for *gso1-1; gso2-1* double mutants (Tsuwamoto et al 2008), the cellular identity of epidermal cells has not been examined. To analyze embryonic epidermis specification in double mutants, we examined transcriptional activity of the epidermal specific marker, *pATML1:: HTA6-YFP* . At the heart stage of embryogenesis, when initial epidermal defects were first reported (Tsuwamoto et al 2008), the expression is similar in wild type and *gso1-2; gso2-1*, indicating that differentiation of epidermis is not affected up to the stage when ATML1 is required for epidermal specification. (Fig. 2A,F). Despite differences in size and shape of mature wild-type and *gso1-2; gso2-1* embryos, the *ATML1* marker expression is similar(Fig. 2B,G).

Since embryonic epidermal specification of *gso1-2; gso2-1* appears similar to that of wild type, we analyzed root epidermal specification and patterning from germination through six DAG. In wild-type roots, *pATML1::HTA6-YFP* marker expression is detected in contiguous longitudinal files and in one of the two resulting clonal files if a longitudinal anticlinal division had occurred (Fig. 2K). Using the ratio of H to N cells in their corresponding longitudinal files as a criteria to distinguish between the two types of cell files (H/N ≈1.3 due to increased number of anticlinal transverse divisions in H file) (Berger et al., 1998) we interpret that expression of *pATML1::HTA6-*

YFP is detected in the N cells. In double mutant *gso1-2; gso2-1* roots, YFP is detected in cells forming shorter files that do not extend over the entire length of the meristem, correlating with the generation of frequent epidermal T-clones (Fig. 2K, asterisks) and is not detected in all cells of a contiguous file (Fig. 2K, arrowheads). This indicates aberrant specification of cells within a longitudinal file in the mutant epidermis.

To characterize specification of root epidermal cell subtypes, we used the markers *pGL2::GUS* and *pCPC::GUS*, normally expressed in the N cell types. In wild-type plants, the epidermal N cell files expressing the reporter genes stain blue, in the presence of the X-Gluc substrate (see methods), while epidermal H cell files that do not express these markers do not stain (Fig 2C-E). In contrast, 70% of *gso1-2; gso2-1* mutant roots (n=85), largely overlapping the short root phenotypic class, misexpress *pGL2::GUS* in H cells (Fig. 2H-J). To quantify the H cell types (based on their file position) misexpressing the marker, we counted the number of blue-staining cells in four non- staining H-type cell files for each root. We found that all *gso1-2; gso2-1* roots that arrest growth by six DAG show a scrambled expression of the *GUS* marker, containing 29% (±10%, n=57) blue cells in a H file while fewer cells are affected in the mutants that are able to elongate (17% ±5%, n=21). As previously mentioned, when seedlings are grown on media containing 1% sucrose, the root length of double mutants is increased, but the ectopic expression of *pGL2::GUS* is still detected in 88% (n=25) of the *gso1-2; gso2-1* roots similarly to roots grown in the absence of sucrose. Misexpression of *pGL2::GUS* in the H files occurs at a low frequency and with large variation from plant to plant in wild-type and single mutant *gso1-2* and *gso2-1* plants (5% ±6.2%, n=15; 8%

±8%, n=14; and 3% ±5%, n=30, respectively) (Fig. 2L). In addition to detecting isolated blue-staining cells within non-staining H-files, we frequently observed blocks of several stained cells contiguous with non-stained cells within a file, correlating with the occurrence of multiple epidermal T-clones within the same or neighboring files (Fig. 2L asterisks, Fig. 2H-J). The abnormal patterning of both GUS reporter types indicates that root epidermal patterning is disrupted in double mutants of both the short and long root phenotypic classes.

Double mutant *gso1-2; gso2-1* seedlings abnormally pattern root radial cell layers

Since epidermal cell sub-types are determined by their position relative to underlying cortical cells, we analyzed transverse root sections of *gso1-2; gso2-1* and wild-type plants expressing *pGL2::GUS* to test for defects in other radial cell layers that could cause miss-expression of the epidermal reporter gene. In *gso1-2; gso2-1* mutants, the epidermal pattern formed by specification of H and N cells is no longer maintained and radial symmetry is lost (Fig. 3). The LRC cells are enlarged, and the anticlinal planes of cell division between cells deviate from the normal orientation observed in the wild type (Fig. 3A). In addition, cells positioned as LRC cells express the epidermal *pGL2::GUS* marker, indicating misspecification of cells in the LRC position (Fig. 3D, black arrows). Through analysis of serial cross-sections from the MZ into the EZ, we found that some cells positioned initially as LRC cells become intermixed with cells in the epidermal cell position. Some of these intermixed cells still retain a partial LRC fate and are shed from the root in the TZ and the EZ, leaving gaps

in the epidermis that sometimes expose underlying cortical cells (Fig. 3D, red arrowheads). Although still present, the intermixing of LRC cells with epidermal cells was detected less frequently in plants grown on MS media supplemented with 1% sucrose (Fig. 3A,C). As epidermal cells are generated from their initials and progress towards the TZ, they lose their *pGL2::GUS* expression when flanked on their outer periclinal wall by LRC cells expressing the *pGL2::GUS*. Extra cells between the epidermal and cortex layers were also detected (Fig. 3A,C-D). Epidermal cells abutting the extra cells show abnormal expression of *pGL2::GUS*, indicating that these extra cells are not fully specified as cortical cells, as would be expected by their positioning. Therefore, as a result of misspecification of cells in the position of LRC and inner cell layers, epidermal sub-specification is abnormal.

To quantify the epidermal cell-type defects, the fate and position of 300 epidermal cells in 5 *gso1-2; gso2-1* mutant plants for each growth condition (with and without added sucrose) were analyzed (Fig. 3B). While the number of N cells at the A-position, , (12.16 ±2.1), was not found to be significantly different compared to wild type (12.2± 1.8) there were many more N cells at the T position (3.9±1.8) in *gso1-2; gso2-1* mutants compared to wild type (0.3±0.4). A reduced number of H cells (5.8±1.4) are found at the T position compared to wild type (7.8±0.3), however this phenotype is not observed in plants grown in presence of sucrose (7.1±1.8 in *gso1-2; gso2-1* mutants, 8±0.0 in wild type). A large variation in the number of the H cells at the A-position is observed in the *gso1-2; gso2-1* mutants (1.1±0.9), but significantly more cells than in the wild type (0.08±0.2). Quantification of total number of epidermal cells (H and N

types) in *gso1-2; gso2-1* mutants (22.5±1.7 on MS media and 23.3±2.2 on MS media plus 1% sucrose) indicates that supernumerary cells are present along the circumference of epidermal layer compared to wild type (20.3±1.6 and 20.7±0.7 respectively, $P < 0.005$).

Because of the presence of extra cells in the epidermis, we also examined the inner layers for the presence of additional cells. The average number of cortical cells per section also varies, from 10.3±1.2 on MS to 11.3±1.8 on MS containing 1% sucrose in the *gso1-2; gso2-1* mutants compared to wild-type plants (8.0±0.0 on MS and 8.1±0.3 on MS plus sucrose).The endodermal layer also contains more cells in *gso1-2; gso2-1* plants grown on MS plus sucrose (10.4±1.8) compared to wild type (8.0±0.0) (Fig. 3C). These results indicate the mutants have more cells along the circumference of radial layers that could be explained by additional longitudinal anticlinal cell divisions that are not restricted in the mutants.

Analyses of transverse root sections also reveal that radial symmetry is disrupted in the *gso1-2; gso2-1* mutants; cells in one layer appear to be contiguous with the layer immediately subjacent. In transverse sections through the MZ and EZ of plastic embedded roots, a spiral pattern of cell layers could be detected in the mutants but not in the wild type (Fig. 3A,D). The spiral pattern of cell generation in the RAM was proposed to be rapidly offset by frequent anticlinal divisions in the daughter cells (Baum and Rost, 1993). In the *gso1-2; gso2-1* mutants, we hypothesize that the spiral pattern is enhanced by ectopic LRC cells that displace cells in the neighboring epidermal layer

and an aberrant succession of periclinal/anticlinal divisions of E/LRC initials that disrupt the progression of periclinal cell divisions along the gyre of a helix.

Root apical meristem morphology is disrupted in *gso1; gso2* seedlings

The aberrant epidermal differentiation patterns of *gso1-2; gso2-1* roots do not explain why they undergo root growth arrest, as other mutants with similar patterning phenotypes, such as *SCM* mutants, do not arrest root growth (Kwak et al., 2005). To further characterize the shorter growth zone, we analyzed RAM morphology, markers for RAM mitotic activity, and markers for QC and inner root cell specification. Rapidly dividing cells of the RAM display dense cytoplasm and appear yellow when visualized using DIC microscopy after staining with Lugol's solution (Fig. 4A). The RAM length of *gso1-1; gso2-1* and *gso1-2; gso2-1* mutants (332 ±53 μm, n=31, and 323 ±50 μm, n=40, respectively) was compared to the length of RAM in wild type (798 ±128 μm, n=28) (Fig. 4A,B) and is significantly shorter for each allelic combination ($P < 0.001$).

To investigate whether the shorter meristematic region is due to a reduced number of actively dividing cells, we analyzed the expression of *pCYCB1;1::DB-GUS* (Colon-Carmona et al., 1999), that marks only cells in the G2 to M phase of the cell cycle due to the presence of the destruction box (DB) domain of the *CYCB1;1* that triggers its degradation during mitosis. We find that the length of the region in which *pCYCB1;1::DB-GUS* is expressed is greatly reduced in double mutants at six DAG (318 ±113 μm, n=33, in *gso1-2; gso2-1* compared to 689 ±90 μm, n=40, in wild type, $P < 0.001$). These measurements overlap the length of the meristematic region, stained by

Lugol's solution, confirming that *gso1; gso2* double mutants display a reduced meristematic cell division activity which could result in fewer cells being generated into the elongation zone, accounting for shorter roots. The resolution of GUS marker expression did not allow for quantification of individual dividing cells and we used a different method (Fig. 6, below) to accomplish this analysis.

To determine if the mutants have defects in the differentiation of columella cells, wild-type, *gso1, gso2* and *gso1; gso2* seedlings grown on MS media were treated with Lugol's solution, which stains the starch granules in the mature columella cells. Wild-type root tips viewed in mid-longitudinal sections show accumulation of starch granules within 3-4 horizontal tiers, each containing 4 differentiated columella cells, but not in the columella initials (Fig. 4E,I, yellow arrow). Starch granule accumulation in *gso1* and *gso2* single mutants resemble that of wild-type roots (Fig. 4 F,G,K), but , a reduced number of columella cell tiers containing starch granules is detected in roots of *gso1-2; gso2-1* (2.7±0.6 tiers, n=22 compared to 3.5±0.6 in wild type, n=22, Fig. 4H,K) and similar results are observed in *gso1-1; gso2-2* (Fig. 4K). Also, the intensity of starch staining is diminished in the mutants, indicating that fewer starch granules are being formed. The CIs form one cell layer in wild-type plants; following a formative cell division, the CI daughters differentiate without further divisions and accumulate starch granules. In three-day old plants, all wild-type roots contain one CI cell layer (n=17) while 82% of the short root class of double mutants have two cell layers between the QC and the starch containing CCs (n=28) (Fig. 4, yellow arrows). By five DAG, only 29% of *gso1-2; gso2-1* short roots (n=34) still have two tiers of CIs while others have

started to differentiate and accumulate starch granules, usually in only one or two of the four visible CCs in the tier closer to CIs. The number of starch-containing columella tiers is increased in the *gso1-1; gso2-2* mutants when grown on MS media with added sucrose (4.75±0.4 tiers in the mutants, n=20 and 3.75±0.4 in the wild type, n=20) and only one layer of columella stem cells is detected (n=20). In the presence of sucrose, not only does the number of starch containing CCs increases, but it also exceeds the wild-type level, indicating that the mutants respond to the exogenous sucrose by generating more CC tiers. In addition, the staining is more intense and is often detected in the LRC cells (Fig. 4J). Whereas wild-type and *gso1* or *gso2* roots have clearly organized columella cells arranged in cell files and tiers that appear contiguous with cell files of LRC along the longitudinal axis of the root, *gso1-2; gso2-1* mutants show an altered alignment of columella cells without a clear delineation between cells from different tiers (± sucrose, Fig. 4H,J,N,O).

QC marker expression is altered in double mutant *gso1-2; gso2-1* seedlings

Since differentiation of columella cells formed after division of columella stem cells appears to be delayed in the *gso1-2; gso2-1* plants, we investigated the specification of the QC using markers specific for the QC. *QC184::GUS* is expressed only in the QC cells of wild-type plants (Fig. 4L, and (Sabatini et al., 2003). In the *gso1-2; gso2-1* roots (35/35), GUS activity is detected not only in the QC but also in the initials surrounding the QC, including the columella stem cells (Fig. 4N); none of the wild-type roots (0/36) show expression in surrounding cells. Analysis of an additional QC identity marker, *QC46:GUS*, shows a similar staining pattern between wild type and

gso1-2; gso2-1 roots (Fig. 4M,O), indicating that not all aspects of QC specification are affected in the double mutants.

For a more precise analysis of cell fates in the QC and surrounding initials of *gso1; gso2* mutants, we used a marker consisting of the *WOX5* promoter (Haecker et al., 2004; Sarkar et al., 2007; Stahl et al., 2009), upstream of a nuclear localized version of GFP (Zhang et al., 2005; Nodine et al., 2007). The *pWOX5::HTA6-GFP* expression in six DAG wild-type plants is detected in the QC cells and, with a lower intensity, in some of the vascular initials (Fig. 5E-H). We quantified the number of cells expressing GFP in the QC and vascular initial cells and found that in *gso1-2; gso2-1* mutant roots, an average of 3.0±1.0 QC cells and 2.5±0.75 vascular initials express the marker (Fig. 5G), compared to 3.3±0.6 QC cells and 1.7±0.9 vascular initials in the wild type (n=16), (Fig. 5E). This indicates an increased number of vascular cells express *pWOX5::HTA6-GFP* in the mutant, compared to wild-type plants ($P < 0.05$) whereas the number of QC cells with a GFP fluorescent signal is similar. Wild-type seedlings grown in the presence of 1% sucrose express GFP in 3.0±0.5 QC cells and 1.3±0.7 vascular initials, while the double mutants express GFP in 3.3±0.8 QC and 2.7±1.0 vascular initials. The number of *pWOX5::HTA6-GFP* expressing QC cells is similar between the mutant and wild-type roots, but the number of vascular initials is increased in the mutants ($P < 0.005$, n=17). This is consistent with the observation of expanded expression of *QC184::GUS*, as QC184 expression has been shown to be dependent on WOX5 (Sarkar et al., 2007). Analysis of *pWOX5::HTA6-GFP* in the QC reveals that an increased number of QC cells divide in the *gso1-2; gso2-1* mutants (14/54) compared to wild type (4/40) and addition

of sucrose stimulates QC cell division in wild type (7/26) but does not increase its frequency in the mutants (7/30) (Fig. 5E-H, arrows).

Since the stem cell maintenance activity of the QC cells is enabled by the SCR transcription factor, we analyzed the expression of *pSCR::HTA6-YFP* to identify potential misspecification of cells that normally express SCR. In wild-type plants, *pSCR::HTA6-YFP* expression is restricted to endodermal cells, including endodermal initials, and the QC (Fig. 5A). *gso1-2; gso2-1* mutants show an altered expression pattern of SCR (Fig. 5B) when grown on MS media, but not on MS containing sucrose (Fig. 5C,D). SCR is expressed in endodermal cells of double mutant roots similar to wild type, but only in the QC, endodermal initials and younger endodermal cells, located closer to the meristem, and is often absent from mature endodermal cells. This pattern of expression is consistent with the endodermis being specified in the meristem but losing its identity in the elongation zone of the mutant root.

Orientation of cell division planes and the frequency of divisions in RAM is disrupted in the *gso1-2; gso2-1* mutants.

To further analyze the activity of other cells in the root meristem, we fixed and stained 3 day old roots using a modified Schiff propidium iodide staining procedure (Truernit et al., 2008) Using confocal microscopy we analyzed mid-longitudinal optical section images and observed several defects in cell morphology, such as enlarged LRC cells, different sized cortex and epidermal cells, and aberrant cell division planes in the mutants (Fig. 6).

In mid-longitudinal sections of three-day old wild-type roots, two CEIs are normally observed, one on either side of the QC (Fig. 6A, white asterisks). Analysis of *gso1-2; gso2-1* roots reveals that in 50 % of the roots (n=18), the CEI on either or both sides had already divided periclinally, generating the EnI and the CoI. The occurrence of periclinal divisions of CEIs at three DAG in wild-type plants is less frequent (16%, n=12).

The CoI and EnI cells undergo transverse anticlinal divisions to generate daughters that will displace the older daughters towards the shoot. At some distance from the initials, these daughters undergo anticlinal symmetric cell divisions, amplifying the number of cells in the proximal meristem along the respective files. In *gso1-2; gso2-1* mutants, the frequency of transit-amplifying cell divisions is much reduced (Fig. 6B,C) resulting in fewer cells within the cortex file (14.0±1.1 cortical cells compared to 17.0±1.5 in wild type, n=28, $P < 0.005$), correlating with shorter meristems. In addition, the rate of cell divisions in radially opposing cortical files is often unequal, with one cortical cell file showing no or very few anticlinal divisions while the opposing one is more similar to wild type (Fig. 6A,B) correlating with the asymmetric and wavy pattern of root growth observed in the mutants. In *gso1-2; gso2-1* plants grown on media supplemented with sucrose, these divisions were present in more cortical cells and more equally on either side of the root, correlating with a longer MZ and root observed under this condition. Furthermore, the *gso1-2; gso2-1* plants seem to be more sensitive to the sugar-induced increase in cell divisions (18.2±1.3 cortical cells compared with17.4±1.4 in wild type, n=14, $P < 0.05$). These data suggest that GSO1/2 signaling is

important for the control of cortical cell divisions that increase the number of cells in the meristem.

The contiguous cell files of the LRC and the columella have suggested that the cell divisions in the E/LRC and CIs are synchronous (Dolan, 1993). Our analysis of optical longitudinal sections and transverse Z-series sections indicate that in 83% of the *gso1-2; gso2-1* mutants (n=12), one or both visible E/LRC cells in the focal plane do not present synchronous first periclinal divisions with the columella initials, while this was not observed in the wild type (9/9 roots showed synchronous cell divisions) (Fig. 6A, white and yellow arrows). This effect is also observed in mutant plants grown on sucrose (66% of the roots displayed asynchronous divisions of E/LRC and CIs as compared to none in wild type). In addition, some of the E/LRC initials undergo a transverse anticlinal division first (6/15 mutant plants and 0/9 wild-type plants), as early as 24 hours after germination, without the periclinal cell division that generates the LR daughter cell (Fig. 6). In the presence of sucrose, the alteration of sequential periclinal and anticlinal divisions of the E/LRC cells is still present, albeit at a reduced frequency (2/10 *gso1-2; gso2-1* plants and 0/12 wild-type plants). Repeated longitudinal anticlinal divisions in the E/LRC initials also correlate with fewer LRC cell layers observed in the mutant roots (Fig. 6A). Shootward from the QC, where the wild-type plants have three layers of LRC cells visible around the entire section, the *gso1-2; gso2-1* plants often exhibit only two layers, or sometimes, are asymmetrically organized, with two layers on one side and three layers on the other side (Fig. 6A).

To rule out that the extra cells visible in the transverse sections are not middle cortex cells forming earlier in the three DAG roots, we analyzed the longitudinal optical sections for periclinal cell divisions of endodermal cells. We could not detect the middle cortex forming divisions in *gso1-2; gso2-1* mutants or wild type at this stage and conclude that the extra cells visible between our concentric layers must be the result of aberrant cell divisions generated from E/LRC and their daughters. The anticlinal walls of the epidermal, cortex and endodermal cell layers are often not perpendicular to the longitudinal axis of the root, and therefore they intersect the plane of section (optical and physical), creating the appearance of multiple cell layers. Analyzing the z-series sections, we were able to conclude that some sectors of the mutant roots have the normal number and organization of cell files while other sectors contain extra cells, contributing to an asymmetric radial organization of the root.

GSO1 and GSO2 are transcribed in distinctive and overlapping domains in the root

The RAM defects seen in *gso1; gso2* seedlings could be attributed to indirect effects caused by loss of epidermal patterning, or by direct loss of function of these RLKs within the RAM. To better understand the function of *GSO1* and *2* in roots, we analyzed their expression pattern using promoter fusions with GUS. Previous analysis using RT-PCR and promoter-GUS fusions of *GSO1* and *GSO2* indicated that *GSO1* but not *GSO2* is expressed in roots (Tsuwamoto et al., 2008). Using similar promoter sequences to drive the expression of GUS, and various lengths of time for X-Gluc staining, we further refined the expression of *GSO1* and *GSO2* in roots. We

determined that the expression is dynamic and changes significantly over the first six days post-germination. During the first three DAG, a high level of *GSO1* expression is detected throughout the EZ and differentiation zone and restricted to the endodermis and vasculature (Fig. 7A) and a lower level of expression in the QC (Fig. 7C). At six DAG, all roots analyzed show strong QC expression within a few hours of staining, indicating expression of GSO1 in the QC is increasing during the first six DAG. In support of our data, *GSO1* expression in the QC was also reported based on cell sorting and microarray analysis of QC expressed genes (Nawy et al., 2005). *GSO1* expression appears to be downregulated at sites of lateral root primordia (LRP) initiation (Fig. 7E,D), as indicated by the absence of X-Gluc staining in endodermis cells overlaying early stage LRP and is also absent at sites of deliberate wounding in the root (Fig. 7F).

pGSO2::GUS expression is detected in the aerial tissue of 1-3 day old seedlings (Fig. 7G,M), and in the root epidermis and lateral root cap cells (Fig. 7G-I). Within the epidermis, *GSO2* expression during the first three DAG is stronger in H cells. By six DAG, the RAM expression is mostly confined to the QC, while the root epidermal expression is decreased and detected only in mature root H cells (Fig. 7K,M). In general, eFP browser expression data (http://bar.utoronto.ca/efp/cgi-bin/efpWeb.cgi) (Brady et al., 2007) for *GSO1* and *GSO2* is consistent with our analysis of GUS transcriptional fusions and indicates that *GSO1* shows higher overall expression levels in the root compared to *GSO2*. Based on this analysis we note that these two RLKs have a complementary pattern of expression, with *GSO1* mostly in the inner layers of the

mature root, the QC and SAM and *GSO2* in the outer layers of the mature root and the RAM, including the QC.

Exogenous application of sucrose rescues root growth arrest and cell divisions defects but not patterning defects of *gso1; gso2* mutants

We hypothesized that cell fate specification defects in either the epidermis or initial cells of the RAM in *gso1; gso2* mutants cause the arrest of cell division and growth. As described above, mutant phenotypes including arrested root growth (Fig. 1B), less starch accumulation in columella cells (Fig. 4J), and reduced longitudinal anticlinal cell divisions in root cell files (Fig. 6B), are rescued by exogenous application of sucrose to the media. To test mechanisms that could allow the plants to bypass these growth arrest phenotypes, mutant seedlings were grown in the presence of exogenous sucrose, glucose and a non-metabolizable glucose analog, 3-O-Methylglucose (3-OMG). Root growth measurements indicate that the application of exogenous sucrose or glucose is able to rescue the growth arrest defects of mutant seedlings (Fig. 8A,K and Fig. 1B,C). Additionally, the exogenous application of sugars allows the aerial portion of the plant to grow and produce a fertile adult plant. However, the application of 3-OMG has no effect on root growth of *gso1; gso2* mutants (Fig. 8A). This indicates that sugar metabolism and not the activation of sugar signaling pathways is required to rescue the growth defect. The ability to rescue the root growth defects is also not due to changes in osmotic conditions, as the application of NaCl or mannitol did not increase root growth (Table 1). The exogenous application of sucrose may have different effects: 1) sucrose may activate parallel pathways to rescue the patterning defects caused by

loss of both *GSO1* and *2*, or 2) sucrose may activate cell proliferation to bypass the growth arrest defects of *gso1; gso2* seedlings without rescuing the patterning defects.

In order to address these two hypotheses, we first assayed the ability of sucrose to rescue the abnormal TB staining of *gso1; gso2* mutants that was originally reported (Tsuwamoto et al., 2008). Double mutant seedlings grown on media containing sucrose stain purple, similar to the ones grown in the absence of sugar, indicating the permeability defect of the cuticle in *gso1; gso2* seedlings is not rescued by sucrose (Fig. 8H-J). We further analyzed the effects of exogenous sucrose on the expression of *QC184::GUS*, which has an expanded region of expression in *gso1; gso2* seedlings not grown on sucrose. *QC184::GUS* shows no change in expression in wild-type plants grown in presence of sucrose, consistent with sucrose having no effect on patterning in wild-type seedlings (Fig. 8F). In *gso1-2; gso2-1* seedlings grown in the presence of sucrose, *QC148:GUS* expression is not restricted to the position of the presumptive QC as in wild-type plants, but is ectopically expressed in cells neighboring this location (Fig. 8G). However, *gso1-2; gso2-1* mutants grown with sucrose did not have the same expanded expression of *QC184* as seen without sucrose (compare to Fig. 5E), indicating an effect of sucrose on the organization of the RAM in these mutants. Additionally, the ectopic expression of *QC184* in sucrose-treated *gso1-2; gso2-1* mutants is not always located in the presumptive QC region, but is sometimes shifted laterally (Fig. 8G).

Although exogenous sucrose is able to restore growth of *gso1; gso2* seedlings, additional defects were uncovered while analyzing *gso1; gso2* double mutants grown in

the presence of sucrose. We previously used Lugol's solution to stain the starch granules in the CCs in the root tip. The staining of *gso1; gso2* seedlings grown on sucrose with Lugol's solution uncovered the abnormal presence of starch granules in the cotyledons and hypocotyls of mutant seedlings compared to wild-type seedlings (Fig. 8C,E). The increased accumulation of starch granules is not observed in *gso1; gso2* seedlings grown without sucrose (Fig. 8B,D) indicating that the starch granules likely accumulate after germination as an effect of growth in the presence of exogenous sucrose. The excessive starch accumulation is also noted in the columella cells in the *gso1-2; gso2-1* mutants to a greater extent than in wild-type roots when grown on sucrose, as indicated by an increased number of tiers of columella cells staining positive for the presence of starch (Fig. 4K). In addition, despite the *gso1; gso2* seedlings showing aberrant growth on sucrose, including producing more cells than wild type (Fig. 4J and Fig. 3A) and showing fusions of the stem to leaves and abnormal leaf shapes (Fig. 1B), reminiscent of *cr4* defects, the mutants were able to continue their growth (Fig. 8K) and produce a fertile adult plant. Furthermore, the growth on sucrose does not restore normal aerial epidermis function as penetration of TB is still observed (Fig. 8H-J). These results indicate that sucrose allows *gso1; gso2* seedlings to grow, partially restoring the QC and columella defects, but not the epidermal patterning defects and abnormal cell divisions that generate additional cells.

Discussion

Coordinating cell division and cell fate specification is necessary for normal root growth in *Arabidopsis*. Our analysis of *gso1; gso2* phenotypic defects indicates that

altered root meristem function and epidermal differentiation correlates with root growth arrest and seedling lethality. Extending previously published analysis of phenotypic defects in aerial tissues of double mutants (Tsuwamoto et al., 2008), we identified additional morphological defects that primarily affect the seedling root: 1) misregulation of formative cell divisions; 2) altered progression of cell differentiation in both columella stem cell daughters and mature E and LRC cells, 3) reduced frequency of transverse amplifying cell divisions in the RAM, resulting in short cell files and 4) increased frequency of longitudinal anticlinal divisions in the RAM, increasing the number of cells along the circumference of radial layers. The ability of exogenous sucrose to rescue the proximal meristem proliferation and root growth, but not the patterning defects of the RAM, argues that GSO1 and 2 have a major role in maintaining proper patterning and division of RAM cells and that additional pathways, such as those integrating sugar metabolism, have intersecting roles. In addition, the response of *gso1; gso2* double mutants to exogenous sucrose suggests a role for GSO1 and 2 in modulating the sucrose-induced development of seedlings at the transition to autotrophic nutrition. Our model for how GSO1 and 2 function, depicted in Fig. 9, summarizes our findings about the expression domains of these RLKs in the root and makes predictions about the interactions between GSO1 and 2 and some of the previously identified pathways that have a similar role in regulating stem cell proliferation, differentiation and the integration of sugar signaling.

GSO1 and *GSO2* regulate root growth by controlling root apical meristem size

The postembryonic root initiates growth during germination mainly through cell elongation in the proximal region between the root and the hypocotyl (Sliwinska et al., 2009), but also through activation of cell division in the meristem (Masubelele et al., 2005). The RAM reaches its mature size by five days after germination and its proliferative activity is maintained through a complex interplay of long distance signaling molecules such as plant hormones (Gonzalez-Garcia et al., 2011; Cederholm et al., 2012) and small RNAs (Chuck et al., 2009). In addition, metabolic signals such as photosynthesis derived sugars are integrated to coordinate aerial and underground growth (Kircher and Schopfer, 2012; Xiong et al., 2013) (Fig. 9). Cell autonomous or short distance signaling that activates a multitude of transcription factors further refines meristem activity (Smolarkiewicz and Dhonukshe, 2013).

gso1; gso2 double mutant seedling roots arrest growth by three DAG, a phenotype that occurs with three independent combinations of double mutants and does not occur in any of the single mutants. Furthermore, the growth arrest phenotype is not fully penetrant; about 20% of the double mutant roots continue to elongate similar to wild type, indicating that additional pathways that contribute to root growth can bypass the defects of double mutants. The short root phenotype which is associated with reductions of RAM size, cell cycle marker expression and number of putative cortex cells in longitudinal files, leads us to hypothesize that signaling through GSO1 and 2 together is required for regulation of RAM activity, resulting in proper root growth.

GSO1 and *2* control the activity of QC and initial cells in the stem cell niche

In the *Arabidopsis* root, the QC cells are the source of signals that maintain the stem cell features of the directly surrounding initial cells (van den Berg et al., 1997). Based on our analysis of the QC identity markers QC184, SCR and WOX5, we conclude that double mutant *gso1-2; gso2-1* roots maintain their QC cell identity. In addition, considering the ectopic expression of WOX5 in cells around the QC (vascular initials and occasional CEIs), and the ectopic expression of QC184 in all surrounding stem cells, we hypothesize that some QC specific characteristics are maintained in the QC-derived initial cells. An increased mitotic activity of the QC in the double mutants might represent a compensatory strategy to renew the stem cells surrounding the QC, which show aberrant differentiation, patterning and timing of cell division.

Misregulation of signaling from the QC in *gso1; gso2* double mutants could cause the differentiation defects seen in the CI daughters and the reduced starch accumulation in all columella cells. As a result, fewer tiers of columella cells containing starch granules are detected and 80% of the mutant roots contain two layers of CIs. These defects could be attributed to delayed differentiation of columella stem cell daughters after division rather than increased frequency of CI divisions, as we did not observed more than two tiers of cells lacking starch below the QC. Based on the observations that by five DAG, a few cells in the uppermost tier of columella cells start accumulating small starch granules and exogenous addition of sucrose restores the starch accumulation in all columella cells but not in the CIs, we conclude that GSO1 and GSO2 may be required to modulate signaling from the QC that regulates the coupling of CI cell divisions and differentiation of their daughters.

The CI mutant phenotypes of *gso1; gso2* seedlings resemble columella phenotypes of mutants in another RLK, ACR4 in which supernumerary CIs are detected and CCs appear disorganized. ACR4 regulates formative cell divisions in the root columella, likely through perceiving the CLE40 peptide, by repressing WOX5 activity in the root tip (De Smet et al., 2008; Stahl et al., 2009). Supernumerary CIs and delayed differentiation of columella daughters were also observed upon removal of RBR using RNAi (Wildwater et al., 2005) or in regional clones (Wachsman et al., 2011); a reduction of RBR in the RAM results in an expansion of the columella stem cell pool due to differentiation of columella cells at a more distal point from the QC. It is not currently known whether RBR directly controls transcription factors regulating columella stem cell daughter differentiation, as is the case in the CEIs (Cruz-Ramirez et al., 2012) or the effect of RBR is restricted to the control of exit from cell cycle and therefore indirectly promoting cell differentiation (Borghi et al., 2010). As depicted in our model, ACR4 and RBR may function in overlapping pathways to regulate columella cell division or differentiation. Similarly, GSO1 and 2 could mediate inductive signaling leading to differentiation of CCs after CI divisions.

Similar to the lag in differentiation of the distal initial cells in *gso1; gso2* double mutants, there are also defects in the proximal initials and their progeny. Premature differentiation of double mutant CEIs into EnI and CoI could be the result of a requirement for GSO1 and 2 signaling to perpetuate formative anticlinal divisions that regenerate the CEI, or signaling to delay the occurrence of periclinal divisions and maintain the CEI cell fate. The SCR endodermal marker expression in the RAM of *gso1;*

gso2 double mutants is detected in the QC, the CEIs, the EnI and the meristematic endodermal cells, similarly to wild type, but is often absent from cells in the EZ of the root. This indicates that endodermal cells are normally specified in the young meristem but their identity is lost in older cells of the root, suggesting that GSO1 and 2 also reinforce signaling to maintain the cell identities of more mature root cells. Previous studies have shown that mature cells signal to initial cells to guide their differentiation (van den Berg et al., 1995). Loss of identity of mature endodermal cells (in which both GSO1 and 2 are normally expressed) may disrupt signaling to young differentiating cells and the RAM, leading to proliferation and specification defects (Fig. 9). We conclude that GSO1 and 2 signaling pathway acts separately or downstream from the SCR-dependent pathways controlling division patterning of CEIs and endodermal specification (Fig. 9).

GSO1 and *GSO2* regulate alternating cell divisions of E/LRC and epidermal differentiation in roots

Although epidermal defects of *gso1; gso2* mutants, including outer layer permeability and the adherence of cotyledons to the endosperm, were previously described (Tsuwamoto et al., 2008), the specification of the embryonic epidermis is at least partially normal, based on ATML1 marker expression. However, during post-embryonic root development, specification defects of epidermal and sub-epidermal cell fates are apparent, as indicated by GL2, ATML1 and CPC marker expression and analysis of root cell organization.

The scattered expression of non-hair root epidermal markers in *gso1; gso2* mutants could be due to GSO1 and GSO2 function: 1) in the epidermis, to convey positional information, similar to SCM, or 2) in the QC to signal normal division and/or specification of E/LRC stem cells or cortical cells underlying the epidermis and thereby interfere with normal epidermal patterning pathways. Our observations of aberrant cell divisions in the E/LRC initials of double mutants that undergo an anticlinal cell division before dividing periclinally led us to conclude that the GSO receptors function in signaling either an initial cell fate of the E/LRC or the alternating orientation of the cell division plane. As a result of misoriented cell divisions of E/LRC initials, positional information is likely not properly relayed to all LRC cells, and therefore some LRC cells express the epidermal specification marker GL2, and are be aberrantly positioned within the epidermal cell layer. These misoriented cell divisions sometimes generate epidermal cells that express the GL2 marker and are positioned subjacent to LRC cells also expressing the GL2 marker. We hypothesize that due to their location between the cortex and the LRC cells expressing epidermal markers, the relay of positional information between these adjacent cell layers is impacted. In addition, in the mutant roots more epidermal cells, as well as cells of underlying layers, divide anticlinally and longitudinally, increasing the number of cells along the circumference of corresponding radial layers. As a result of intermixing of LRC and E cells, as well as supernumerary cells of unequal size within each layer, cells become displaced radially, often creating an additional incomplete layer. Cells positioned in a new location, regardless of their clonal origin, might then receive aberrant signaling from neighboring cells that results in

a fate change. Based on our observations of the reduced frequency of periclinal divisions of E/LRC and increased longitudinal anticlinal divisions of epidermal cells, we conclude that GSO1 and 2 positively regulate alternating cell division planes in the E/LRC initials and negatively regulate longitudinal anticlinal divisions in the RAM epidermal cells. Our observations of aberrant root cell divisions is also consistent with previously reported cell divisions defects in the aerial tissues of *gso1; gso2* mutants (Tsuwamoto et al., 2008).

Similar phenotypes including short roots, reduced meristem size and epidermal specification defects have been described for mutants in another LRR-RLK, BRI1 (Hacham et al, 2011). Restricting expression of BRI1 to the epidermis is sufficient to rescue the RAM defects in *bri1* mutants, demonstrating the importance of epidermal function in regulating inner cell fates in roots. It is possible that the GSO receptors function through a similar mechanism to relay signals from the outer layers, epidermis and LRC (where GO2 is expressed) to the QC (where both *GSO1* and *2* are expressed), to maintain the proper division and differentiation of initials around the QC. Further analysis is needed to determine if epidermal specification defects precede the cell division defects of initials and to determine whether defects in *gso1, gso2* mutants are due to overlapping functions of these genes within same cell layers or concomitant impairment of signaling through separate layers.

GSO1 and *2* expression is developmentally regulated in seedlings

Analysis of GUS transcriptional fusions indicates that *GSO1* is expressed in the QC, endodermis and cells of the stele in the root differentiation zone, while *GSO*2 is detected mainly in the QC, endodermis, epidermis and lateral root cap cells. The spatial requirements for GSO1 and GSO2 are as yet unknown, but, considering their expression pattern and our marker analysis results, we hypothesize that signaling from the epidermis (GSO2) and vasculature (GSO1) prevails in the first few days after germination, as the seedling uses the stored resources of the embryo. As the plant transitions to autotrophic nutrition and the RAM becomes more active, GSO1 and 2 signaling from the QC could become increasingly more important in regulating cell divisions in the RAM. Although *GSO1* and *GSO2* are expressed in both overlapping and non-overlapping root cell types, the root growth arrest is only seen in *gso1; gso2* double mutants. This suggests that GSO1 and 2 either perform a redundant function in the cell types in which they are expressed or that a combination of distinct functions of each RLK is required simultaneously in multiple tissues to prevent the manifestation of the observed defects. An additive role of these genes in integrating the RAM proliferation and metabolic cues is suggested by findings that GSO1 might be cell cycle regulated, increasing 4.9 fold during mitosis (Menges et al., 2003), contains a binding motif in its promoter for the RBR interacting transcription factor, E2F (Naouar et al., 2009) and is differentially expressed in seedlings in the first days post-germination (Allen et al., 2010). *GSO2* expression is reported to be increased 3.3 fold in plants with reduced RBR protein function and increased 5.5 fold in these plants upon exogenous sucrose addition (Gutzat et al., 2011) but its expression is not changed in wild-type plants upon

sucrose treatment. This suggests that GSO2 sucrose-mediated response requires RBR and that GSO1 and GSO2 together might integrate signals to coordinate the cell growth status with cell proliferation.

Root development of *gso1; gso2* mutants is impaired during the transition from heterotrophic to autotrophic nutrition in the absence of exogenous sucrose

If the root growth arrest is caused by cell proliferation defects in the *gso1; gso2* double mutants, an increase in cell cycle activity through alternative mechanisms should rescue the root growth (Masubelele et al., 2005). By applying sucrose to the growth media, the roots of *gso1; gso2* mutants extend during the first 10 DAG similar to wild-type roots, but in contrast to wild type, they also show overproliferation of specific cells, including columella cells, indicating that GSO1 and 2 are also required to modulate sucrose signaling and metabolism in cell proliferation for proper root growth. Phenotypic root defects caused by abnormal patterning such as the scrambled GL2 expression, supernumerary cells within each radial layer, the presence of extra cells between the presumptive epidermal and cortical layers, the seedling cuticle defects that allow for TB penetration of cotyledons, as well as fusion of cotyledons and the reduced length of hypocotyls, are still present in seedlings grown in the presence of sucrose. Since the non-metabolizable sugar analog 3-OMG did not rescue root growth, we conclude that the metabolism of sucrose and not the activation of sugar signaling pathways is responsible for the observed effect of restoring cell proliferation in the proximal meristem. Responses of *gso1, gso2* mutants to exogenous sucrose, including supernumerary columella cells, increased accumulation of starch granules in the

cotyledons, the hypocotyl and columella cells and the increased radial asymmetry of the root, often shifting the QC location, indicate that GSO1 and 2 negatively regulate sucrose-dependent cell division and starch accumulation. Further analysis is needed to distinguish between whether GSO1 and 2 directly regulate sugar allocation and utilization in the root, or the alternative hypothesis that the observed effects of exogenous sucrose on double mutants is an indirect result of cell specification defects that allow for excessive uptake and accumulation of sugar in the mutants.

As signals from photosynthesis-derived sugars in the cotyledons are required for root growth (Kircher and Schopfer, 2012), the arrested growth in *gso1; gso2* mutants could be attributed to reduced photosynthesis-derived sugars due to cotyledon epidermal defects (Tsuwamoto, et al, 2008). In our model (Fig. 9), GSO1 and GSO2 could have an additional function in integrating cotyledon-to-root signaling regulating sugar-dependent cell proliferation, consistent with the ability of *gso1; gso2* seedlings to germinate and grow for the first 3 days after germination. This correlates with embryo resources being sufficient for seedling development until newly emerged cotyledons are able to photosynthesize and plants transition to photoautotrophic nutrition. While sucrose-induced cell proliferation allows for seedling survival, the primary defects in both aerial and underground tissues are still present in mutant plants germinated and grown on sucrose media and their root defects are not simply a consequence of impaired sucrose metabolism and signaling from the cotyledons. We conclude that **GSO1and 2 function at the transition to autotrophic nutrition to integrate complex**

cell division patterning cues and photosynthesis-derived nutrient availability signals in the root.

The molecular mechanisms that link sugar-induced cell proliferation and patterning by GSO1 and 2 are as yet unknown, but one example of a novel mechanism that functions in the root meristem is represented by regulatory transcriptional changes that precede the transition to photoautotrophic nutrition and require the Target-of-Rapamycin (TOR) signaling pathway (Xiong et al., 2013). The inability of exogenous sugars to rescue the defective meristem of *tor* mutants, unlike in the *gso1, gso2* mutants, directly implicates TOR in sucrose-induced RAM development. Phosphorylation of E2Fa, a cell cycle transcriptional activator (Sozzani, 2006) by the TOR kinase (Xiong, 2013) bypasses the requirement for canonical E2Fa/RBR signaling and provides evidence for a direct link between sugar signaling and induction of cell proliferation. These results, however do not exclude the possibility that growth factors, including sugars, release other E2F/RBR transcriptional repressor complexes to activate E2F target genes (Inzé and De Veylder, 2006). Further genetic analyses are necessary to explore potential connections of GSO1 and 2 with sugar signaling pathways.

Complex signaling networks integrate developmental cues leading to normal root growth

Additional pathways known to control root patterning or cell fate specification have components that are regulated by available sugars. For example, SCR has a

SHR-independent role in sugar signaling with an effect on root growth: *scr* mutants show a hypersensitive response to the inhibitory effects of high sugar content and accumulate high levels of starch in their leaves (Cui et al., 2012). The SCR interacting protein RBR was also implicated in sucrose-mediated seedling development (Gutzat et al., 2011). Seedlings with reduced RBR levels show embryonic features and do not transition to autotrophic nutrition. They also respond very strongly to exogenous sucrose application by inducing ectopic cell divisions and activation of late-embryonic genes. Based on the strong similarities between seedlings with a reduced RBR function and *gso1; gso2* seedlings, we speculate that GSO1 and 2 signaling possibly intersects the pathway mediated by SCR and RBR (Fig. 9).

Mutations in *STIMPY* (*STIP*)/*WOX9* also cause a seedling lethal phenotype which can be rescued with growth on exogenous sucrose. The phenotypes of *stip* loss of function mutants resemble *gso1; gso2* mutants, including smaller cotyledons and smaller embryos, reduced expression of cell cycle markers in the RAM, arrested seedling growth and the rescue of the growth arrest with the application of sucrose (Wu et al., 2005; Tsuwamoto et al., 2008). STIP also has an overlapping expression patterns with *GSO1* in the maturation region in the root and with *GSO2* in the lateral root cap (http://bar.utoronto.ca/efp/cgi-bin/efpWeb.cgi). Based on their double mutant phenotypes, GSO1 and 2 could function upstream of the STIP in the same pathway (Fig. 9).

Thus far, it appears that a network of RLKs regulates the identity of the epidermis, the spatio-temporal differentiation of the epidermis, and the activity of the

root meristem (Fig. 9). The control of meristem maintenance from the epidermis through BRI1 (Gonzalez-Garcia et al., 2011; Hacham et al., 2011), the ACR4 interaction with ABNORMAL LEAF SHAPE 2 (ALE2) receptor kinase (Watanabe et al., 2004; Tanaka et al., 2007) determining epidermal characteristics, and the ACR4-CLV1 interaction (Stahl et al., 2013) in controlling root stemness, exemplify the complexity of RLK signaling in root growth regulation. The potential cross-talk of these patterning pathways is illustrated by several common hubs in which signaling from different pathways converge, creating a complex root growth regulatory network. One example is the interaction of JKD not only with SCR/SHR (Ogasawara et al., 2011) but also with the LRR-RLK SCM in epidermal patterning (Hassan et al., 2010). Another example is the modulation of the RLK ACR4 function in epidermal patterning by its interacting partner ABNORMAL LEAF SHAPE1 (ALE1) (Tanaka et al., 2001) that also has an input into the GSO1 and 2 mediated epidermal cuticle formation (Xing et al., 2013). Other transcription factors controlling subsets of developmental and patterning mechanisms might also function as points of crosstalk between pathways. Examples include WOX9, which controls root growth by stimulating cell proliferation and preventing premature differentiation and modulating sucrose signaling (Wu et al., 2005) and the transcription factors *FEZ* and *SOMBRERO* (*SMB*) that control periclinal divisions of the epidermal/lateral root cap and LRC cell fate specification without affecting root growth (Willemsen et al., 2008) (Fig. 9). Determining the signaling pathways upstream of these transcription factors, as well as the genetic interactions among various RLKs controlling

root development will increase our understanding of how networks of RLKs modulate the connection between cell proliferation and cell fate specification.

Conclusion

Based on the analysis of postembryonic spatial and temporal expression of *GSO1* and *2*, as well as their double mutant phenotypes, we conclude that these two RLKs are required in the RAM to restrict longitudinal anticlinal cell divisions (that result in increased number of cells along the circumference of each cell layer) and to promote transverse amplifying cell divisions (that increase meristem length), possibly by integrating signals from mature endodermis/vasculature and epidermis. Consistent with the localized expression of *GSO1* and *2* in the QC, and the additional *GSO2* expression in E/LRC and their derivatives, the function of both RLKs is required to maintain proper cell division patterns and specification of cells in the stem cell niche and epidermis. Further research is needed to address whether stem cell specification is primarily controlled by GSO1 and 2, resulting in altered cell division or whether the primary role of these RLKs is to directly control the orientation and timing of cell divisions and subsequent cell differentiation. The hypersensitive response of these double mutants to sucrose, combined with a lack of a response of sucrose to ameliorate patterning defects, suggest a model in which both GSO1 and 2 not only act to modulate sucrose-induced cell cycle reactivation, but they also function in sucrose-independent signaling

regulating development of embryo and seedling root tissues. By integrating these signaling modules, GSO1 and 2 function as positive regulators of seedling development at the transition from embryo-specific heterotrophic nutrition to photosynthesis-driven autotrophic growth.

Experimental Procedures

Genetic analyses and growth conditions

The *gso1-1* (SALK_064029), *gso1-2* (SALK_043539), *gso2-1* (SALK_130637), and *gso2-2* (SALK_147249) alleles used in this analysis were identified in the SALK Insertion collection (Alonso et al., 2003). The *gso1-1* and *gso2-1* insertion alleles were characterized as knockouts (Tsuwamoto et al., 2008) and our genetic results with *gso1-2* and *gso2-2* are consistent with the interpretation that all four of these alleles are nulls. The *Arabidopsis* Columbia ecotype (*Col-0*) was used as wild-type control. The GL2::GUS (CS8851), CPC::GUS (CS6497), marker lines were obtained from the Arabidopsis Biological Resource Center (Columbus, OH).The promoter trap lines QC184::GUS, and QC46::GUS were described by Sabatini et al, 2003. All lines were plated on 0.5X MS (Murashige and Skoog) media and stratified at 4°C for 48 hours, then grown at 22 °C in a Conviron growth chamber with a 16 hour light/8 hour dark cycle. Seedling roots were analyzed at three and six days after germination (DAG). All plate assays used the same growth conditions as above, but also contained the

indicated concentrations of sucrose, glucose, 3-O-Methylglucose (3OMG), NaCl, or mannitol. Growth measurements were taken at three and five DAG. To genotype the *gso* mutant alleles, three primer polymerase chain reactions were performed using Ex-Taq polymerase (TaKaRa Bio Inc., Japan). GSO1 F 5' GTGAATGTAAAGTGTACTACTCCAC, GSO1 R 5' TGACATATCTAACAAGGACAGCTC, GSO2 F 5' TCTTAACGGCATTAGAACTGTT, GSO2 R 5' CTCTTCATCAAACATTGCTTCG, LBb1 5' GCGTGGACCGCTTGCTGCAACT.

Cloning and generation of marker lines

To create the promoter-YFP fusion constructs, the promoter regions of ATML1 (At4g21750) and SCR (At3g54220) were PCR amplified (using Prime Star polymerase, TaKaRa Bio Inc., Japan) and the primers ATML1-T1 (5′-ATTGATTCTGAACTGTACCC-3′), ATML1-T2 (5′-TTTAAGCTTAACCGGTGGATTCAGGG-3′) described previously (Takada and Jurgens, 2007) and SCR F (5'-AAGGGATAGAGGAAGAGGACT-3') and SCR R (5'-GGAGATTGAAGGGTTGTTGG-3'), respectively. The PCR products were cloned into the pCR8-TOPO Gateway vector using the TOPO cloning kit (Invitrogen) and subcloned into the Gateway-adapted T-DNA binary vector pFYTAG (GenBank acc.DQ370421) using the LR Gateway system (Invitrogen).The pFYTAG vector clones therefore contain the respective promoters fused with the coding region of Yellow Fluorescent Protein (YFP) and the coding region of a histone 2A gene (HTA6; At5g59870) allowing for nuclear localization of the synthesized protein.

To generate GSO1 (At4g20140) and GSO2 (At5g44700) promoter fusions with GUS, putative promoter sequences were amplified using primers GSO1pF (5'-TCTAGACTGAGTTATACAGAACCATAAGCAA -3'), GSO1pR (5'-TCTAGACATGTTTTCTTCTTCGTCGTCTTA-3') and GSO2pF (5'-GGATCCCTGGTTAAAATCTTGAAT-3'), GSO2pR (5'-GGATCCAAGAAGAACAGAGTTTTGCTG3'), respectively. The primers amplify a 3kb region, upstream of the ATG start codon of GSO1 sequence while adding a restriction site for XbaI. The primers for GSO2 incorporate a site for BamHI flanking a 2kb region of GSO2 promoter, upstream of the corresponding coding region. The PCR products were each cloned into pCR2.1TOPO (Invitrogen), digested with the corresponding restriction enzyme and ligated into digested pBI101:GUS destination vector (Jefferson et al., 1987).

The CYCB1;1 (At4g37490) promoter and destruction box (Colon-Carmona et al., 1999) were amplified using Prime Star polymerase and the primers CYCB1 F 5' TTTAAAGTTCCTCGAGAGATGACTAAATT, CYCB1 R 5' TATATCACCAAGAACTTGACGGTTTCT) and cloned into the pCR8-TOPO Gateway entry vector (Invitrogen). Entry clones were subcloned via Gateway recombination cloning (Invitrogen) into a binary expression vector, pBIB-GUS-BASTA (Gou et al., 2010). The *pWOX5::HTA6-GFP* construct was previously described (Nodine et al., 2007). All constructs were transformed into wild type (*Col-0* ecotype) and/or *gso2-1* plants using *Agrobacterium*-mediated transformation and crossed with *gso1-2* to create double mutants.

Microscopy and staining

Images of seedlings were obtained using a Canon Power Shot SX110 digital camera mounted on a Leica dissecting microscope or by scanning seedlings on agar plates (Epson Perfection 2400 Photo flatbed scanner). Seedlings containing the GL2, CPC and CYCB1;1 marker lines and GSO1 and GSO2::GUS promoter fusions were fixed in 80% acetone and stained with 1mM X-Gluc (5-Bromo-4-chloro-3-indoxyl-beta-D-glucuronide cyclohexylammonium salt) (Gold Bio Technology) dissolved in DMSO (2% final concentration) in a solution of 10 mM EDTA, 0.5 mM potassium ferricyanide, 0.5 mM potassium ferrocyanide, 0.1% Triton X-100, 100 mM NaH_2PO4, pH 7.0 for 2-24 hours at 37°C. Seedlings were fixed at room temperature in 9:1 (v/v) ethanol: acetic acid and mounted in a chloralhydrate solution (chloralhydrate: distilled water: glycerol, 8:2:1, w/v/v). Seedlings were imaged using a Zeiss Axioplan microscope equipped with a digital camera and QCapture Pro 5.0 imaging software. Wild-type and mutant seedlings containing *QC184::GUS* and *QC46::GUS* markers were stained with X-Gluc for 2-6 hours at 37°C and mounted in 6:1 chloralhydrate: Lugol's solution and imaged using a Zeiss Axioplan microscope. Root lengths were measured six DAG using Image J software.

Embryos carrying the ATML1 marker were dissected from developing ovules and stained for 5 minutes with 2 μM FM4-64, and six DAG roots of WOX5, ATML1 and SCR marker line plants were stained for 5 minutes with 10 μM propidium iodine, mounted in sterile water and imaged using a Zeiss 510 Meta confocal microscope equipped with a laser line with excitation at 488nm. Images were captured and processed using the BP

505-530 filter sets for YFP and GFP and LP560 for PI and FM4-64 and AxioVision image processing software.

Toluidine blue (TB) staining was performed as described by Tsuwamoto et al, 2008. Briefly, seedlings grown on agar plates were transferred to a 0.05% aequeous solution of TB, immersed for 3 minutes, rinsed in water and immaged using an Epson Perfection 2400 Photo flatbed scanner.

Staining of whole seedlings at one and three DAG using a modified Schiff propidium iodide procedure was carried out as described by (Truernit et al., 2008), with the exception that seedlings were mounted in chloralhydrate solution.

Imaging of transverse root sections

Three day old mutant and wild-type seedlings expressing the GL2::GUS marker were stained as described above, rinsed three times in water and placed in a plate containing warm 1% agarose in 100 mM sodium phosphate buffer, pH 6.8. Solidified agarose blocks containing the roots were cut to about 1 X 0.4 X 0.4 cm and placed in fixation solution (2% gluteraldehide, 3% paraformaldehyde in 50 mM sodium phosphate buffer, pH 7.2) for 4 hours on a rotating platform. Samples were rinsed twice for 15 min. in 50 mM sodium phosphate buffer and then dehydrated for 20 min. each time in 10%, 30%, 50%, 70%, 90% and 100% (twice) ethanol. The samples were embedded in

Technovit 7100 resin (Electron Microscopy Sciences, Hatfield, PA, USA) following the manufacturer's protocol, with the modification that pre-infiltration step was performed in a series of 2:1, 1:1, 1:2 ethanol: Technovit solution H1 for 2 hours each. After plastic polymerization, samples were removed from histoforms and root cross-sections of 7µm were obtained using a Sorvall MT2-B Ultra Microtome. Sections were mounted on Superfrost plus slides (Thermo Fisher Scientific Inc.,Waltham, MA, USA) and imaged with and without staining in 0.05% TB for 5 min and rinsing with water. Images were captured on a Zeiss Axioplan microscope equipped with a digital camera and QCapture Pro 5.0 imaging software.

Acknowledgements

We are grateful to the members of the Tax lab for their helpful comments and discussions of the manuscript. We thank C. Zhang for providing the *pWOX5::HTA6-GFP* construct and pFYTAG vector. The pBIB::GUS-BASTA vector was kindly provided by Jia Li. This work was supported by NSF 2010: MCB 0418946, NSF IOS-0922678, and NSF IOS 1257316, awarded to Frans E Tax. A. C. B. and A. R. received funding from NIH T32 GM08659. A.R. was also funded by NSF IGERT DGE-0114420.

References

Aichinger E, Kornet N, Friedrich T, Laux T. 2012. Plant stem cell niches. Annu Rev Plant Biol 63:615-636.

Allen E, Moing A, Ebbels TM, Maucourt M, Tomos AD, Rolin D, Hooks MA. 2010. Correlation Network Analysis reveals a sequential reorganization of metabolic and

transcriptional states during germination and gene-metabolite relationships in developing seedlings of Arabidopsis. BMC Syst Biol 4:62.

Alonso JM, Stepanova AN, Leisse TJ, Kim CJ, Chen H, Shinn P, Stevenson DK, Zimmerman J, Barajas P, Cheuk R, Gadrinab C, Heller C, Jeske A, Koesema E, Meyers CC, Parker H, Prednis L, Ansari Y, Choy N, Deen H, Geralt M, Hazari N, Hom E, Karnes M, Mulholland C, Ndubaku R, Schmidt I, Guzman P, Aguilar-Henonin L, Schmid M, Weigel D, Carter DE, Marchand T, Risseeuw E, Brogden D, Zeko A, Crosby WL, Berry CC, Ecker JR. 2003. Genome-wide insertional mutagenesis of Arabidopsis thaliana. Science 301:653-657.

Baum SF, Dubrovsky JG, Rost TL. 2002. Apical organization and maturation of the cortex and vascular cylinder inArabidopsis thaliana (Brassicaceae) roots. Am J Bot 89:908-920.

Baum SF, Rost TL. 1996. Root apical organization inArabidopsis thaliana 1. Root cap and protoderm. Protoplasma 192:178-188.

Berger F, Hung C-Y, Dolan L, Schiefelbein J. 1998. Control of Cell Division in the Root Epidermis ofArabidopsis thaliana. Developmental Biology 194:235-245.

Borghi L, Gutzat R, Fütterer J, Laizet Y, Hennig L, Gruissem W. 2010. Arabidopsis RETINOBLASTOMA-RELATED is required for stem cell maintenance, cell differentiation, and lateral organ production. Plant Cell 22:1792-1811.

Brady SM, Orlando DA, Lee JY, Wang JY, Koch J, Dinneny JR, Mace D, Ohler U, Benfey PN. 2007. A high-resolution root spatiotemporal map reveals dominant expression patterns. Science 318:801-806.

Campilho A, Garcia B, Toorn HV, Wijk HV, Scheres B. 2006. Time-lapse analysis of stem-cell divisions in the Arabidopsis thaliana root meristem. Plant J 48:619-627.

Cederholm HM, Iyer-Pascuzzi AS, Benfey PN. 2012. Patterning the primary root in Arabidopsis. Wiley Interdiscip Rev Dev Biol 1:675-691.

Chuck G, Candela H, Hake S. 2009. Big impacts by small RNAs in plant development. Curr Opin Plant Biol 12:81-86.

Colon-Carmona A, You R, Haimovitch-Gal T, Doerner P. 1999. Technical advance: spatio-temporal analysis of mitotic activity with a labile cyclin-GUS fusion protein. Plant J 20:503-508.

Cruz-Ramirez A, Diaz-Trivino S, Blilou I, Grieneisen VA, Sozzani R, Zamioudis C, Miskolczi P, Nieuwland J, Benjamins R, Dhonukshe P, Caballero-Perez J, Horvath B, Long Y, Mahonen AP, Zhang H, Xu J, Murray JA, Benfey PN, Bako L, Maree AF, Scheres B. 2012. A bistable circuit involving SCARECROW-RETINOBLASTOMA integrates cues to inform asymmetric stem cell division. Cell 150:1002-1015.

Cui H, Hao Y, Kong D. 2012. SCARECROW has a SHORT-ROOT-independent role in modulating the sugar response. Plant Physiol 158:1769-1778.

De Smet I, Vassileva V, De Rybel B, Levesque MP, Grunewald W, Van Damme D, Van Noorden G, Naudts M, Van Isterdael G, De Clercq R, Wang JY, Meuli N, Vanneste S, Friml J, Hilson P, Jurgens G, Ingram GC, Inze D, Benfey PN, Beeckman T. 2008. Receptor-Like Kinase ACR4 Restricts Formative Cell Divisions in the Arabidopsis Root. Science 322:594-597.

Di Cristina M, Sessa G, Dolan L, Linstead P, Baima S, Ruberti I, Morelli G. 1996. The Arabidopsis Athb-10 (GLABRA2) is an HD-Zip protein required for regulation of root hair development. Plant J 10:393-402.

Di Laurenzio L, Wysocka-Diller J, Malamy JE, Pysh L, Helariutta Y, Freshour G, Hahn MG, Feldmann KA, Benfey PN. 1996. The SCARECROW gene regulates an asymmetric cell division that is essential for generating the radial organization of the Arabidopsis root. Cell 86:423-433.

Dolan L, Janmaat K, Willemsen V, Linstead P, Poethig S, Roberts K, Scheres B. 1993. Cellular organisation of the Arabidopsis thaliana root. Development 119:71-84.

Gonzalez-Garcia MP, Vilarrasa-Blasi J, Zhiponova M, Divol F, Mora-Garcia S, Russinova E, Cano-Delgado AI. 2011. Brassinosteroids control meristem size by promoting cell cycle progression in Arabidopsis roots. Development 138:849-859.

Gou X, He K, Yang H, Yuan T, Lin H, Clouse SD, Li J. 2010. Genome-wide cloning and sequence analysis of leucine-rich repeat receptor-like protein kinase genes in Arabidopsis thaliana. BMC Genomics 11:19.

Guo Y, Han L, Hymes M, Denver R, Clark SE. 2010. CLAVATA2 forms a distinct CLE-binding receptor complex regulating Arabidopsis stem cell specification. Plant J 63:889-900.

Gutzat R, Borghi L, Futterer J, Bischof S, Laizet Y, Hennig L, Feil R, Lunn J, Gruissem W. 2011. RETINOBLASTOMA-RELATED PROTEIN controls the transition to autotrophic plant development. Development 138:2977-2986.

Hacham Y, Holland N, Butterfield C, Ubeda-Tomas S, Bennett MJ, Chory J, Savaldi-Goldstein S. 2011. Brassinosteroid perception in the epidermis controls root meristem size. Development 138:839-848.

Haecker A, Gross-Hardt R, Geiges B, Sarkar A, Breuninger H, Herrmann M, Laux T. 2004. Expression dynamics of WOX genes mark cell fate decisions during early embryonic patterning in Arabidopsis thaliana. Development 131:657-668.

Hassan H, Scheres B, Blilou I. 2010. JACKDAW controls epidermal patterning in the Arabidopsis root meristem through a non-cell-autonomous mechanism. Development 137:1523-1529.

Helariutta Y, Fukaki H, Wysocka-Diller J, Nakajima K, Jung J, Sena G, Hauser MT, Benfey PN. 2000. The SHORT-ROOT gene controls radial patterning of the Arabidopsis root through radial signaling. Cell 101:555-567.

Inzé D, De Veylder L. 2006. Cell cycle regulation in plant development. Annu Rev Genet 40:77-105.

Jefferson RA, Kavanagh TA, Bevan MW. 1987. GUS fusions: beta-glucuronidase as a sensitive and versatile gene fusion marker in higher plants. EMBO J 6:3901-3907.

Kircher S, Schopfer P. 2012. Photosynthetic sucrose acts as cotyledon-derived long-distance signal to control root growth during early seedling development in Arabidopsis. Proc Natl Acad Sci U S A 109:11217-11221.

Kuppusamy KT, Chen AY, Nemhauser JL. 2009. Steroids are required for epidermal cell fate establishment in Arabidopsis roots. Proc Natl Acad Sci U S A 106:8073-8076.

Kwak SH, Schiefelbein J. 2007. The role of the SCRAMBLED receptor-like kinase in patterning the Arabidopsis root epidermis. Dev Biol 302:118-131.

Kwak SH, Schiefelbein J. 2008. A feedback mechanism controlling SCRAMBLED receptor accumulation and cell-type pattern in Arabidopsis. Curr Biol 18:1949-1954.

Kwak SH, Shen R, Schiefelbein J. 2005. Positional signaling mediated by a receptor-like kinase in Arabidopsis. Science 307:1111-1113.

Masubelele NH, Dewitte W, Menges M, Maughan S, Collins C, Huntley R, Nieuwland J, Scofield S, Murray JA. 2005. D-type cyclins activate division in the root apex to promote seed germination in Arabidopsis. Proc Natl Acad Sci U S A 102:15694-15699.

Menges M, Hennig L, Gruissem W, Murray JA. 2003. Genome-wide gene expression in an Arabidopsis cell suspension. Plant Mol Biol 53:423-442.

Naouar N, Vandepoele K, Lammens T, Casneuf T, Zeller G, van Hummelen P, Weigel D, Rätsch G, Inzé D, Kuiper M, De Veylder L, Vuylsteke M. 2009. Quantitative RNA expression analysis with Affymetrix Tiling 1.0R arrays identifies new E2F target genes. Plant J 57:184-194.

Nawy T, Lee JY, Colinas J, Wang JY, Thongrod SC, Malamy JE, Birnbaum K, Benfey PN. 2005. Transcriptional profile of the Arabidopsis root quiescent center. Plant Cell 17:1908-1925.

Nodine MD, Yadegari R, Tax FE. 2007. RPK1 and TOAD2 are two receptor-like kinases redundantly required for arabidopsis embryonic pattern formation. Dev Cell 12:943-956.

Ogasawara H, Kaimi R, Colasanti J, Kozaki A. 2011. Activity of transcription factor JACKDAW is essential for SHR/SCR-dependent activation of SCARECROW and MAGPIE and is modulated by reciprocal interactions with MAGPIE, SCARECROW and SHORT ROOT. Plant Mol Biol 77:489-499.

Sabatini S, Heidstra R, Wildwater M, Scheres B. 2003. SCARECROW is involved in positioning the stem cell niche in the Arabidopsis root meristem. Genes Dev 17:354-358.

Sarkar AK, Luijten M, Miyashima S, Lenhard M, Hashimoto T, Nakajima K, Scheres B, Heidstra R, Laux T. 2007. Conserved factors regulate signalling in Arabidopsis thaliana shoot and root stem cell organizers. Nature 446:811-814.

Sliwinska E, Bassel GW, Bewley JD. 2009. Germination of Arabidopsis thaliana seeds is not completed as a result of elongation of the radicle but of the adjacent transition zone and lower hypocotyl. Journal of Experimental Botany 60:3587-3594.

Smolarkiewicz M, Dhonukshe P. 2013. Formative cell divisions: principal determinants of plant morphogenesis. Plant Cell Physiol 54:333-342.

Sozzani R, Cui H, Moreno-Risueno MA, Busch W, Van Norman JM, Vernoux T, Brady SM, Dewitte W, Murray JA, Benfey PN. 2010. Spatiotemporal regulation of cell-cycle genes by SHORTROOT links patterning and growth. Nature 466:128-132.

Stahl Y, Grabowski S, Bleckmann A, Kühnemuth R, Weidtkamp-Peters S, Pinto KG, Kirschner GK, Schmid JB, Wink RH, Hülsewede A, Felekyan S, Seidel CA, Simon R. 2013. Moderation of Arabidopsis root stemness by CLAVATA1 and ARABIDOPSIS CRINKLY4 receptor kinase Complexes. Curr Biol 23:362-371.

Stahl Y, Wink RH, Ingram GC, Simon R. 2009. A signaling module controlling the stem cell niche in Arabidopsis root meristems. Curr Biol 19:909-914.

Takada S, Jurgens G. 2007. Transcriptional regulation of epidermal cell fate in the Arabidopsis embryo. Development 134:1141-1150.

Tanaka H, Onouchi H, Kondo M, Hara-Nishimura I, Nishimura M, Machida C, Machida Y. 2001. A subtilisin-like serine protease is required for epidermal surface formation in Arabidopsis embryos and juvenile plants. Development 128:4681-4689.

Tanaka H, Watanabe M, Sasabe M, Hiroe T, Tanaka T, Tsukaya H, Ikezaki M, Machida C, Machida Y. 2007. Novel receptor-like kinase ALE2 controls shoot development by specifying epidermis in Arabidopsis. Development 134:1643-1652.

Truernit E, Bauby H, Dubreucq B, Grandjean O, Runions J, Barthélémy J, Palauqui JC. 2008. High-resolution whole-mount imaging of three-dimensional tissue organization and gene expression enables the study of Phloem development and structure in Arabidopsis. Plant Cell 20:1494-1503.

Tsuwamoto R, Fukuoka H, Takahata Y. 2008. GASSHO1 and GASSHO2 encoding a putative leucine-rich repeat transmembrane-type receptor kinase are essential for the normal development of the epidermal surface in Arabidopsis embryos. Plant J 54:30-42.

van den Berg C, Willemsen V, Hage W, Weisbeek P, Scheres B. 1995. Cell fate in the Arabidopsis root meristem determined by directional signalling. Nature 378:62-65.

van den Berg C, Willemsen V, Hendriks G, Weisbeek P, Scheres B. 1997. Short-range control of cell differentiation in the Arabidopsis root meristem. Nature 390:287-289.

Wachsman G, Heidstra R, Scheres B. 2011. Distinct cell-autonomous functions of RETINOBLASTOMA-RELATED in Arabidopsis stem cells revealed by the Brother of Brainbow clonal analysis system. Plant Cell 23:2581-2591.

Wada T, Tachibana T, Shimura Y, Okada K. 1997. Epidermal cell differentiation in Arabidopsis determined by a Myb homolog, CPC. Science 277:1113-1116.

Watanabe M, Tanaka H, Watanabe D, Machida C, Machida Y. 2004. The ACR4 receptor-like kinase is required for surface formation of epidermis-related tissues in Arabidopsis thaliana. Plant J 39:298-308.

Welch D, Hassan H, Blilou I, Immink R, Heidstra R, Scheres B. 2007. Arabidopsis JACKDAW and MAGPIE zinc finger proteins delimit asymmetric cell division and stabilize tissue boundaries by restricting SHORT-ROOT action. Genes Dev 21:2196-2204.

Wildwater M, Campilho A, Perez-Perez JM, Heidstra R, Blilou I, Korthout H, Chatterjee J, Mariconti L, Gruissem W, Scheres B. 2005. The RETINOBLASTOMA-RELATED gene regulates stem cell maintenance in Arabidopsis roots. Cell 123:1337-1349.

Willemsen V, Bauch M, Bennett T, Campilho A, Wolkenfelt H, Xu J, Haseloff J, Scheres B. 2008. The NAC domain transcription factors FEZ and SOMBRERO control the orientation of cell division plane in Arabidopsis root stem cells. Dev Cell 15:913-922.

Wu X, Dabi T, Weigel D. 2005. Requirement of homeobox gene STIMPY/WOX9 for Arabidopsis meristem growth and maintenance. Curr Biol 15:436-440.

Xing Q, Creff A, Waters A, Tanaka H, Goodrich J, Ingram GC. 2013. ZHOUPI controls embryonic cuticle formation via a signalling pathway involving the subtilisin protease ABNORMAL LEAF-SHAPE1 and the receptor kinases GASSHO1 and GASSHO2. Development 140:770-779.

Xiong Y, McCormack M, Li L, Hall Q, Xiang C, Sheen J. 2013. Glucose-TOR signalling reprograms the transcriptome and activates meristems. Nature 496:181-186.

Zhang C, Gong FC, Lambert GM, Galbraith DW. 2005. Cell type-specific characterization of nuclear DNA contents within complex tissues and organs. Plant Methods 1:7.

Figure Legends

Figure 1. Root growth is arrested in *gso1; gso2* T-DNA insertion mutants.

A: GSO1 (top) and GSO2 (bottom) gene models, indicating the positions of conserved domains and T-DNA insertions (arrowheads); LRRs - Leucine-rich repeats. **B:** Seedling morphology and root length of wild type (Col), *gso1-1, gso1-2, gso2-1*, and *gso2-2* single mutants and the *gso1-1*; *gso2-1*, *gso1-2*; *gso2-1*, *gso1-1; gso2-2* double mutants at three and five days after germination (DAG), grown on MS plates or MS with 1% sucrose. Scale bars = 2 mm**. C:** Quantification of root growth at three and five DAG on MS media (no sucrose added) of the wild type, *gso1-2*, *gso2-1* and *gso1-2; gso2-1* (n=30, mean ± SD*)*. Asterisks mark significant differences in root length, **P* < 0.001. **D:** The distance from the root tip to the root hair zone (brackets) is reduced in *gso1-2; gso2-1* mutants. Scale bar = 1 mm.

Figure 2. Analysis of epidermal cell identity markers in embryos and seedlings of single and double mutants.

A,B,F,G,K: Confocal images of heart stage embryos (A,F), mature embryos (B,G) and six DAG roots (K) expressing *pATML1::HTA6-YFP* and counterstained with propidium iodide. Wild-type embryos (Col) (A,B) shown at the same developmental stage as *gso1-2; gso2-1* (F, G). Scale bars = 50 μm. Surface view and mid-longitudinal optical sections of six DAG roots (K), scale bars =20 μm. **C-E, H-J, L:** Wild-type (Col) (C-E) and *gso1-2; gso2-1* (H-J) seedlings grown on MS media (C,E,H,J) or MS containing 1% sucrose (D,I) and stained for GUS activity show expression of *pGL2::GUS* (C,D,H,I) and *pCPC::GUS* (E,J) in three DAG roots. Root expression of *pGL2::GUS* at six DAG detected in wild type, *gso1-2*, *gso2-1*, and *gso1-2; gso2-1* seedlings grown on MS media (I). Asterisks in (K) and (L) mark epidermal cells forming T-clones, arrows mark cells lacking the GFP signal. Scale bars = 50 μm.

Figure 3. Abnormal patterning of root cell types in *gso1; gso2* double mutants.

A: Expression pattern of *pGL2::GUS* in transverse root sections of the meristematic (MZ) and transition zones (TZ) of 3-day old double mutant and wild-type (Col) seedlings. Black arrows mark non-hair cell type specified at the trichoblast (T) cell position in the epidermis. Red asterisks - endodermis, green - cortex, blue - extra cells between cortex and epidermis. E- epidermis, L- lateral root cap (LRC), A- atrichoblast position, S - MS media + 1% sucrose. Scale bars = 20 μm. **B,C**: Quantification of

epidermal hair and non-hair cell types at the A and T position based on *pGL2::GUS* expression (B) and quantification of cells along the circumference of each radial layer (C) at three independent positions in the root apical meristem (mean ±SD). * $P < 0.005$, n=5 for each condition. **D:** Representative serial sections of *gso1-2; gso2-1* roots. Cells in the epidermal layer (black arrowheads) and enlarged cells in the position of the inner LRC (black arrows) express *pGL2::GUS*. Red arrowheads mark dying cells of the LRC in the elongation zone. Asterisks mark cells in the epidermal file position that are initially specified as A-type cells. Approximate distance of sections from the root tip indicated in µm. Scale bar = 20 µm.

Figure 4. RAM size is reduced and QC marker expression is altered in *gso1; gso2* double mutant seedlings.

A–B: Chloralhydrate: Lugol's staining of wild-type Col (A) and *gso1-2; gso2-1* (B) roots at six DAG shows meristematic cells with dense cytoplasm (brackets) and starch-containing cells in the columella. **C-D:** X-Gluc staining for *pCYCB1;1::GUS* in wild-type Col (C) and *gso1-2; gso2-1* (D) seedlings at six DAG. **E-J:** Starch granule accumulation in the columella cells of seedlings grown on MS media (E-H) or MS + 1% sucrose (I, J). The wild-type Col (E, I), *gso1-2* (F), *gso2-1* (G), and *gso1-2; gso2-1* (H, J) roots are shown at six DAG. The arrowheads and dashed lines (in E and H insets, different plants are shown) indicate the location of the QC (blue) and columella initials (yellow). **K:** Quantification of starch granule-containing columella cells in wild-type Col and mutant seedlings grown for 6 days on MS media or MS containing 1% sucrose (+S). *$P < 0.005$ (n=22 for each genotype on MS, n=20 for MS +1% sucrose grown plants). **L-O:** QC

marker expression in wild-type (L,M) and *gso1-2; gso2-1* (N,O) six DAG roots grown on MS media. X-Gluc staining of roots carrying the *QC184::GUS* (L.N) and the *QC46::GUS* (M,O) markers. The position of QC cells is marked by dashed line circles. Scale bars =20 μm.

Figure 5. RAM cells show abnormal marker expression and increased QC cell division in *gso1-2; gso2-1* mutant seedlings.

A-H: Expression of *pSCR::HTA6-YFP* (A-D) and *pWOX5::HTA6-GFP* (E-H) in roots counterstained with propidium iodide. Confocal medial optical sections of wild-type Col (A,C, E,F) and *gso1-2; gso2-1* (B,D,G,H) six DAG roots, grown on MS media (A,B,E,G) and on MS with 1% sucrose (C,D,F,H). Scale bars are 50 μm (A-D) and 20 μm (E-H). Arrows indicate the position of cell walls in dividing QC cells.

Figure 6. Abnormal cell divisions and altered RAM patterning in *gso1-2; gso2-1* mutants.

A: Longitudinal optical sections of three DAG roots stained using a modified pseudo Schiff propidium iodide method. Asterisks indicate the position of central cells and initials: yellow - QC cells, white – cortical/endodermal initials (CEI), red - endodermal stem cells, green - cortical stem cells. E - epidermis, C - cortex, En - endodermis and L - lateral root cap (LRC) cell files, Col – wild-type control. The positions of E/LRC initials are indicated by white arrows. Cell divisions of columella initials are indicated by yellow arrows, and abnormal planes of cell division in the meristem are indicated by red arrows. **B:** Close-up view of mid-longitudinal sections;

white arrows indicate newly formed cell walls between two cortical daughter cells. **C:** Number of cortex file cells within the first 100 μm immediately above the CEI/stem cells in the meristem. +S indicates plants grown on MS media containing 1% sucrose. ** $p < 0.001$ (n=20); *$P < 0.05$ (n=14). **D:** Detailed view of columella and E/LRC initial divisions. Yellow arrows indicate the position of the distal cell wall of columella stem cells; white arrows indicate the plane of cell division of E/LRC initials. Scale bars = 20 μm. **E:** Transverse root sections at the columella stem cell zone (marked by asterisks). E/LRC initials divide periclinally along the gyre of a helix (red arrowheads perpendicular to the plane of cell division) in wild type Col but not in the *gso1-2; gso2-1* roots. L - lateral root cap cells; bracket -group of cells with aberrant orientation of cell division planes.

Figure 7. Dynamic expression of *GSO1* and *GSO2* in wild-type Col seedlings.

A-F: *pGSO1::GUS* activity in wild-type seedlings. At 2 DAG, the histochemical GUS assay shows *GSO1* promoter activity in the vasculature of the root, extending from above the elongation zone to the root-hypocotyl junction (A) and by six DAG in the QC and the SAM (B-C). *pGSO1::GUS* expression displays an alternating pattern in root endodermal cells close to the root-hypocotyl junction (D) and is not detected at sites of lateral root initiation (arrow in E) or at sites of wounding (arrow in F). **G-K**: *pGSO2::GUS* expression in 2 (G), 3(H,I) and six DAG (J,K) seedlings. Expression is detected in roots in E and LRC at two DAG (G), restricted by three DAG to mostly cotyledons, hypocotyls and root tips (H,I), and detected in the QC by six DAG (K). **L, M:** Expression of

pGSO1::GUS (L) and *pGSO2::GUS* (M) in 3 day old wild-type seedlings. Scale bars are 200 µm in A and G, 100 µm in B-F and H-K, and 1 mm in L and M (n >20 for each time-point and each genotype).

Figure 8. Addition of sucrose to the growth media rescues the growth arrest but not the cell specification defects in *gso1; gso2* mutants.

A: Quantification of root length at six DAG in seedlings grown on MS media or MS media containing 1% sucrose, glucose or 3-O-methlyglucose (3-OMG). Asterisks mark significant differences between root growth of wild-type Col and double mutants. * $P < 0.001$ (n>30). **B-E:** Accumulation of starch granules in cotyledons of plants grown on MS media or MS containing 1% sucrose, cleared and mounted in chloralhydrate: Lugol's solution. Wild-type Col seedlings (B, D) are compared to *gso1-2; gso2-1* (C, E). **F-G:** *QC184::GUS* expression in wild-type Col (F) and *gso1-2; gso2-1* (G) seedlings grown in MS + 1% sucrose. **H-J:** TB staining of cotyledons is observed in double mutant seedlings grown with (I), or without (J**)** 1% sucrose but not in the wild type or single mutants (H). **K:** Double mutant seedlings, shown at 10 DAG, grow at comparable rates to wild-type seedlings in the presence of 1% sucrose, forming true leaves and lateral roots.

Figure 9. Model for control of root growth, cell proliferation and cell differentiation by GSO1 and 2 integrated with known pathways.

A. Model of signaling mechanisms mediated by GSO1 and 2 in the differentiated root and in the RAM. H-hair cell file, N-non-hair cell file. Expression domains of GSO1

and 2 are shaded in blue and pink, respectively, and overlapping domains in purple. **B.** Activity of GSO1 and 2 in the stem cell niche controls stem cell fate maintenance and division (black arrows and bars) integrated with known pathways (red arrows and bars) contributing to RAM patterning and control of cell division. Arrows represent positive regulation, bars, negative regulation and double arrows, co-regulation or genetic interaction. Dotted lines symbolize potential crosstalk among components of the RAM signaling network that could involve GSO1/2. ACD - asymmetric cell divisions. Gene names for abbreviations and references can be found in the text.

Fig 1

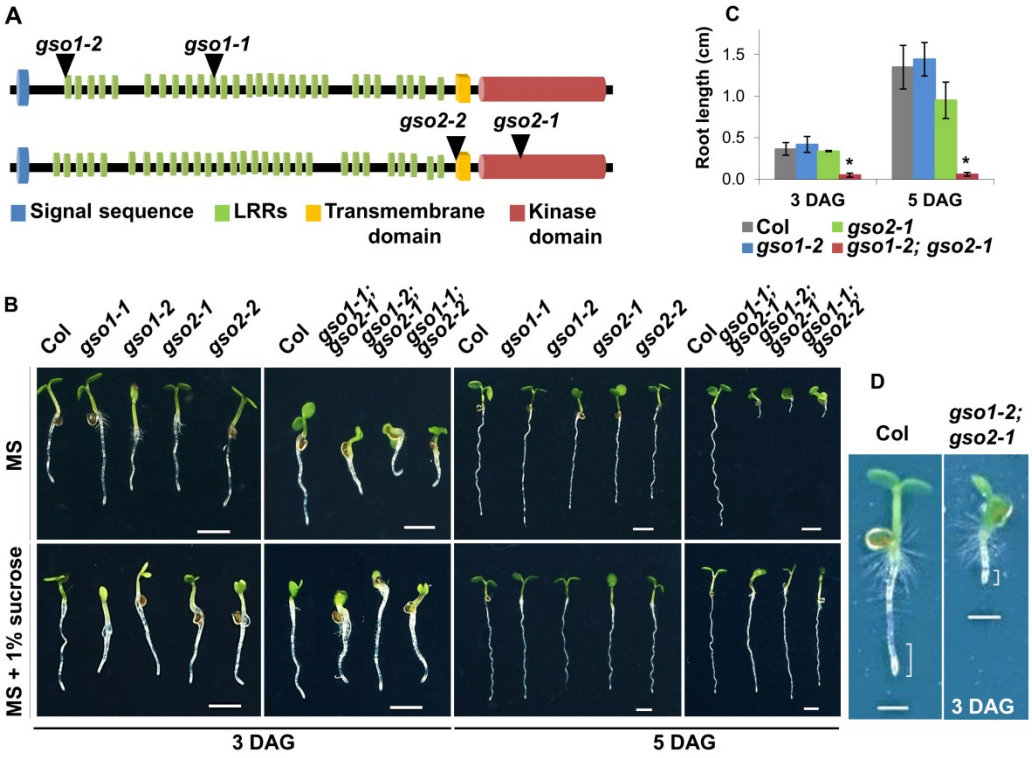
A
gso1-2
gso1-1
gso2-2
gso2-1
Signal sequence
LRRs
Transmembrane domain
Kinase domain
C
Root length (cm)
1.5
1.0
0.5
0.0
3 DAG
5 DAG
Col
gso2-1
gso1-2
gso1-2; gso2-1
B
Col
gso1-1
gso1-2
gso2-1
gso2-2
gso1-1; gso2-1
gso1-2; gso2-1
gso1-1; gso2-2
MS
MS + 1% sucrose
3 DAG
5 DAG
D
Col
gso1-2; gso2-1
3 DAG

Fig 2

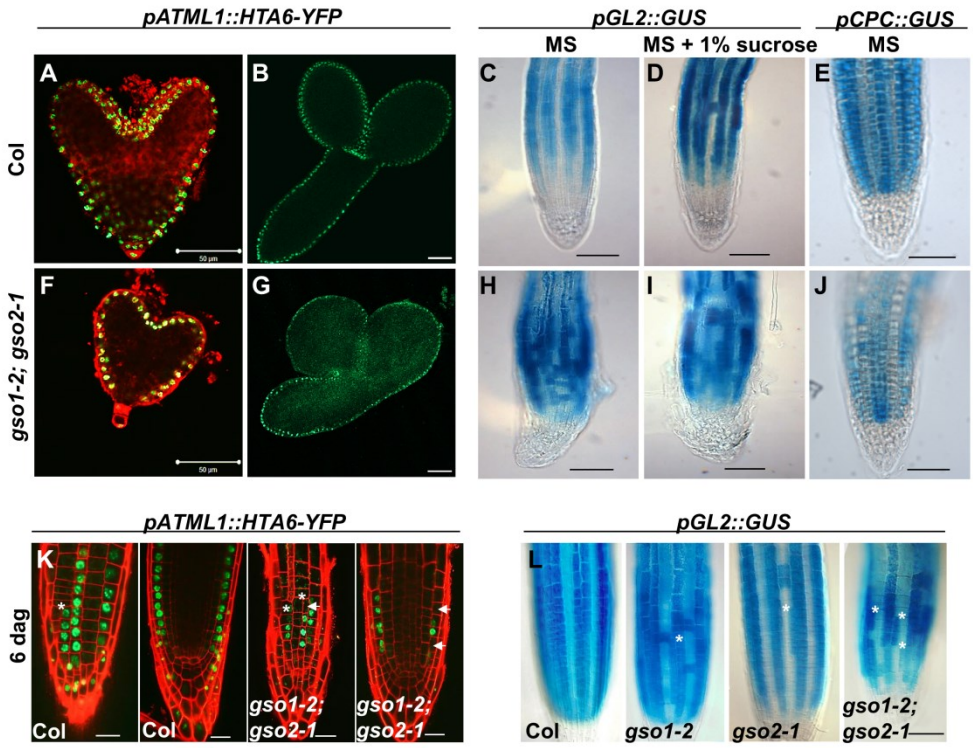
pATML1::HTA6-YFP
pGL2::GUS
pCPC::GUS
MS
MS + 1% sucrose
MS
Col
gso1-2; gso2-1
A
B
C
D
E
F
G
H
I
J
pATML1::HTA6-YFP
pGL2::GUS
6 dag
K
L
Col
Col
gso1-2; gso2-1
gso1-2; gso2-1
Col
gso1-2
gso2-1
gso1-2; gso2-1

Fig 3

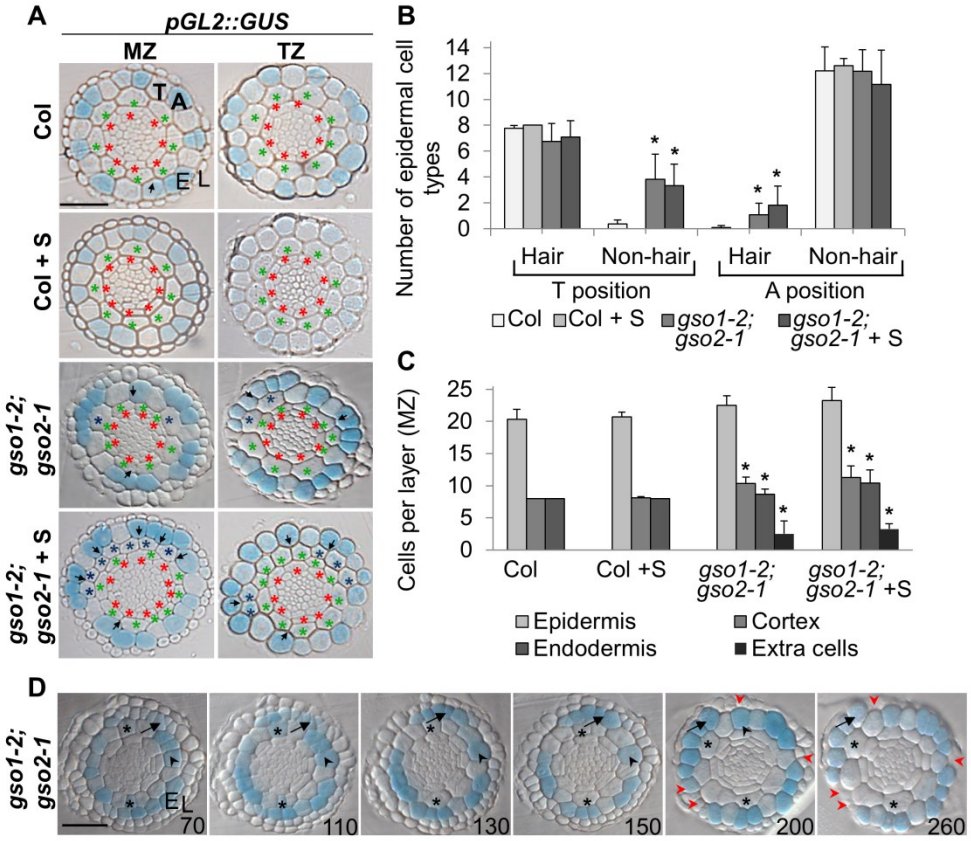
A
pGL2::GUS
MZ
TZ
Col
Col + S
gso1-2; gso2-1
gso1-2; gso2-1 + S
T
A
E
L
B
Number of epidermal cell types
14
12
10
8
6
4
2
0
Hair
Non-hair
Hair
Non-hair
T position
A position
Col
Col + S
gso1-2; gso2-1
gso1-2; gso2-1 + S
C
Cells per layer (MZ)
25
20
15
10
5
0
Col
Col +S
gso1-2; gso2-1
gso1-2; gso2-1 +S
Epidermis
Cortex
Endodermis
Extra cells
D
gso1-2; gso2-1
E
L
70
110
130
150
200
260

Fig 4

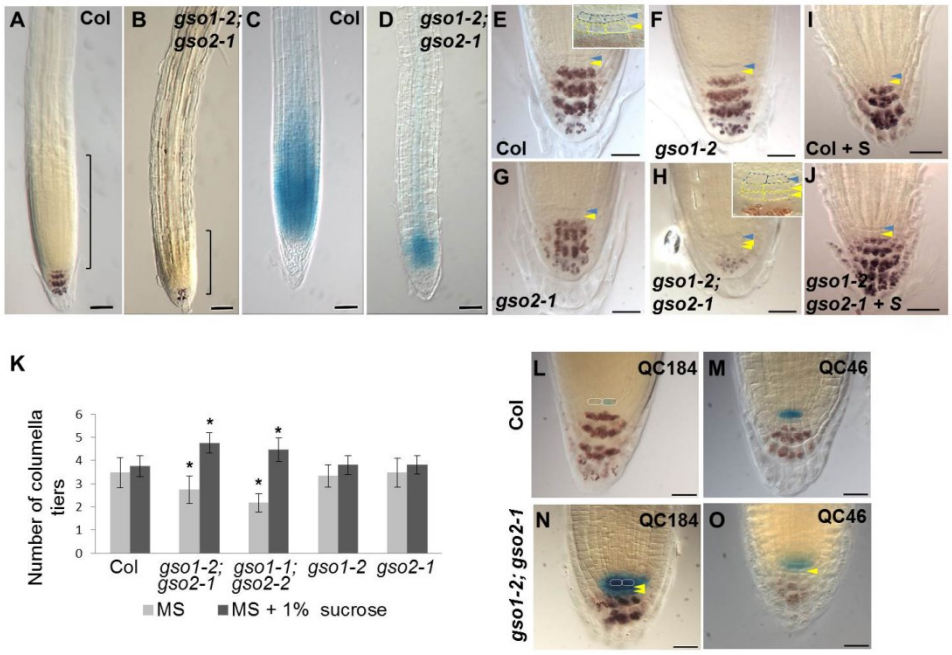
A
Col
B
gso1-2; gso2-1
C
Col
D
gso1-2; gso2-1
E
Col
F
gso1-2
I
Col + S
G
gso2-1
H
gso1-2; gso2-1
J
gso1-2; gso2-1 + S
K
Number of columella tiers
0
1
2
3
4
5
6
Col
gso1-2; gso2-1
gso1-1; gso2-2
gso1-2
gso2-1
MS
MS + 1% sucrose
L
QC184
M
QC46
Col
N
QC184
O
QC46
gso1-2; gso2-1

Fig 5

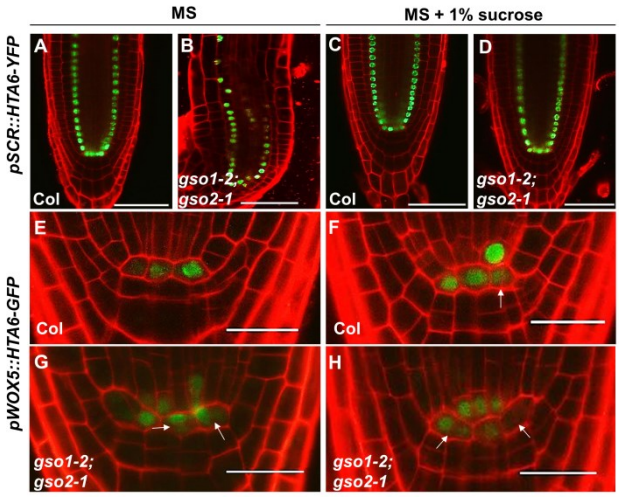
MS
MS + 1% sucrose
pSCR::HTA6-YFP
pWOX5::HTA6-GFP
A
B
C
D
E
F
G
H
Col
gso1-2;
gso2-1

Fig 6

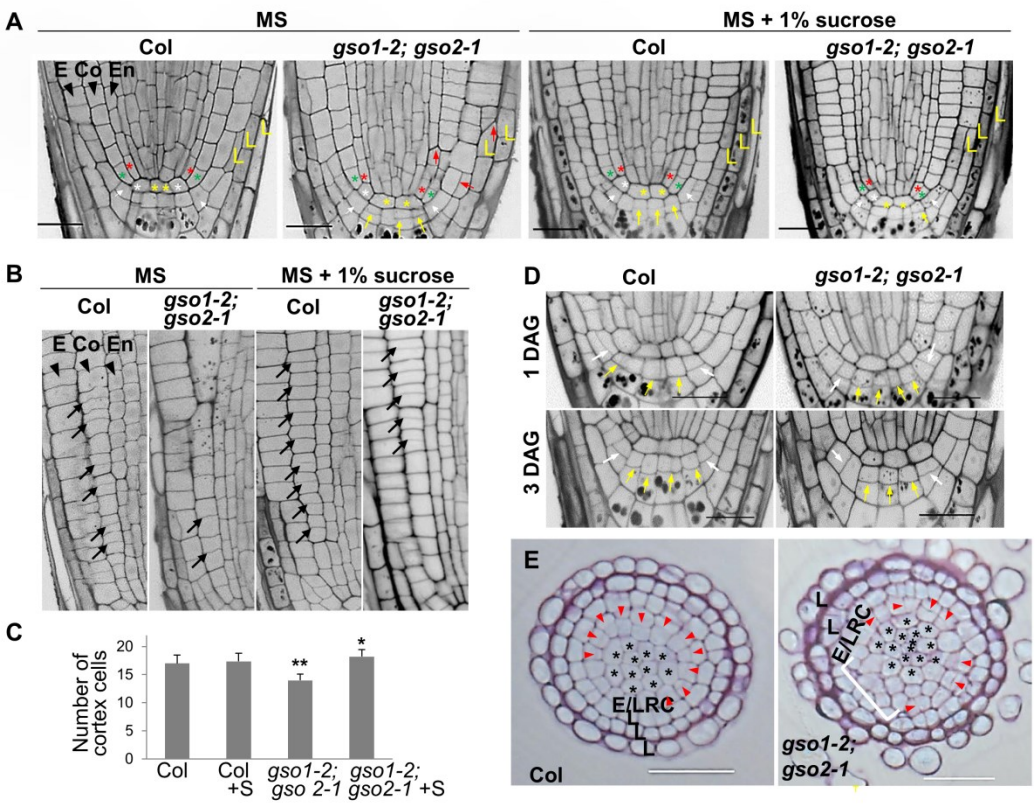
A
MS
MS + 1% sucrose
Col
gso1-2; gso2-1
Col
gso1-2; gso2-1
E Co En
B
MS
MS + 1% sucrose
Col
gso1-2; gso2-1
Col
gso1-2; gso2-1
E Co En
C
Number of cortex cells
20
15
10
5
0
**
*
Col
Col +S
gso1-2; gso 2-1
gso1-2; gso2-1 +S
D
Col
gso1-2; gso2-1
1 DAG
3 DAG
E
E/LRC
L
L
Col
E/LRC
L
L
gso1-2; gso2-1

Fig 7

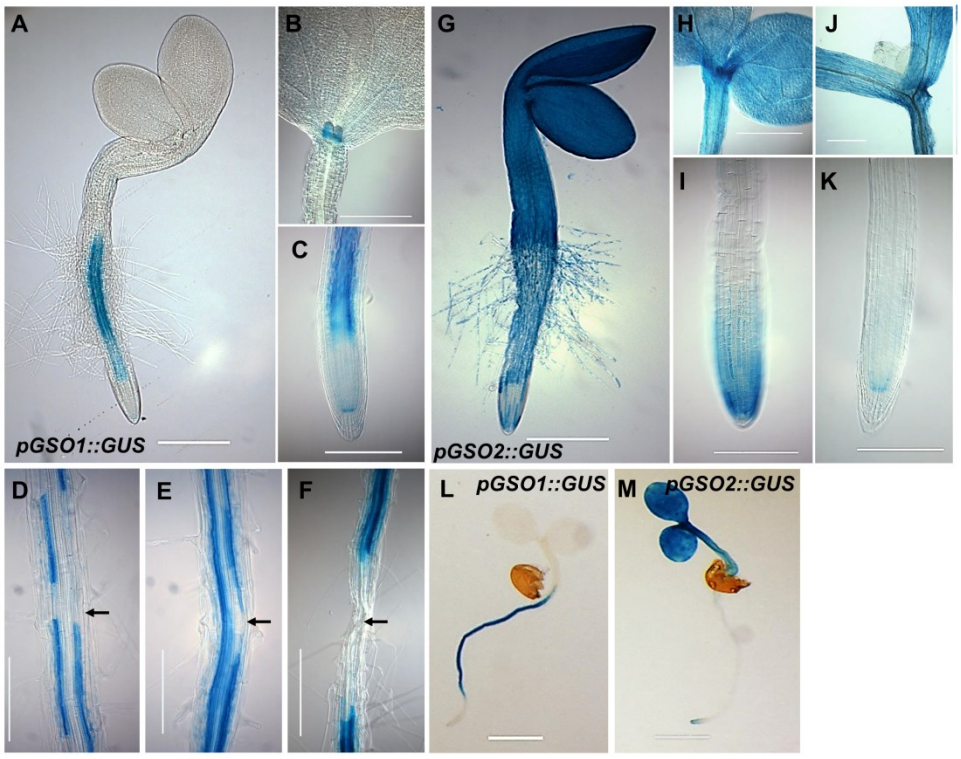

Fig 8

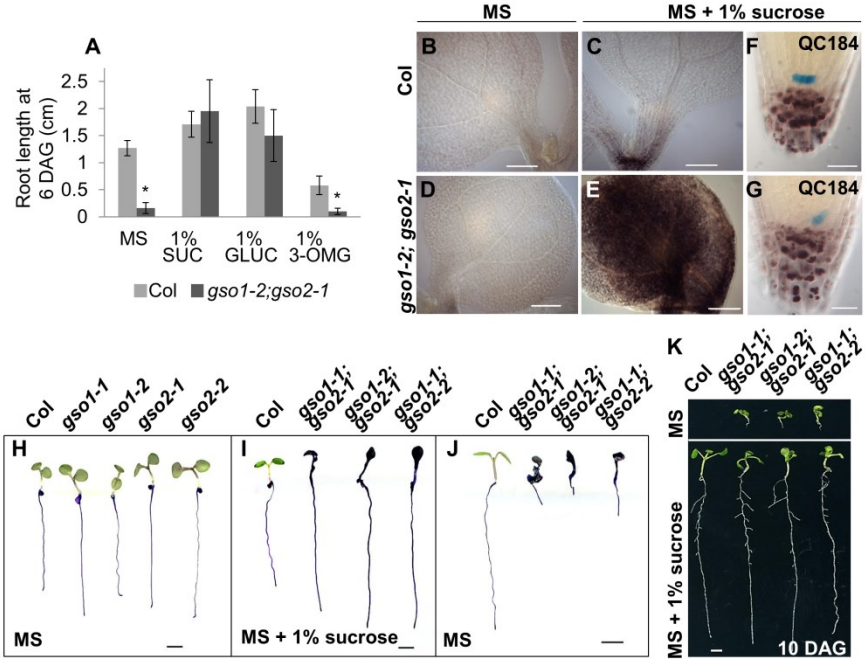
A
Root length at 6 DAG (cm)
2.5
2
1.5
1
0.5
0
MS
1% SUC
1% GLUC
1% 3-OMG
Col
gso1-2;gso2-1
MS
MS + 1% sucrose
B
C
F
QC184
Col
D
E
G
QC184
gso1-2; gso2-1
Col
gso1-1
gso1-2
gso2-1
gso2-2
gso1-1; gso2-1
gso1-2; gso2-1
gso1-1; gso2-2
H
I
J
MS
MS + 1% sucrose
MS
K
MS
MS + 1% sucrose
10 DAG

Fig 9

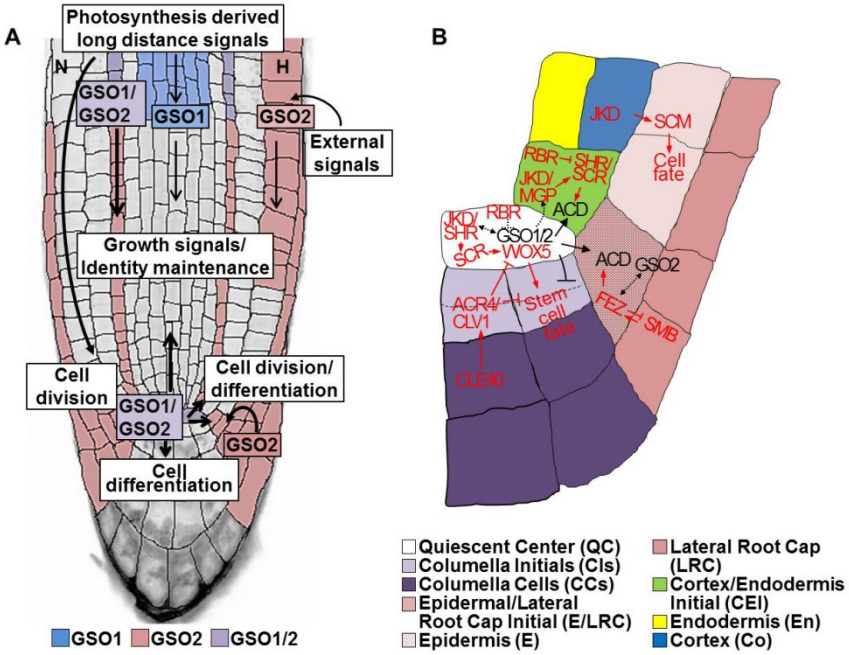
A
Photosynthesis derived long distance signals
N
H
GSO1/ GSO2
GSO1
GSO2
External signals
Growth signals/ Identity maintenance
Cell division
GSO1/ GSO2
Cell division/ differentiation
GSO2
Cell differentiation
GSO1
GSO2
GSO1/2
B
JKD
SCM
Cell fate
RBR
SHR/ SCR
JKD/ MGP
ACD
JKD/ SHR/ SCR
RBR
GSO1/2
WOX5
ACD
GSO2
ACR4/ CLV1
Stem cell fate
FEZ
SMB
CLE40
Quiescent Center (QC)
Columella Initials (CIs)
Columella Cells (CCs)
Epidermal/Lateral Root Cap Initial (E/LRC)
Epidermis (E)
Lateral Root Cap (LRC)
Cortex/Endodermis Initial (CEI)
Endodermis (En)
Cortex (Co)

Table 1

Table1. Root length of 6 DAG seedlings grown under osmotic conditions

Growth condition	MS	MS + 3% sucrose	MS + 3% Manitol	MS + 100 mM NaCl
WT	10.76 (± 1.95)	19.10 (± 3.69)	9.65 (± 2.38)	5.66 (± 1.70)
gso1-2; gso2-1	1.78 (± 0.76)	15.00 (± 5.71)	1.34 (± 1.09)	1.28 (± 0.51)

Values represent mean length ±SD (mm). n=30

APPENDIX B: CLE-MEDIATED REGULATION OF ROOT GROWTH REQUIRES SIGNALING THROUGH THE RECEPTOR KINASES TOAD2 AND RPK1

CLE-mediated regulation of root growth requires signaling through the receptor kinases *TOAD2* and *RPK1*

Adriana Racolta[1], Michael Nodine[3], Scott Rowe[1] and Frans E. Tax[1,2]

[1]Department of Molecular and Cellular Biology

[2]School of Plant Sciences

University of Arizona, Tucson, AZ 85721, USA

Phone: (520) 622-1186

Fax: (520) 621-3709

Corresponding author: Frans E. Tax (fetax@email.arizona.edu)

[3]Current address:
Gregor Mendel Institute of Molecular Plant Biology GmbH
Dr. Bohr-Gasse 3
1030 Vienna, Austria
T: +43 1 79044-9000
F: +43 1 79044-9001
E: office(at)gmi.oeaw.ac.at

Running title: Roles of RPK1 and TOAD2 in CLE signaling in roots

Keywords: receptor-like kinase, CLE, root apical meristem, root development

Key findings:

- *rpk1* and *rpk1; toad2/+* mutants show a low penetrance short root phenotype
- short root mutants have a disorganized RAM due to misoriented cell divisions in the lateral root cap, epidermis and cortex and QC
- *toad2* mutants are insensitive to CLE peptide treatment

- *RPK1-GFP* protein downregulation upon CLE treatment requires TOAD2

Abstract

Cell-cell communication is essential for plants to integrate developmental programs with external cues that affect their growth. Recent advances in plant signaling have uncovered similarities in shoot, root and vascular meristem signaling that involves receptor-like kinases and small signaling peptides. Often these signaling modules act redundantly in different regions of the plant. Here we report the receptor-like kinases TOAD2 and RPK1 regulate root growth by controlling cell proliferation affecting meristem size. TOAD2 mutant plants are insensitive to root meristem inhibition effect of CLE17 treatment, suggesting that TOAD2 may function as a receptor for CLE peptides. Two types of developmental defects were observed upon exogenous CLE treatment: defects identified in both sensitive and insensitive phenotypes, and defects specific to the sensitive phenotypes. The overlapping set of defects in sensitive and insensitive plants comprises increased proliferative activity of cells in the stem cell niche and a delay of progression to differentiation of daughter cells. The specific defects found only in the sensitive genotypes revealed a large decrease in the occurrence of anticlinal transit-amplifying cell divisions in longitudinal files, correlating with short meristems and cessation of root growth. A strong downregulation of RPK1 protein upon CLE treatment, dependent on TOAD2 suggests these two RLKs mediate CLE signaling in a common pathway to control root growth.

Introduction

Formation of new tissues and organs occurs during both embryonic and post-embryonic plant development through precise coordination of division of stem cells (meristems) and differentiation of their daughter cells. Studying the molecular mechanisms that generate and maintain the precisely regulated patterns underlying cell-fate decisions of cells departing from an undifferentiated meristematic cell state establishes a foundation for understanding plant development. Increasing experimental evidence, compiled from research in *Arabidopsis thaliana* and other plant systems, has uncovered complex networks of interacting receptors, hormones, small peptides, RNAs, transcription factors and other molecules regulating the patterning of meristems (Stahl and Simon, 2010; Azpeitia and Alvarez-Buylla, 2012; Petricka et al., 2012). Less is known, however, about how external and internal signals are perceived by the plant and how the receptor-ligand interaction translates into controlled downstream molecular steps that will ultimately generate precise patterns of growth.

The paradigm of signaling through plasma membrane receptors implies that ligands bind to the extracellular domain of receptors and a signaling cascade triggers changes in post-translational and transcriptional programs, modulating plant growth. In *Arabidopsis*, a large monophyletic family of more than 400 genes encodes receptor-like protein kinases (RLKs), with a predicted extracellular domain (containing Leucine-Rich Repeat motifs (LRRs) in more than half of these RLKs), a single-pass transmembrane domain and a cytoplasmic serine/threonine/tyrosine kinase domain (Shiu and Bleecker, 2001b, a; Diévart and Clark, 2004; Oh et al., 2009). Despite the large number of

identified RLKs, the specific functions are known for only a fraction of them (fewer than 50). The functions ascribed to these RLKs thus far indicate they play key signaling roles in regulating cell fate specification or maintenance, cell growth, cell death and pathogen response (Diévart and Clark, 2004) and that they bind a variety of ligand molecules ranging from steroid hormones to peptides and small secreted proteins (Torii, 2008). In addition, some RLKs may not only function in directly binding ligand,s but also as a regulatory components of other RLK complexes (Li, 2010).

A well characterized signaling pathway includes the LRR-RLK CLAVATA1 (CLV1) that functions to control the size of the shoot apical meristem (SAM) by binding to a small secreted peptide, CLAVATA3 (CLV3) (Ogawa et al., 2008), which ultimately restricts the expression domain of the homeodomain transcription factor *WUSCHEL*(*WUS*) that defines a stem cell fate (Schoof et al., 2000). In addition, the receptor protein kinase CORYNE (CRN), lacking an extracellular domain and the receptor-like protein CLAVATA2 (CLV2), lacking an intracellular kinase domain, form a heteromeric receptor complex that also binds CLV3 and regulates WUS in a pathway independent of CLV1 (Müller et al., 2008; Guo et al., 2010). The common phenotypic read-out of defects in the CLV pathway are marked by an enlarged SAM and supernumerary floral and fruit organs (Clark et al., 1997; Schoof et al., 2000; Durbak and Tax, 2011).

In addition to its well-established role in modulating the maintenance of the SAM, CLV1 was recently identified to play a similar role in the root apical meristem (RAM) (Stahl et al., 2013). The RAM, located at the tip of the root, contains a niche of

stem cells (also called initials), a group of frequently dividing cells surrounding three or four cells with a low mitotic activity, called the quiescent center (QC). The stem cell niche is the source of all cells that arise in layers from the stem cells and form concentrically arranged files of tissue types. CLV1 expression in cells distal to the QC (towards the root tip) overlaps that of a non-LRR receptor kinase, ARABIDOPSIS CRINKLY4 (ACR4), which was previously shown to regulate formative cell divisions in lateral roots (LRs) and to control the integrity of the epidermal cell layer (Gifford et al., 2003; De Smet et al., 2008). Root phenotypes caused by ACR4 mutations, similar to mutations in a CLV3 homolog CLAVATA3/ENDOSPERM SURROUNDING REGION-LIKE (ESR)40 (CLE40), include the expanded expression of a WUS-RELATED HOMEOBOX 5 (WOX5) and supernumerary meristematic columella initials (De Smet et al., 2008; Stahl et al., 2009). Application of exogenous CLE 40 results in transcriptional upregulation of ACR4 but not CLV1, and even though a direct binding between ACR4 and CLE 40 was not demonstrated, CLV1 has the potential to directly bind CLE40 (Guo et al., 2010). These findings further demonstrate the importance of receptor complexes containing different receptors in modulating intricate signaling responses triggered by peptides in the CLV3 family.

Intercellular communication through small regulatory peptides, as described above, emerges as a key component of developmental programs (Fukuda and Higashiyama, 2011; Delay et al., 2013). The regulatory peptides encoded by the CLE (CLAVATA3/ESR-related) family of 32 genes in *Arabidopsis,* have been implicated not only in meristem maintenance but also in a variety of developmental processes such as

LR development, gravitopism and protoxylem differentiation (Qiang et al.; Kiyohara and Sawa, 2012; Qiang et al., 2013). The CLE proteins have a conserved 12–14 amino acid CLE motif at or near the C-terminus (Cock and McCormick, 2001) and are proteolytically processed and further modified (Ni et al., 2011; Tamaki et al., 2013) to generate extracellular signaling molecules. Based on the response triggered by overexpression or exogenous treatment of *Arabidopsis* seedlings, CLE peptides are classified as type A and B CLE peptides. Treatment of roots with type A CLE peptides can induce early termination of meristem activity and cessation of growth (Fiers et al., 2005; Ito et al., 2006; Whitford et al., 2008) while type B CLE peptides can suppress tracheary element differentiation (Ito et al., 2006; Kinoshita et al., 2007; Hirakawa et al., 2008), but do not have an effect on root length. Overexpression and exogenous application experiments are used (Strabala et al., 2006; Kinoshita et al., 2007; Jun et al., 2010) largely due to the absence of visible phenotypes of CLE mutants ((Jun et al., 2010). While functional assays clearly suggest that CLE peptides can signal through RLKs to regulate meristem size and activity in both SAM and RAM, few direct interactions have been demonstrated (Matsubayashi et al., 2002; Hirakawa et al., 2008; Ogawa et al., 2008).

The RECEPTOR-LIKE PROTEIN KINASE 2 (RPK2)/TOADSTOOL 2 (TOAD2) is another RLK that functions downstream of the CLV3 in regulation of SAM size (Kinoshita et al., 2010; Betsuyaku et al., 2011). The mutant phenotypes of TOAD2 resemble the increased size of the SAM observed in CLV1 and CLV2 mutants, and those phenotypes are additive in higher order mutants containing *toad2*, *clv1* and *clv2*

(Kinoshita et al., 2010) suggesting they may act in parallel pathways. In addition, a partial insensitivity to the effect of CLV3-induced short root phenotype was reported for *toad2* mutants, similar to *crn* and *clv2.* Unlike CRN (Müller et al., 2008), the overexpression of RPK2 resembles the phenotypes of CLV3 overexpression and the *wus* mutant phenotype in which the size of the SAM is reduced (Kinoshita et al., 2010). Biochemical studies of CLV pathway component interactions using a transient gene expression system in *N. benthamiana* revealed that CLV1 is potentially forming multiprotein complexes with CLV2/ CRN and with TOAD2 in a CRN-dependent manner (Betsuyaku et al., 2011b), but whether a single large complex forms, or several independent complexes function in parallel remains to be uncovered.

The LRR-RLK TOAD2 was also reported to be a key regulator of other developmental mechanisms that involve cell differentiation and specification of cell fates. Phenotypic analysis of *toad2* mutants revealed enhanced shoot growth and male sterility due to pollen defects caused by abnormal differentiation of microspores and hypertrophy of the tapetum (Mizuno et al., 2007). TOAD2 also genetically interacts with another LRR-RLK, the RECEPTOR-LIKE PROTEIN KINASE 1 (RPK1) to coordinate central domain protoderm patterning during the late globular stage of embryogenesis (Nodine et al., 2007). Double homozygous *rpk1; toad2* mutants are embryo lethal and arrest their development during early stages of embryogenesis and lack the normal radial specification of cell types. Analysis of molecular markers indicates that outer layer specification is lost and an outward expansion of inner markers is detected. However, whether the ground tissue cell fate of outer layers is an indirect consequence of

misspecification of protoderm or directly due to a specific role of these RLKs in the ground tissue is still an unsolved issue. Interestingly, about half of the *rpk1; toad2/+* embryos developing from *rpk1; toad2/+* plants exhibit a similar arrest as the double mutant embryos, while the other half are able to complete their development and reach the mature stage (Nodine et al., 2007). However, further analysis of *rpk1; toad2/+* embryos that do not arrest at the globular stage revealed that additional developmental processes are affected at a lower penetrance in this mutant background, with about 16% of *rpk1; toad2/+* embryos developing only one cotyledon primordia and consequently emerging as seedlings with just one cotyledon (Nodine and Tax, 2008). The single cotyledon phenotype is also characteristic of *rpk1* embryos but occurs at a much lower frequency (4.6%) (Nodine and Tax, 2008). This phenotype indicates that failure to specify the outer layer at early stages perturbs subsequent patterning events. For instance, the accumulation of the phytohormone auxin, one of the key regulators of cotyledon patterning (Moller and Weijers, 2009) is not detected at the site where cotyledon primordia should initiate in the *rpk1; toad2/+* mutants (Nodine and Tax, 2008). The auxin flux, and therefore the establishment of an auxin maxima is regulated by PIN-FORMED (PIN) efflux carrier proteins family through their polar localization in the plasma membrane (Friml, 2010). The auxin efflux carrier PIN-FORMED1 (PIN1) is not expressed In the defective half of the embryos lacking one cotyledon primordial, correlating with absence of auxin maxima. A link between missregulated polarity of PIN1 in the epidermis of *rpk1* and the occurrence of plants with one cotyledon was also recently demonstrated in the *rpk1* embryos with cotyledon defects (Luichtl et al., 2013).

Spatiotemporal regulation of RLK activity contributes to coordination of plant growth and development. The LRR-RLK BRASSINOSTEROID INSENSITIVE1 (BRI1), functions in brassinosteroid hormone perception, and mutations in BRI1 cause a dwarf phenotype due to reduced growth and development (Li and Chory, 1997; Clouse and Sasse, 1998). The growth defects of *bri1* mutants, but not vascular tissue defects, are rescued by expression of a functional BRI1 receptor from the *Arabidopsis thaliana MERISTEM LAYER 1* (*AtmL1)* promoter that has a restricted expression domain within the epidermis. This suggests that signaling in the epidermis is sufficient to restore cell-cell communication with inner layers in order to coordinate the growth of the entire plant. Additional experiments in which BRI1 expression is restricted to specific radial layers shows that signaling in the outer layer has the most significant effect on regulating root meristem size and QC identity (Hacham et al., 2011). These data suggest that signaling mechanisms taking place in the outer layers drive plant growth, although there is also evidence for “inside-out” signaling (Gallagher et al., 2004; Cui et al., 2007; Yadav et al., 2008).

Here we report that signaling mediated by TOAD2 and RPK1 controls RAM activity. *rpk1* mutants display an incompletely penetrant short root phenotype that is enhanced when an additional *toad2* allele is mutated. The short roots display misoriented cell divisions in the RAM that affects primarily cells of the lateral root cap, epidermis and cortex and QC, and a decrease in the number of columella cell tiers. Signaling through RPK1 and TOAD2 in the outer epidermal layer is sufficient to restore normal root growth in the mutant plants, supporting a model of “outside-in” signaling to

coordinate overall root growth. *toad2* mutants are insensitive to the root growth arrest induced by exogenous application of CLE17 and CLE19 peptides. This implies TOAD2 might function as a receptor for these or similar CLE peptides, alone or in a complex with CLV2 and CRN or other components. Transcript and protein levels of RPK1 are reduced upon CLE treatment and the protein reduction requires the presence of functional TOAD2 protein. Finally, the incompletely penetrant phenotype of *rpk1* and the observed CLE responses suggest additional unknown components of this regulation play an important role.

Results

Root growth defects of *rpk1* mutants are dominantly enhanced by *toad2* mutations.

To investigate the role of *RPK1* and *TOAD2* in the regulation of primary root growth in *Arabidopsis*, wild-type (Col-0 ecotype) plants and *rpk1-1, rpk1-5, toad2-1, toad2-3* and *rpk1-1; toad2-1/+* and *rpk1-5; toad2-3/+* mutants were germinated and grown on MS plates and their root growth was measured every 24 hours for six days after germination (DAG). Homozygous *rpk1; toad2* double mutants cannot be recovered due to their embryo lethal phenotype (Nodine, et al 2007), and *toad2-1* and *toad2-3* are typically maintained as heterozygous lines due to their sterility. While roots of *toad2*/+ and *toad2* seedlings grow similarly to wild type (Fig 1 A), *rpk1* mutants exhibit an

incompletely penetrant root growth arrest leading to variable root length by six DAG (Fig 1A). A sub-population of *rpk1-1* (13%, n=130) and *rpk1-5* (16%, n=130) roots slow down their growth abruptly by two to three DAG and their length by six DAG is less than 15% of that of wild type (the short (S) phenotypic class, Fig 1A, B, C). A smaller fraction of roots (4% in *rpk1-1* and 5% in *rpk1-5*) elongate more, to reach between 15 and 70% of the wild type root length, and constitute the medium length (M) phenotypic class (Fig 1A, B, C). An increase in the frequency of S and M root phenotypes is observed in the *rpk1; toad2/+* seedlings independently of the allelic combinations analyzed (22% of *rpk1-1; toad2-1/+* roots are S and 22% are M type, n=45; 24% of *rpk1-5; toad2-3/+* roots are S and 22% are M type, n=45) (Fig 1 C). A significant fraction of *rpk1* and *rpk1; toad2/+* seedlings also elongate their roots similar to wild type (Fig 1) and the single *toad2* mutants (long phenotypic class, L).

Root morphology is altered in the short roots of *rpk1* and *rpk1; toad2/+* mutants

In the RAM, the radially organized layers of epidermis(E), cortex (Co), endodermis (En) and the central stele (St) (Fig 1 D) are maintained by precisely oriented cell divisions of their corresponding initials located in the stem cell niche. To determine specific phenotypic defects in the RAM in the medium and short root phenotypic classes, we analyzed the patterning of different cell types in *rpk1* and *rpk1; toad2/+* mutants. In the S phenotypic class, and to a less extent in the M class, we observed that all plants display abnormally oriented cell division planes, a lack of organization of cells in distinguishable files and irregular size of cells within files,

indicating a loss of patterning in the mutants (arrows, Fig 1D). At five DAG, at least one cortical endodermal initial (CEI) was visible in a mid-section (rarely an undivided daughter is also present, asterisks in Fig 1 D) in 12 out of 16 wild type, 8 out of 18 long *rpk1-1*, and 6 out of 12 *toad2-1* plants. In the mutants of the S phenotypic class, rarely up to 3-4 cortical daughter cells are present (3 out of 18 *rpk1-1* and 2 out of 10 *rpk1-1; toad2-1/+* mutant roots) (asterisks in Fig 1D), forming a single cell file distal to the cell that first undergoes the periclinal division that generates the two separate cortical layers (Co and En).

The lack of typical organization and easily identifiable QC in the stem cell niche does not allow for clear cell type quantification based on positioning. One exception is the markedly reduced number of the columella cell (CC) tiers containing starch-accumulating cells associated with the S and M phenotypes. At five DAG, an average of 3.25±0.4 (n=16) CC tiers were observed in the wild type plants and 3.25±0.5 (n=12) tiers in *toad2-1* but only 2.3±0.4 (n=10) CC tiers in the *rpk1-1; toad2-1/+* mutants (Fig 1D, compare S, M to L). This phenotype correlates with an increased asymmetry of the root tip, as all short roots display an overproliferation of cells in the RAM, mostly in the radial dimension, affecting the epidermis, cortex, the lateral root cap cells (LRC) and cells in the stem cell niche (Fig 1 D, black arrows). In addition to aberrant cell division planes, the LRC and CC appear rounded in shape compared to wild type and also lack a distinguishable organization in clearly defined cell tiers.

Marker analysis indicates that specification of cell types and organization of longitudinal cell files is disrupted in *rpk1-1; toad2-1/+* mutant roots

To determine the nature of root defects and the identity of cells affected in the abnormal patterning of the RAM, the activity of several molecular markers expressing GFP or GUS was analyzed in double mutant *rpk1-1; toad2-1/+* (long, medium and short) roots and compared to wild type. The *DR5rev::GFP* construct comprises a synthetic auxin-responsive promoter (DR5) fused to the GFP reporter gene. The expression of DR5 driven reporters is therefore induced by the plant hormone auxin and has been previously used to indicate the auxin maxima in *Arabidopsis* (Friml et al., 2003). The basipetal transport of auxin from the columella through the lateral root cap cells towards the epidermis creates a gradient of the growth hormone that stimulates faster cell growth at a lower concentration rather than a high concentration (Swarup et al., 2005). Here, we analyzed whether the root apical auxin maxima would be altered in *rpk1-1; toad2-1/+* mutants by comparing *DR5rev::GFP* expression in the root apex of wild type and mutant seedlings. The short phenotypic class of *rpk1-1; toad2-1/+* mutants (n=12) express the *DR5rev::GFP* marker in the QC and CSC similar to wild type (n=15), but a clear expression gradient cannot be detected; often columella cells in the lowest tier contain the highest GFP signal (Fig 2 A-C). This aberrant distribution is more severely disrupted in the short phenotypic class than in the medium length class (n=6). This might indicate a defect in auxin transport through the misshapen columella cells that lack a clearly delineated apical and basal membrane that affects the distribution of auxin and auxin carrier proteins (Swarup, et al, 2005).

To further analyze the root growth defects of mutant seedlings, we evaluated the localization of the auxin carrier protein, PIN1 which, in the wild type localizes mainly to

the basal membrane of the vascular cells, but weak PIN1 signals can be also detected in the En and the Co (Blilou et al., 2005). *PIN1p::PIN1-GFP* expression in the wild type was detected in the plasma membrane of vascular, En and Co cells (Fig 2 D). In contrast, *rpk1-1; toad2-1/+* mutants show mainly cytoplasmic localization of the PIN1 protein in the vasculature and very weak expression in the endodermis and cortex (Fig 2 D´-F´). This distribution is likely affecting the maintenance of instructive auxin gradients that are required for proper root growth. We did not detect an outward expansion of the expression pattern of these markers, as seen in the Toadstool phenotypic class of embryos (Nodine et al, 2007), indicating that patterning and cell fate specification occurred normally in the embryos that survived past the globular stage and that patterning is largely maintained postembryonically. The defects that we can detect in the short roots are more subtle, affecting sub-cellular functions, rather than broad cell layer specification.

To analyze the identity of cell types in the RAM, the expression of *SCRp::GFP-NLS* and *WOX5p::GFP-NLS* markers was compared in the wild type and *rpk1-1; toad2-1/+* roots. The SCARECROW (SCR) transcription factor of the GRAS family is specifically expressed in the CEIs, the QC and the endodermal cells. The nuclear localized GFP driven by the *SCR* promoter was similar in wild type and the mutant roots (n=47), indicating that the respective cells are present in the mutant plants (Fig 2 G-I). In the short root class of *rpk1-1; toad2-1/+* mutants (n=20), the GFP expression is not detected in all cells and it also is not detected in a linear file of cells (arrowheads, Fig 2

H,I), indicating the patterning and specification of some endodermal cells is aberrant in the double mutants.

The WUS-RELATED HOMEOBOX 5 (WOX5) homeodomain transcription factor acts downstream of SCR, and functions in the QC to maintain columella stem cell signaling (Sarkar et al., 2007) and is often used as a marker for QC cell identity. In the wild type roots, *WOX5p::GFP-NLS* is expressed in the QC cells and occasionally in one or a few vascular initials, with an average of 4.9±0.9 (n=18) cells expressing the GFP in their nuclei. In contrast, *WOX5p::GFP-NLS* expression in the *rpk1-1; toad2-1/+* mutants is often detected in more cells, located mainly in the QC and in the cells above the putative QC cells (7.4±1.4, n=29, t-test $p < 0.001$) (Fig 2. J-L). This indicates that some aspects of QC cell fate are maintained in the cells generated through cell divisions of the QC and displaced proximally in the region of vascular initials. To further characterize the specification of cells in the stem cell niche, we analyzed the expression of the QC specific markers *QC184::GUS* and *QC25::GUS.* These markers are expressed only in the QC cells of wild type plants (n=20) (arrows in Fig 2M, and (Sabatini et al., 2003). In the *rpk1-1; toad2-1/+* roots, GUS activity is detected not only in the QC but also in the initials surrounding the QC, including the vascular initials (for QC25, 12/12 plants) and columella stem cells (QC184, 14/14 plants, QC 25, 3/12 plants), indicating that select subsets of transcriptional programs are altered in the initials surrounding the QC in the double mutants (Fig 2 M).

RPK1 and *TOAD2* have partially overlapping expression domains in the Arabidopsis roots

RPK1 and *TOAD2* were previously reported to function redundantly in early stages of *Arabidopsis* embryogenesis, where their partially overlapping expression was detected using GFP translational fusions (Nodine, 2007). Because we detected defects in root growth in *rpk1* mutants and an increased frequency of defective roots in the *rpk1, toad2/+* mutant seedlings, we tested the expression of these genes postembryonically by analyzing *RPK1p::YFP-NLS* and *TOAD2p::YFP-NLS* transcriptional fusions and *RPK1p::RPK1-GFP* and *TOAD2p::TOAD2-GFP* translational fusions in wild type plants from two to seven days after germination (DAG). While fluorescent signals from transcriptional and translational fusions of both RLKs were detected throughout the roots, a more intense signal was detected in the RAM (Fig 3). *RPK1* shows strong expression in the E, Co and St as well as in the QC and initial cells of the RAM (Fig 3 A-D). Reduced expression is also detected outside of the RAM and is not observed in the root vasculature or in the mature root cap cells. *TOAD2* has a similar expression pattern as *RPK1* in the root tip with the exception of mature LRC cells where *TOAD2* is expressed more strongly (Fig 3 E-H). Beyond the RAM, *TOAD2* is also strongly expressed in St cells throughout the entire root. Both fusion proteins appear to be plasma membrane-localized based on their fluorescent signal overlapping with the PI staining outlining the cells. While for the RPK1 transcriptional and translational fusions the expression domains are largely overlapping, in the case of TOAD2, we observed that *TOAD2p::YFP-NLS* expression is detected to a very low level in the inner cell

layers compared to the LRC and RAM epidermis. We hypothesized this might be due to specific post transcriptional stabilizing processes that allow for the endogenous protein to be maintained in all cells, while the TOAD2 mRNA levels are very low in cells other than LRC and E.

The function of *RPK1* and *TOAD2* in the outer radial layers of the root contribute to correct patterning of roots

RPK1 and *TOAD2* have overlapping expression domains in the root, but functionally, only *rpk1* mutants present a low penetrant short root phenotype that is enhanced in a heterozygous *toad2* genotype, and is not observed in *toad2* single mutants. We asked whether the expression domain of the two kinases is functionally overlapping and whether the specific localization is important for gene function. By swapping the promoters of the two genes, we created *TOAD2p::RPK1-GFP* and *RPK1p::TOAD2-GFP* transgenes, transformed them into r*pk1-1; toad2-1/+* and wild type *Arabidopsis* plants and analyzed their expression and effect on the short root phenotype (Fig 4 A). r*pk1-1; toad2-1/+* plants expressing RPK1 and TOAD2 transgenes show a reduction in the frequency of short roots compared with the r*pk1-1; toad2-1/+* plants (Fig 4 B, compare with Fig 1). This indicates that in r*pk1-1; toad2-1/+* plants, the *TOAD2p::RPK1-GFP* transgene reintroduced a functional RPK1 kinase and that expression from the TOAD2 promoter is sufficient for normal RPK1activity. The r*pk1-1; toad2-1/+; RPK1p::TOAD2* plants also have a reduced frequency of short roots, more similar to single *rpk1-1* mutants, indicating that TOAD2 receptor kinase expressed from the RPK1 promoter is functional and rescues the short root phenotype (Fig 4 A, B).

We then asked whether these kinases function throughout the radial layers, or within specific subdomains, some of which might be more important than others in controlling the short root phenotype. We expressed *RPK1-GFP* and *TOAD2-GFP* under the control of promoters with specific transcriptional activity in restricted radial layers of the root: *AtmL1p,* restricted to the epidermis*, SCRp* (SCARECROW) in the endodermis, CEI, and the QC*,* and *PNHp* (PINHEAD), in the St and the QC*.* Using the GFP tag, we detected the expression of *RPK1* and *TOAD2* and the fluorescent protein localized at the plasma membrane in the corresponding radial layers in the mutant background, similar to the wild type (Fig 4 A). When *RPK1* was expressed from the promoters specific for inner cells (*SCR, PNH*), the short root phenotype was not rescued (Fig 4 A, B), indicating that RPK1 activity in the endodermis, the QC, CEIs or in the stele is not sufficient for suppressing the short root phenotype. Expression of *RPK1* from the *AtmL1* promoter, fully rescued the short root phenotype indicating that RPK1 activity in the outer layer is sufficient to restore a normal root length. Similar to RPK1, TOAD2 localization and activity in the epidermis was sufficient to restore the frequency of short roots to the level found in *rpk1* single mutants (Fig 4 B). However, the inner layer expression of TOAD2 in the stele results in fewer short roots while the endodermal localization does not, indicating a more spatially expanded activity of TOAD2 on root growth.

toad2 mutants are insensitive to *in vitro* treatment with CLE peptide

Recent functional studies of plant meristems indicate that small peptides from the CLE family play an important role in signaling through receptor kinases in the RAM, the

SAM and in vascular meristem development (reviewed in (Betsuyaku et al., 2011a). In *Arabidopsis*, at least 18 of the 32 CLE genes are transcribed in specific or overlapping regions of the root (Jun, 2010). Wild-type roots overexpressing CLE genes or treated with exogenous CLE peptides (CLV3, CLE19, and CLE40) are shorter and have a reduced number of meristematic cells compared to untreated roots (Fiers et al., 2005). To verify the presence of root-expressed CLE genes, we generated transcriptional fusions with YFP and a nuclear localization signal for two genes: *CLE17p::YFP-NLS* and *CLE19p::YFP-NLS*, transformed them in wild type plants and analyzed their expression in four independent T3 generation lines (Fig 5). CLE17 is expressed in the RAM, in the lateral root cap cells and in the epidermis (Fig 5 A-C) and CLE19 has a more restricted expression domain in the lateral root cap cells (Fig 5 D-F). In the elongation and differentiation zone, both CLE genes are expressed mainly in the epidermal and cortical cells (Fig 5, B, E). The RAM expression of *CLE17* and *CLE19* therefore partially overlap the outer layer expression domains of *RPK1* and *TOAD2*.

Due to phenotypic similarities betweeen *rpk1; toad2/+* mutant roots and the CLE treated wild-type roots, we tested the effect of CLE17 and CLE19 peptides on plants lacking functional copies of RPK1 and TOAD2. Previously, the receptor-like protein CLV2 (Guo et al., 2010) and the receptor-like cytoplasmic kinase CRN (Miwa et al., 2008) were shown to be required for transmission of the CLE signals and therefore, in this study, we used plants carrying the mutant *crn-1* and *clv2-8* alleles as positive controls. In preliminary experiments, the root growth inhibitory effect of different amounts of peptide (0.5, 1.0 and 10.0μM) was tested on wild type plants. While the

plants responded to all treatments, the 10 µM peptide concentration triggered the fastest response within two to three days after seedling transfer, similar to reports by others (Fiers, 2005) and this concentration was therefore selected for the root growth assay.

We generated the peptides corresponding to the 12 amino acid conserved CLE motif of two type A CLE peptides, CLE17 and CLE19, one type B CLE peptide, CLE41 and an additional peptide, CLE19-MOD, derived from the CLE19 sequence in which all proline residues were replaced by alanine, to render the peptide non-functional (Song et al., 2012) (Fig 6 C). Progeny of wild type, *crn-1*, *clv2-8*, *rpk1-1, rpk1-5, toad2-1/+, toad2-3/+* and *rpk1-1; toad2-1/+* and *rpk1-5; toad2-3/+* plants were grown for three days on MS plates and then transferred and monitored for root growth on control or CLE containing MS media (Fig 6 A). Wild-type seedlings, as well as *toad2-1/+, toad2-3/+*, *rpk1-5* and *rpk1-1* seedlings show sensitivity to CLE19 and CLE17 peptide treatment and their root growth ceases within two to three days after transfer to test plates (Fig 6 A, B) and significant differences in their root length are observed. In contrast, the root length of homozygous *toad2-1, toad2-3, crn-1*, and *clv2-8* seedlings grown on CLE17 and CLE19 peptide-containing MS media is not significantly different when compared to plants grown on control plates after the five-day treatment period, demonstrating insensitivity to CLE peptide treatment (Fig 6 A, B). In addition, all plant genotypes tested on CLE41, CLE19-MOD, and the no-peptide control plates do not show altered root growth phenotypes when compared to wild type seedlings, indicating that the CLE41 and CLE19-MOD have no effect on root length.

CLE17 treatment causes a short root phenotype by negatively regulating the frequency of cell divisions in the proximal meristem

To analyze the mechanisms leading to cessation of root growth in response to CLE treatment, progeny of heterozygous *toad2-1/+, toad2-3/+*, and homozygous *rpk1-5, rpk1-1, crn-1*, and *clv2-8* and control wild-type seedlings were grown on plates containing added peptides, fixed and stained using a modified pseudo Schiff propidium iodide (mPS-PI) method and visualized using confocal microscopy. The root growth and cell number of different RAM domains were quantified in these genotypic backgrounds and compared to wild type when grown in the presence of 10.0 μM CLE17, CLE19, CLE41, CLE19-MOD peptides and on control plates.

We found that the roots of *rpk1-5, rpk1-1* and wild type respond to CLE17 and CLE19 treatment through a reduction of the overall length of their RAM, and no effect was observed on roots grown in the presence of CLE41, CLE19-MOD and on control plates (Fig 7 A, B). The size of RAM is not decreased in the *clv2-8, crn-1* or *toad2* homozygous mutants after five days of treatment; therefore, *toad2-1* and *toad2-3,* similar to *crn-1* and *clv2-8* mutants, are insensitive to the exogenously applied CLE peptide effect of reducing root meristem growth (Fig 7 A, B).

To further analyze the cause of the short root meristems, we quantified the number of cells in longitudinal E and Co cell files. The average number of E and Co cells observed in mid-longitudinal optical sections of wild type, *rpk1-1*, and *rpk1-5* roots was found to be significantly less that the number of cells in *crn-1*, *clv2-8*, *toad2-1* or

toad2-3 ($p<0.001$, n=12). Similar results are observed with CLE19 treated roots (data not shown). In the mPS-PI stained roots, recently dividing cells are marked by a very thin cell wall formed between the two daughter cells that have not yet elongated and therefore appear half the length of non-dividing cells (Fig 7 A). This series of anticlinal (perpendicular to the long axis of the root) cell divisions in the distal meristem generate more cells and increases the root length, in a process called transit-amplifying cell divisions. Upon analysis of dividing cells in longitudinal files, we found that the short roots of *rpk1-5, rpk1-1* and wild type present a decreased frequency of transit-amplifying cell divisions along the epidermal and cortical cell files after treatment with CLE17 peptide (Fig 7 C, D) resulting in fewer cells comprising the RAM portion of these files. This effect is not observed in the long roots of *toad2-1, toad2-3, crn-1* and *clv2-8* upon CLE17 treatment, and the frequency of cell divisions is similar to that of untreated controls (Fig 7 C, D).

An increased number of presumptive QC cells is also detected, associated with increased cell divisions, both anticlinal and periclinal, noted in the cells at the position of QC ($p<0.05$ between treated and non-treated controls) after CLE17 and CLE19 peptide treatment. More importantly, division of QC cells results in two layers of cells at the position of QC. In most of the wild-type roots, a single QC cell layer is visible in an apical-basal optical section and this layer is contiguous with the cells of CEI or Co and En. However, upon CLE peptide treatment cells at the position of QC divide, generating smaller cells that occupy the same position in the stem cell niche (Fig 8 A, B). This response is stronger in *toad2*, *clv2* and *crn* mutants and it was not detected in

rpk1 mutants indicating that the effect of CLE peptide to increase the frequency of QC cell division is negatively regulated by TOAD2, CLV2 and CRN and positively regulated by RPK1 (Fig 8 A, B).

A similar increased frequency of cell division was observed in the CSCs of wild type. The CSCs form a single cell layer contiguous with the LRC/E initial in untreated plants. After CLE peptide treatment, often two complete or incomplete layers of cells was observed at the position of CSCs and a very few of the distally located cells in the CSCs position differentiate and accumulate starch granules (Fig 8 A, B). The CSCs response of *toad2* and *rpk1* to CLE treatment was also contrasting. While treated *toad2* roots (similar to *clv2* and *crn*) have mostly two layers of cells at the position of CSCs, these cells also accumulate starch granules indicating their differentiation. In treated *rpk1* mutants, cells at the position of CSCs form mostly one layer and in the cases of two incomplete layers, the cells do not accumulate starch, similarly to wild type (Fig 8 A, B). This indicates a common mechanism by which CLE peptides act to increase cell division in the stem cell niche, but the response of *toad2* and *rpk1* mutants is rather opposite.

To understand the effect of CLE peptide treatment on other cells of the stem cell niche, we analyzed the CEI cells and their daughters in mid-longitudinal optical sections (Fig 8 C). We found an increased number of CEIs and their daughters present in all treated roots. These results suggest that one effect of CLE treatment is a delay in the CEI divisions into the two separate types of cortex stem cells (En and Co stem cells) as well as a delay in the occurrence of periclinal divisions of their daughters, generating the

separated initial cells in the respective files (Fig 8 C). At eight to nine DAG the majority of wild type roots have already divided their CEI into En and Co stem cells. We detected that in all genotypes tested, less than 50% of the roots still have one or two CEIs in a medial optical section (n>12). After CLE17 and CLE19 treatment, the number of CEIs detected, as well as their daughters that do not undergo a periclinal (parallel to the long axis) division, often forming a single cortical file of cell extending from the CEI, is increased. For instance, 60% of wild type, 100% of *crn-1*, 80% *clv2-8*, 90% of *rpk1* and 100% *of toad2* (n>12) roots have one or two visible CEIs and 30% of wild type, 70% of *crn-1*, 80% of *clv2-8*, 40% of *rpk1* and 60% of *toad2* have at least one undivided daughter, but the number of non-separated CEI daughters varies from one to eight.

***RPK1* is downregulated in CLE treated roots and this process requires the presence of functional TOAD2**

All *toad2* roots respond to CLE treatment similarly, by continuous growth on the CLE plates (n=142) while the *rpk1* mutants, similarly to wild type, cease their root growth; very rarely we observed *rpk1* mutant roots that elongated on CLE plates (4 out of 224). To unravel the potential genetic interactions between RPK1 and TOAD2 in root development and the regulation of the CLE-mediated signaling pathway in RAM growth, we analyzed the transcriptional and translational regulation of these receptor kinases upon CLE treatment. The expression of the *RPK1p::YFP-NLS* and *TOAD2p::YFP-NLS* transcriptional fusions was analyzed in wild type plants treated with CLE17 and CLE19 peptides (Fig 9 A, D). The expression of *RPK1p::YFP-NLS* marker is significantly reduced in the CLE17 (Fig 9 A) and CLE19 (not shown) treated plants. We measured

the YFP signal intensities in treated and untreated roots using ImageJ software and found that in 80% of treated plants (n=30) the YFP signal intensity is reduced to the background level and in 20% of the plants the signal is reduced between six to ten fold compared to untreated plants (Fig 9 A). Interestingly, the reduction in fluorescence intensity is specific to the main root RAM, and the fluorescence intensity is not changed in the lateral roots of treated plants compared to untreated controls (Fig 9 A). In contrast, the fluorescence generated by *TOAD2p::YFP-NLS* activation is only partially reduced (two to four fold) in the roots treated with the CLE17 peptide (n=24), while the signal from the fluorescence in the emerged lateral roots is not different compared to control plants (Fig 9 D).

Analysis of *RPK1p::RPK1-GFP* and *TOAD2p::TOAD2-GFP* translational fusions in the wild type plants treated with CLE17 and CLE19 peptides indicates a similar pattern. The signal from RPK1-GFP protein localized at the plasma membrane in the CLE17 treated plants is greatly reduced in the RAM but not in the lateral root primordia (Fig 9 B, B´), while the TOAD2-GFP signal is still detected in the plasma membrane of RAM cells of treated plants (Fig 9 E). The expression of *RPK1p::RPK1-GFP* in *toad2-1* plants is unchanged upon CLE17 treatment (Fig 9 C, C´), indicating that CLE17-induced downregulation of *RPK1* is not activated that in the *toad2-1* mutant background. Also, RPK1-GFP is normally localized at the plasma membrane and in numerous intracellular vesicles (Fig 9 C, C´) and in CLE-treated roots we noted a residual fluorescent signal from internal vesicles, but not at the plasma membrane (Fig 9, B, B´) We also analyzed the expression of *TOAD2p::TOAD2-GFP* in *rpk1-1* mutant plants and did not detect a

change in the fluorescence intensities of membrane localized TOAD2-GFP after CLE17 treatment (Fig 9 F).

Transgenic homozygous plants expressing *TOAD2p::TOAD2-GFP* display a slower root growth over a period from 3 to 8 days after germination compared to wild-type plants or plants expressing *RPK1p::RPK1-GFP* (Fig 10), indicating that the presence of more TOAD2 gene copies has an effect on slowing root growth, similar to exogenous CLE treatment. When the *TOAD2p::TOAD2-GFP* expressing plants are treated with CLE17 or CLE19, their root growth ceases at least 24 h sooner than the control plants, and their overall root length after five days of treatment is smaller compared to wild type plants (Fig 10 B and data not shown). However, homozygous *rpk1-1* plants containing the *TOAD2p::TOAD2-GFP* do not elongate differently than wild type, when grown on control, CLE17 or 19 plates (Fig 10 B), indicating that RPK1 functions as an important regulatory component of TOAD2-mediated response to both the endogenous and exogenously applied CLE peptides. Plants that express the *RPK1p::RPK1-GFP* transgene have similar root growth in the wild type or *toad2-1* mutant background, and their response to CLE treatment is similar to that observed in wild type plants and *toad2-1* mutants, respectively (Fig and Fig). Interestingly, although the root length of *RPK1p::RPK1-GFP* expressing plants is not significantly increased (at least until eight days post-germination), the size and patterning of their distal meristem is different than in control plants. Wild-type plants at this stage have 4.5±0.5 columella cell tiers, while *RPK1p::RPK1-GFP* have 6.0±0.0 and *toad2-1; RPK1p::RPK1-GFP*

have 6.7±0.6 (n=20, each) columella tiers. In addition, the cell alignment and the columella tiers appear disorganized in the distal meristem (Fig 10A).

Transcription levels of SCR and WOX5 markers does not change upon CLE treatment

To test that downregulation of RPK1 gene expression after CLE treatment is specific to the RPK1 gene and not the result of a more general transcriptional silencing occurring in the RAM, we analyzed the expression of the molecular markers SCRp::GFP, SCR::GFP-NLS and WOX5::GFP-NLS, after five days of growth in the presence of CLE17 peptide.

The GFP signal from *SCRp::GFP* accumulates in the cytoplasm of QC, CEI and endodermal cells of untreated plants (Fig 11 A). The expression of SCR is also detected in the endodermal cells of all wild type (n=20) and *toad2-1* (n=12) plants at similar levels as in the wild type plants, but is often reduced in the QC and CEIs of CLE treated plants (arrowheads in Fig 11). Using a nuclear localized version of GFP, under the control of the same SCR promoter, we detected a GFP signal from QC cells (Fig 11 A), indicating that transcription from the SCR promoter occurs in the QC, but the cytoplasmic GFP is probably unstable in the QC. This might indicate that some intrinsic characteristics of QC cells are not maintained upon CLE treatment.

WOX5 expression, described above, is also detected in the CLE17 treated plants similar to the control plants. In addition, the number of cells expressing WOX5-GFP increases in the treated plants (6.2±1.3, n=18) compared to the untreated controls

(4.5±1.2, n=12). Importantly, the cells expressing the WOX5 marker are localized above the putative QC cells (arrows in Fig 11, lower panel) in 67% of the analyzed plants(n=18 plants), and 33% of the plants show WOX5 expression in both, QC and vascular initial cells. These results indicate that the mechanisms restricting the WOX5-dependent QC cell fate are disrupted in the CLE17 treated roots, leading to misexpression of these markers in a larger group of cells, resulting from division of QC.

Discussion

Using analysis of mutants, transgene expression and exogenous CLE treatment in *Arabidopsis,* we uncovered a role for the RLKs *RPK1* and *TOAD2* in the control of root growth and meristem patterning. Previously, TOAD2 was shown to function redundantly with RPK1 to maintain the protoderm cell fate in *Arabidopsis* embryos (Nodine et al., 2007); the loss of the regulatory role of protoderm in the central domain of embryos leads to more defects, including a failure to specify cotyledon primordia (Nodine and Tax, 2008). Genetic analyses also revealed TOAD2 has a role in tapetum specification in the anther (Mizuno et al., 2007) and contributes to shoot apical homeostasis by transmitting the CLV3 signal (Kinoshita et al., 2010), possibly via its CRN-mediated interaction with CLV1 (Betsuyaku et al., 2011b). RPK1 was also shown to integrate environmental signals and to control ABA-dependent cell proliferation (Osakabe et al., 2005; Osakabe et al., 2010; Lee et al., 2011). Here we show that RPK1 and TOAD2 have a role in the maintenance of root growth by controlling cell

proliferation in the RAM; the main defects of mutant roots are arrested growth due to a short meristem, and aberrant cell divisions that result in supernumerary and disorganized radial cell layers. The penetrance of these *rpk1* mutant phenotypes is enhanced in heterozygous *toad2* mutants indicating a dose-dependent requirement for both genes in the pathway controlling root meristem maintenance.

Root meristem size is determined by a precise balance between cell proliferation and differentiation. The formation of auxin maxima in the RAM is an important signaling mechanism that controls cell division and differentiation and therefore instructs morphogenesis and depends on the spatial distribution of PIN proteins (Grieneisen et al., 2007; Hacham et al., 2011). The interplay of different mechanisms that control root meristem size is supported by examples of BR signaling affecting the post-transcriptional regulation of PIN protein localization; this implies that BR-mediated root meristem growth is controlled, to some extent, by auxin reallocation (Hacham et al., 2012). Here we show that root proliferation defects of *rpk1; toad2/+* mutants correlate with a disrupted auxin gradient in the root proximal meristem, and with a reduction in the cellular distribution of PIN1 protein. If cortical and endodermal cell specification and function is disrupted in *rpk1; toad2/+* as a result of aberrant signaling, the abnormal distribution of PIN protein in these cells could in turn, perturb the auxin flow and therefore the cell division patterns and differentiation.

Another level of control of root growth is represented by the patterning transcription factors. Mutations in SCR affect radial root patterning and cause a short root phenotype (Scheres et al., 1995) and cause ectopic cell divisions of the QC,

leading to disorganized QC and LRC (Wysocka-Diller et al., 2000). The WOX5 transcription factor specifies some aspects of QC cell fate that are under the control of the SCR gene; in *scr* mutants, the expression of WOX5 is reduced or undetectable (Sarkar et al., 2007). Due to changes in cell morphology in *rpk1; toad2/+* mutants, the QC cells are not easily distinguishable and therefore we employed the analysis of specific markers for the QC and the endodermis. The RPK1/TOAD2 pathway does not appear to function upstream of SCR, as transcription of SCR was detected in the En, CEI and QC cells of *rpk1-1; toad2/+* mutants, albeit irregularly absent in some cells. In wild type plants the expression of the WOX5 marker is detected in the QC cells and occasionally with a lower intensity in the vascular initials. In the *rpk1-1; toad2/+* plants we did not detect ectopic WOX5 expression in cells other than the ones observed in wild type; the expression of WOX5 indicates an increased division of QC cells and generation of small cells that reside at the center of the stem cell niche and continue to express the marker. A similar pattern was observed with the QC184 marker that acts downstream of WOX5 (Sarkar et al., 2007) and QC25, indicating that cells around the presumptive QC still maintain some aspects of QC specification.

The role of epidermis as a key regulator of inner cell fates was explored in the process of BR-mediated root growth (Hacham et al., 2011). Epidermis- restricted expression of BRI1 was shown to be sufficient to promote root meristem growth, providing evidence for signaling from the outer layers to the inner meristem. Both RPK1 and TOAD2 protein localize at the plasma membrane of epidermal cells but are also expressed in inner cells throughout the RAM. Due to the prevalence of root proliferation

defects in the short roots of *rpk1; toad2/+* in the LRC, E and Co we asked whether epidermal function of these kinases is sufficient for signaling for proper meristem activity. Indeed, using the short root phenotype as a readout of RPK1 and TOAD2 function, we were able to conclude that a signal from epidermis is sufficient for the RPK1/TOAD2 pathway to restore the defects seen in the mutants. In addition, TOAD2 signaling in the inner layer may be functionally equivalent to the signaling in the epidermis.. More analysis is needed for partial overlapping root subdomains (for instance, *SCR* and *PNH* together) for a more clear answer to the inner sub-domain expression of TOAD2. These results, however, support a model in which epidermis signaling is sufficient to promote growth of the inner cell layers and ascribe a function to RPK1 and TOAD2 in signaling from the epidermis to maintain a normally developing root meristem.

If these two receptor kinases function in signaling from the epidermis, what are the ligands for RPK1 and TOAD2? How is the signal transmitted from cell to cell? Does their activity follow a ligand sequestration model (Stahl and Simon, 2009) or a ligand-induced trafficking and degradation of receptors model (Nimchuk et al., 2011)? Previous reports of CLV3 signal perception by TOAD2 prompted us to search for candidate ligands among root-specific CLE genes that have an expression pattern similar or overlapping with that of the receptors. CLE17 and CLE19, among others (Jun et al, 2010) are expressed in the RAM, so we tested the effect of the exogenously applied synthetic peptides corresponding to the CLE motif of these two genes on mutant roots. As previously reported (Fiers et al, 2005), treatment with type A CLE peptides caused a

short root meristem phenotype of wild type plants. We uncovered that *rpk1* as well as *rpk1; toad2/+* mutants are also sensitive to CLE treatment, whereas *toad2* mutants similar to *clv2-8* and *crn-1,* are insensitive to CLE19 and 17 treatment. We analyzed the effects of CLE treatment at a cell-type specific level, in both sensitive and insensitive plants, and found a common set of CLE-induced responses, as well as responses specific to the insensitive plants only. As a general response, found in all genotypes, we observed an increase in the number of cells in the stem cell niche, due to increased number of cell divisions in the QC and CSCs. In addition, we concluded that TOAD2 (similar to CLV2 and CRN) negatively regulate CLE-mediated cell division of QC and CSCs and negatively regulate differentiation of CSCs daughters. An opposite effect was observed by analyzing rpk1 mutants, which led us to conclude that RPK1 acts as a negative regulator of QC and CSCs division and has a positive role in differentiation of CSCs daughters.

The maintenance of CEI cells as well as their daughters, and a delay in their periclinal division was positively affected by CLE 17 and CLE19, regardless of the phenotype tested indicating the control of stem cell niche by RPK1 and TOAD2 was not primarily acting on the CEI cells.

A specific response to CLE treatment was the reduced proliferative activity of cells in the proximal meristem, resulting in fewer cells comprising the longitudinal files. In conclusion, despite the increased frequency of cell division of QC cells and the increased stem cell niche size of CLE treated plants, this mechanism is not sufficient to overcome the reduction in the number of cells in the proximal meristem that accounts

for shorter roots. Roots of *toad2, clv2-8*, and *crn-1* mutants are insensitive to the CLE17 and CLE19-mediated reduction of transit-amplifying cell divisions and present longer roots indicating a common mechanism by which CLE peptides act to control root growth. This implicates that TOAD2 might function as a CLE receptor in a multi-protein receptor complex, containing CLV2 and CRN, which perceives the CLE signals, or the individual contribution of TOAD2, CLV2 and CRN to root growth converges on some unknown downstream general mechanism controlling root cell division and growth.

As RPK1 does not appear to function directly in CLE perception, we tested the regulation of both RPK1 and TOAD2 by exogenous CLE treatment. A strong downregulation of RPK1 transcriptional activity as well as RPK1-GFP protein accumulation at the plasma membrane was observed five days after CLE treatment. Normally, we observe RPK1-GFP localization in the plasma membrane and also in structures we believe are part of intracellular vesicular membrane system, but after CLE treatment, the residual protein detected was localized mostly to the inner membranes. A slight reduction in TOAD2 protein levels was also detected, but in all plants the protein was still present in the plasma membrane after treatment. In the absence of TOAD2, however, the level of RPK1 in the plasma membrane of treated plants remains unchanged. Our conclusion is that TOAD2 mediates this response by triggering RPK1 turnover at the transcript and protein level. The shorter root and increased sensitivity to CLE treatment of plants expressing additional TOAD2 phenocopy the CLE treatment, providing further support for a role for TOAD2 in perceiving the CLE signal. A similar phenotype of shorter roots and increased sensitivity to CLE peptides was reported for

plants overexpressing TOAD2 under the control of the cauliflower mosaic virus 35S promoter (Kinoshita et al., 2010).

The response to CLE treatment by downregulating gene expression is not a general response as other genes (SCR, WOX5) are still expressed at similar levels to untreated plants. The WOX5 misexpression in cells at the position of vascular initials and absence from the putative QC cells might indicate a proximal shift in the QC activity. If QC cells lose their activity as a result of CLE action, it is possible that new QC cells are specified proximally from the presumptive QC. This observation also correlates with the increased cell division rates of cells at the center of the stem cell niche.

Our findings suggest that RPK1 and TOAD2 function to balance positive and negative regulation of root meristem growth, and the gene dosage or the level of activation by exogenous peptides is very important in tipping the balance. Our model indicates that CLE peptides are perceived by TOAD2 (or a complex containing TOAD2) (Fig 12). Upon ligand binding, a signaling cascade is initiated and results in downregulation of RPK1 transcription and protein internalization. In the absence of RPK1, growth signals are no longer transmitted, resulting in short roots, but this is not a all-or-none process, as additional unidentified components als play a similar, redundant role. In *rpk1* mutants, upon TOAD2 stimulation by exogenous CLE, the *rpk1* pathway is already interrupted and therefore short roots are observed (similar to the phenotype of *rpk1* mutants). Additional components of the RPK1 pathway, that might act in parallel and account for the low penetrance of short root phenotype in RPK1, might also be downregulated upon TOAD2-ligand interaction (Fig 12).

Further molecular and biochemical studies are needed to validate the potential binding of CLE to the extracellular domain of TOAD2 and the mechanisms leading to either sequestration of ligand molecules or ligand-receptor internalization model of action. Processes reminiscent of ligand-induced receptor endocytosis in animals were shown to occur in plants. For instance, the LRR RLK FLAGELLIN-SENSING 2 (FLS2) that functions in plant innate immunity was shown to trigger an immune response after ligand binding and internalization in endocytic vesicles (Robatzek et al., 2006). Endocytosis of receptors and signaling from internal membranes was also described for the steroid receptor BRI1 where endocytic trafficking and signaling appear to be constitutive, and does not changes with changes in ligand levels (Geldner et al., 2007). Contrary to sequestration models, signaling in the CLV1 pathway were also shown to be dependent on internalization of the receptor regardless of the expanded diffusion of the CLV3 ligand (Nimchuk et al., 2011). In the case of ACR4, its internalization is dependent on its functionality, suggesting this as a mechanism of signaling regulation (Gifford et al., 2005). Is TOAD2 sequestering ligands that are expressed in the outer layers, such that their movement towards the stem cell niche is limited? Is TOAD2 binding CLE ligands and possibly being internalized, alongside RPK1? Future molecular dissection of this pathway is necessary to reveal the details of RPK1/TOAD2 interplay in the CLE mediated root growth.

Thus far it appears that several RLKs and CLE ligands function in sometimes overlapping processes mediating root primary and secondary meristem growth. ACR4 and CLV1 regulate distal root meristem maintenance (Stahl et al., 2013) by responding

to CLE40 signaling. The LRR-RLK BARELY ANY MERISTEM (BAM3) and its putative ligand, CLE45 control the development of the protophloem, a secondary meristem (Depuydt et al., 2013). The CLE41/44 signal perceived by the LRR-RLK PHLOEM INTERCALATED WITH XYLEM (PXY) in the procambial cells, inhibits their differentiation and promotes their proliferation (Hirakawa et al., 2010).

RPK1 and TOAD2 are now also implicated in controlling the balance between proliferation and differentiation of root cell types. The CLE treatment affects only the main root and not the lateral root growth even though TOAD2 and RPK1 are also expressed in the lateral roots; exploring the bases of differential regulation of main and lateral roots might shed some light on the CLE regulation of root growth.

Materials and Methods

Plant material

The *Arabidopsis* seeds used in this study were wild-type *Columbia-0* (*Col-0) toad2-1/+, rpk1-1, rpk1-5 (Nodine et al., 2007) toad2-3/+ (*a new loss-of-function insertion mutant in the fourth LRR, generated by the Wisconsin *Arabidopsis* Knockout Facility,(Sussman et al., 2000), backcrossed five times into *Col-0*), *rpk1-1; toad2-1/+, rpk1-5; toad2-3/+* and *crn-1* and *clv2-8* (Durbak and Tax, 2011). The seeds were

surface-sterilized with a solution of 70 % ethanol and 0.1% Triton X-100 for 20 minutes, washed three times in 95% ethanol, air dried and plated at a distance of aproximately 4mm on 1% (w/v) agar plates containing 0.5X Murashige and Skoog (MS) media and 0.05% 2-(*N*-Morpholino) ethane sulfonic acid (MES), pH 5.8. After stratification at 4°C in the dark for 3 days the seeds were grown vertically at 22 °C under a 16 h light/8 h dark cycle in a Conviron growth chamber. Seedlings used for CLE peptide assay were transferred to media containing different peptides at five days after germination.

Root growth inhibition assay

The root length was measured from the base of the hypocotyl to the tip of the primary root at the time of transfer, and then every 24 hours for the next five days. CLE peptides (Mimotopes, http://www.mimotopes.com/) with a purity of >70% were dissolved in 50 µL DMSO and then diluted to a final concentration of 2mM using sterile sodium phosphate buffer (50 mM, pH 6.0). Peptides were added to the cooled sterilized media to a final concentration of 10 µM. Control plates were prepared by adding the same volume of DMSO/phosphate buffer that did not contain any CLE peptide. Plates were scanned and root lengths were measured on the captured images using ImageJ software.

Generation of transcriptional and translational fusions

To generate transcriptional fusions, the genomic regions upstream of *RPK1* (2913bp) and *TOAD2* (1314 bp) coding sequences were amplified using primers RPK1pF/RPK1pR and TOAD2pF/TOAD2pR respectively, and TOPO TA cloned into

the GATEWAY entry vector pCR8 (Invitrogen). DNA sequences immediately upstream of *CLE19* (2283bp) and *CLE17* (523bp) start codons were amplified with primers CLE19pF/CLE19pR and CLE17pF/CLE17pR respectively, and cloned into the pCR8 vector. The entry clones above were used in the Gateway LR reaction (Invitrogen) to insert the corresponding regulatory sequences into the Gateway-adapted T-DNA binary vector pFYTAG (GenBank acc.DQ370421, donated by Zhang,C. and Galbraith,D.W). The resulting expression vectors carrying the promoter sequences driving the expression of EYFP (enhanced yellow fluorescence protein) fused with the coding region of a histone 2A gene (HTA6; At5g59870) (Zhang et al., 2005) were used for *Agrobacteium*-mediated transformation of *Col-0 Arabidopsis* using the floral dip method (Clough and Bent, 1998). Seeds (T1) were harvested, germinated on soil and selected using 50mg/L BASTA (1:1000 dilution of Finale, Farnam Comp Inc, Phoenix, AZ). At least five independently transformed lines were analyzed for the presence of transgenes using PCR genotyping and microscopy to visualize the YFP signal. The RPK1p::GFP-NLS and TOAD2::GFP-NLS translational fusions used in this study were described by Nodine et al, 2007.

Primer Name	Primer Sequence 5´ to 3´
RPK1pF	ACCCGAGTTTTCTTTGTGTTGCTA
RPK1pR	CTTCTTTTTCTTCACAAGAG
TOAD2pF	GATCCCTCTTCTTATGTGTAAATTG
TOAD2pR	CTTCGTAACTTATCCCCAAAAATG
CLE19pF	CTCGAGGTAGTGTTTCAGGGATTGGA
CLE19pR	CTCGAGTTGTCTATTTTTGGTCAAAT
CLE17pF	GCCTCTATTTGTAGAAGAATGAGTGAGA
CLE17pR	CATCTCACAAAACCTTGTTCCGGA
RPK1cF	CTCGAGATGAAACTTCTGGGTTTGGT
RPK1cR	CTCGAGCAATCTAGAAGGCTGGATTC
TOAD2cF	ACTAGTCAGATCTACCATACACGACGGAGGTTGTAGCTGCT
TOAD2cR	ACTAGTATGACTTCTTTGCCTTCTTCAG
SCR F	AAGGGATAGAGGAAGAGGACT
SCR R	GGAGATTGAAGGGTTGTTGG
ATML1-T1	ATTGATTCTGAACTGTACCC
ATML1-T2	TTTAAGCTTAACCGGTGGATTCAGGG
PNHGWF	TATTGTTGCGAACAGAATTG
PNHGWR	TTTTTGTTGTTTGGATTTTC

To create the promoter swap constructs, a Gateway-adapted T-DNA binary vector derived from pBIB-GW-GFP-Kan was constructed by inserting the RPK1 or TOAD2 coding region, amplified with primers RPK1cF/RPK1cR and

TOAD2cF/TOAD2cR (table below) upstream of the GFP vector sequence to generate the destination vectors pRPK1-GFP and pTOAD2-GFP.

These vectors were then used in the LR recombination reactions with entry clones vector containing the promoters to obtain the expression clones. The following promoter entry clones were generated using the primer pairs in parenthesis: *SCRp* (SCR F/SCR R), *PNHp, AtmL1p* (ATML1-T1/ ATML1-T2), *RPK1p** (RPK1pF/ RPK1pF) and *TOAD2** (TOAD2pF/ TOAD2pR).

Microscopy

For confocal images, fresh roots were counterstained with 10 µg/ml propidium iodide, PI (Sigma, St Louis, MO, USA) for 1 to 2 minutes, rinsed and mounted in water on microscope slides. GFP and YFP fluorescence was imaged by confocal microscopy using a Zeiss 510 Meta confocal microscope equipped with 10x Plan Neofluar, 0.3NA, 20x Plan Apo, 0.8NA; 40x Plan Neofluar , 1.3NA; 63x Plan Apo, 1.4NA objective lenses and a laser line with excitation at 488nm. Images were captured using filter sets of BP505-530 for GFP and YFP and LP560 for PI and the AxioVision image processing software and Adobe Photoshop Elements 9.0 (Adobe Systems Inc., San Jose, CA) for image processing. Staining of whole seedlings using a modified Schiff propidium iodide procedure was carried out as described by (Truernit et al., 2008), with the exception that seedlings were mounted in chloralhydrate solution. Wild-type and mutant seedlings containing QC184::GUS and QC25::GUS markers were stained with X-Gluc for 2-6

hours at 37°C and mounted in 6:1 chloralhydrate: Lugol's solution and imaged using a Zeiss Axioplan microscope. Root lengths were measured using Image J software. Measurements of fluorescence intensity of GFP signal was done using the basic measuring tools feature of ImageJ software (Hartig, 2013).

Acknowledgements

We are grateful to the members of the Tax lab, especially Yulemi Velazco, Rachel Wellington, and Cameron Lee for their technical assistance. We thank C. Zhang for providing the *pWOX5::GFP-NLS* construct and pFYTAG vector. This work was supported by NSF 2010: MCB 0418946, NSF IOS-0922678, and NSF IOS 1257316, awarded to Frans E Tax. A. R. received funding from NIH T32 GM08659 and NSF IGERT DGE-0114420.

References

Azpeitia, E., and Alvarez-Buylla, E.R. (2012). A complex systems approach to Arabidopsis root stem-cell niche developmental mechanisms: from molecules, to networks, to morphogenesis. Plant Mol Biol **80,** 351-363.

Betsuyaku, S., Sawa, S., and Yamada, M. (2011a). The Function of the CLE Peptides in Plant Development and Plant-Microbe Interactions. Arabidopsis Book **9,** e0149.

Betsuyaku, S., Takahashi, F., Kinoshita, A., Miwa, H., Shinozaki, K., Fukuda, H., and Sawa, S. (2011b). Mitogen-activated protein kinase regulated by the CLAVATA receptors contributes to shoot apical meristem homeostasis. Plant Cell Physiol **52,** 14-29.

Blilou, I., Xu, J., Wildwater, M., Willemsen, V., Paponov, I., Friml, J., Heidstra, R., Aida, M., Palme, K., and Scheres, B. (2005). The PIN auxin efflux facilitator network controls growth and patterning in Arabidopsis roots. Nature **433,** 39-44.

Clark, S.E., Williams, R.W., and Meyerowitz, E.M. (1997). The CLAVATA1 gene encodes a putative receptor kinase that controls shoot and floral meristem size in Arabidopsis. Cell **89,** 575-585.

Clough, S.J., and Bent, A.F. (1998). Floral dip: a simplified method for Agrobacterium-mediated transformation of Arabidopsis thaliana. Plant J **16,** 735-743.

Clouse, S.D., and Sasse, J.M. (1998). BRASSINOSTEROIDS: Essential Regulators of Plant Growth and Development. Annu Rev Plant Physiol Plant Mol Biol **49,** 427-451.

Cock, J.M., and McCormick, S. (2001). A large family of genes that share homology with CLAVATA3. Plant Physiol **126,** 939-942.

Cui, H., Levesque, M.P., Vernoux, T., Jung, J.W., Paquette, A.J., Gallagher, K.L., Wang, J.Y., Blilou, I., Scheres, B., and Benfey, P.N. (2007). An evolutionarily conserved mechanism delimiting SHR movement defines a single layer of endodermis in plants. Science **316,** 421-425.

De Smet, I., Vassileva, V., De Rybel, B., Levesque, M.P., Grunewald, W., Van Damme, D., Van Noorden, G., Naudts, M., Van Isterdael, G., De Clercq, R., Wang, J.Y., Meuli, N., Vanneste, S., Friml, J., Hilson, P., Jürgens, G., Ingram, G.C., Inzé, D., Benfey, P.N., and Beeckman, T. (2008). Receptor-like kinase ACR4 restricts formative cell divisions in the Arabidopsis root. Science **322,** 594-597.

Delay, C., Imin, N., and Djordjevic, M.A. (2013). Regulation of Arabidopsis root development by small signaling peptides. Front Plant Sci **4,** 352.

Depuydt, S., Rodriguez-Villalon, A., Santuari, L., Wyser-Rmili, C., Ragni, L., and Hardtke, C.S. (2013). Suppression of Arabidopsis protophloem differentiation and root meristem growth by CLE45 requires the receptor-like kinase BAM3. Proc Natl Acad Sci U S A **110,** 7074-7079.

Diévart, A., and Clark, S.E. (2004). LRR-containing receptors regulating plant development and defense. Development **131,** 251-261.

Durbak, A.R., and Tax, F.E. (2011). CLAVATA signaling pathway receptors of Arabidopsis regulate cell proliferation in fruit organ formation as well as in meristems. Genetics **189,** 177-194.

Fiers, M., Golemiec, E., Xu, J., van der Geest, L., Heidstra, R., Stiekema, W., and Liu, C.M. (2005). The 14-amino acid CLV3, CLE19, and CLE40 peptides trigger consumption of the root meristem in Arabidopsis through a CLAVATA2-dependent pathway. Plant Cell **17,** 2542-2553.

Friml, J. (2010). Subcellular trafficking of PIN auxin efflux carriers in auxin transport. Eur J Cell Biol **89,** 231-235.

Friml, J., Vieten, A., Sauer, M., Weijers, D., Schwarz, H., Hamann, T., Offringa, R., and Jürgens, G. (2003). Efflux-dependent auxin gradients establish the apical-basal axis of Arabidopsis. Nature **426,** 147-153.

Fukuda, H., and Higashiyama, T. (2011). Diverse functions of plant peptides: entering a new phase. Plant Cell Physiol **52,** 1-4.

Gallagher, K.L., Paquette, A.J., Nakajima, K., and Benfey, P.N. (2004). Mechanisms regulating SHORT-ROOT intercellular movement. Curr Biol **14,** 1847-1851.

Geldner, N., Hyman, D.L., Wang, X., Schumacher, K., and Chory, J. (2007). Endosomal signaling of plant steroid receptor kinase BRI1. Genes Dev **21,** 1598-1602.

Gifford, M.L., Dean, S., and Ingram, G.C. (2003). The Arabidopsis ACR4 gene plays a role in cell layer organisation during ovule integument and sepal margin development. Development **130,** 4249-4258.

Gifford, M.L., Robertson, F.C., Soares, D.C., and Ingram, G.C. (2005). ARABIDOPSIS CRINKLY4 function, internalization, and turnover are dependent on the extracellular crinkly repeat domain. Plant Cell **17,** 1154-1166.

Grieneisen, V.A., Xu, J., Maree, A.F., Hogeweg, P., and Scheres, B. (2007). Auxin transport is sufficient to generate a maximum and gradient guiding root growth. In Nature (England), pp. 1008-1013.

Guo, Y., Han, L., Hymes, M., Denver, R., and Clark, S.E. (2010). CLAVATA2 forms a distinct CLE-binding receptor complex regulating Arabidopsis stem cell specification. Plant J **63,** 889-900.

Hacham, Y., Sela, A., Friedlander, L., and Savaldi-Goldstein, S. (2012). BRI1 activity in the root meristem involves post-transcriptional regulation of PIN auxin efflux carriers. Plant Signal Behav **7,** 68-70.

Hacham, Y., Holland, N., Butterfield, C., Ubeda-Tomas, S., Bennett, M.J., Chory, J., and Savaldi-Goldstein, S. (2011). Brassinosteroid perception in the epidermis controls root meristem size. Development **138,** 839-848.

Hartig, S.M. (2013). Basic image analysis and manipulation in ImageJ. Curr Protoc Mol Biol **Chapter 14,** Unit14.15.

Hirakawa, Y., Kondo, Y., and Fukuda, H. (2010). TDIF peptide signaling regulates vascular stem cell proliferation via the WOX4 homeobox gene in Arabidopsis. Plant Cell **22,** 2618-2629.

Hirakawa, Y., Shinohara, H., Kondo, Y., Inoue, A., Nakanomyo, I., Ogawa, M., Sawa, S., Ohashi-Ito, K., Matsubayashi, Y., and Fukuda, H. (2008). Non-cell-autonomous control of vascular stem cell fate by a CLE peptide/receptor system. Proc Natl Acad Sci U S A **105,** 15208-15213.

Ito, Y., Nakanomyo, I., Motose, H., Iwamoto, K., Sawa, S., Dohmae, N., and Fukuda, H. (2006). Dodeca-CLE peptides as suppressors of plant stem cell differentiation. Science **313,** 842-845.

Jun, J., Fiume, E., Roeder, A.H., Meng, L., Sharma, V.K., Osmont, K.S., Baker, C., Ha, C.M., Meyerowitz, E.M., Feldman, L.J., and Fletcher, J.C. (2010). Comprehensive analysis of CLE polypeptide signaling gene expression and overexpression activity in Arabidopsis. Plant Physiol **154,** 1721-1736.

Kinoshita, A., Nakamura, Y., Sasaki, E., Kyozuka, J., Fukuda, H., and Sawa, S. (2007). Gain-of-function phenotypes of chemically synthetic CLAVATA3/ESR-related (CLE) peptides in Arabidopsis thaliana and Oryza sativa. Plant Cell Physiol **48,** 1821-1825.

Kinoshita, A., Betsuyaku, S., Osakabe, Y., Mizuno, S., Nagawa, S., Stahl, Y., Simon, R., Yamaguchi-Shinozaki, K., Fukuda, H., and Sawa, S. (2010). RPK2 is an essential receptor-like kinase that transmits the CLV3 signal in Arabidopsis. Development **137,** 3911-3920.

Kiyohara, S., and Sawa, S. (2012). CLE Signaling Systems During Plant Development and Nematode Infection. Plant Cell Physiol.

Larkin, M.A., Blackshields, G., Brown, N.P., Chenna, R., McGettigan, P.A., McWilliam, H., Valentin, F., Wallace, I.M., Wilm, A., Lopez, R., Thompson, J.D., Gibson, T.J., and Higgins, D.G. (2007). Clustal W and Clustal X version 2.0. Bioinformatics **23,** 2947-2948.

Lee, I.C., Hong, S.W., Whang, S.S., Lim, P.O., Nam, H.G., and Koo, J.C. (2011). Age-dependent action of an ABA-inducible receptor kinase, RPK1, as a positive regulator of senescence in Arabidopsis leaves. In Plant Cell Physiol (Japan), pp. 651-662.

Li, J. (2010). Multi-tasking of somatic embryogenesis receptor-like protein kinases. Curr Opin Plant Biol **13,** 509-514.

Li, J., and Chory, J. (1997). A putative leucine-rich repeat receptor kinase involved in brassinosteroid signal transduction. Cell **90,** 929-938.

Luichtl, M., Fiesselmann, B.S., Matthes, M., Yang, X., Peis, O., Brunner, A., and Torres-Ruiz, R.A. (2013). Mutations in the Arabidopsis RPK1 gene uncouple cotyledon anlagen and primordia by modulating epidermal cell shape and polarity. Biology Open.

Matsubayashi, Y., Ogawa, M., Morita, A., and Sakagami, Y. (2002). An LRR receptor kinase involved in perception of a peptide plant hormone, phytosulfokine. In Science (United States), pp. 1470-1472.

Miwa, H., Betsuyaku, S., Iwamoto, K., Kinoshita, A., Fukuda, H., and Sawa, S. (2008). The receptor-like kinase SOL2 mediates CLE signaling in Arabidopsis. Plant Cell Physiol **49,** 1752-1757.

Mizuno, S., Osakabe, Y., Maruyama, K., Ito, T., Osakabe, K., Sato, T., Shinozaki, K., and Yamaguchi-Shinozaki, K. (2007). Receptor-like protein kinase 2 (RPK 2) is a novel factor controlling anther development in Arabidopsis thaliana. Plant J **50,** 751-766.

Moller, B., and Weijers, D. (2009). Auxin control of embryo patterning. Cold Spring Harb Perspect Biol **1,** a001545.

Müller, R., Bleckmann, A., and Simon, R. (2008). The receptor kinase CORYNE of Arabidopsis transmits the stem cell-limiting signal CLAVATA3 independently of CLAVATA1. Plant Cell **20,** 934-946.

Ni, J., Guo, Y., Jin, H., Hartsell, J., and Clark, S.E. (2011). Characterization of a CLE processing activity. Plant Mol Biol **75,** 67-75.

Nimchuk, Z.L., Tarr, P.T., Ohno, C., Qu, X., and Meyerowitz, E.M. (2011). Plant stem cell signaling involves ligand-dependent trafficking of the CLAVATA1 receptor kinase. Curr Biol **21,** 345-352.

Nodine, M.D., and Tax, F.E. (2008). Two receptor-like kinases required together for the establishment of Arabidopsis cotyledon primordia. Dev Biol **314,** 161-170.

Nodine, M.D., Yadegari, R., and Tax, F.E. (2007). RPK1 and TOAD2 are two receptor-like kinases redundantly required for arabidopsis embryonic pattern formation. Dev Cell **12,** 943-956.

Ogawa, M., Shinohara, H., Sakagami, Y., and Matsubayashi, Y. (2008). Arabidopsis CLV3 peptide directly binds CLV1 ectodomain. Science **319,** 294.

Oh, M.H., Clouse, S.D., and Huber, S.C. (2009). Tyrosine phosphorylation in brassinosteroid signaling. Plant Signal Behav **4,** 1182-1185.

Osakabe, Y., Maruyama, K., Seki, M., Satou, M., Shinozaki, K., and Yamaguchi-Shinozaki, K. (2005). Leucine-rich repeat receptor-like kinase1 is a key membrane-bound regulator of abscisic acid early signaling in Arabidopsis. Plant Cell **17,** 1105-1119.

Osakabe, Y., Mizuno, S., Tanaka, H., Maruyama, K., Osakabe, K., Todaka, D., Fujita, Y., Kobayashi, M., Shinozaki, K., and Yamaguchi-Shinozaki, K. (2010). Overproduction

of the membrane-bound receptor-like protein kinase 1, RPK1, enhances abiotic stress tolerance in Arabidopsis. J Biol Chem **285,** 9190-9201.

Petricka, J.J., Winter, C.M., and Benfey, P.N. (2012). Control of Arabidopsis root development. Annu Rev Plant Biol **63,** 563-590.

Qiang, Y., Wu, J., Han, H., and Wang, G. CLE Peptides in Vascular Development.

Qiang, Y., Wu, J., Han, H., and Wang, G. (2013). CLE Peptides in Vascular Development. Journal of Integrative Plant Biology **Volume 55, 389–394**.

Robatzek, S., Chinchilla, D., and Boller, T. (2006). Ligand-induced endocytosis of the pattern recognition receptor FLS2 in Arabidopsis. Genes Dev **20,** 537-542.

Sarkar, A.K., Luijten, M., Miyashima, S., Lenhard, M., Hashimoto, T., Nakajima, K., Scheres, B., Heidstra, R., and Laux, T. (2007). Conserved factors regulate signalling in Arabidopsis thaliana shoot and root stem cell organizers. Nature **446,** 811-814.

Scheres, B., Di Laurenzio, L., Willemsen, V., Hauser, M.T., Janmaat, K., Weisbeek, P., and Benfey, P.N. (1995). Mutations affecting the radial organisation of the Arabidopsis root display specific defects throughout the embryonic axis. Development **121,** 53-62.

Schoof, H., Lenhard, M., Haecker, A., Mayer, K.F., Jürgens, G., and Laux, T. (2000). The stem cell population of Arabidopsis shoot meristems in maintained by a regulatory loop between the CLAVATA and WUSCHEL genes. Cell **100,** 635-644.

Shiu, S.H., and Bleecker, A.B. (2001a). Receptor-like kinases from Arabidopsis form a monophyletic gene family related to animal receptor kinases. Proc Natl Acad Sci U S A **98,** 10763-10768.

Shiu, S.H., and Bleecker, A.B. (2001b). Plant receptor-like kinase gene family: diversity, function, and signaling. Sci STKE **2001,** re22.

Song, X.F., Yu, D.L., Xu, T.T., Ren, S.C., Guo, P., and Liu, C.M. (2012). Contributions of individual amino acid residues to the endogenous CLV3 function in shoot apical meristem maintenance in Arabidopsis. Mol Plant **5,** 515-523.

Stahl, Y., and Simon, R. (2009). Is the Arabidopsis root niche protected by sequestration of the CLE40 signal by its putative receptor ACR4? Plant Signal Behav **4,** 634-635.

Stahl, Y., and Simon, R. (2010). Plant primary meristems: shared functions and regulatory mechanisms. Curr Opin Plant Biol **13,** 53-58.

Stahl, Y., Wink, R.H., Ingram, G.C., and Simon, R. (2009). A signaling module controlling the stem cell niche in Arabidopsis root meristems. Curr Biol **19,** 909-914.

Stahl, Y., Grabowski, S., Bleckmann, A., Kühnemuth, R., Weidtkamp-Peters, S., Pinto, K.G., Kirschner, G.K., Schmid, J.B., Wink, R.H., Hülsewede, A., Felekyan, S., Seidel, C.A., and Simon, R. (2013). Moderation of Arabidopsis root stemness by CLAVATA1 and ARABIDOPSIS CRINKLY4 receptor kinase complexes. Curr Biol **23,** 362-371.

Strabala, T.J., O'donnell, P.J., Smit, A.M., Ampomah-Dwamena, C., Martin, E.J., Netzler, N., Nieuwenhuizen, N.J., Quinn, B.D., Foote, H.C., and Hudson, K.R. (2006). Gain-of-function phenotypes of many CLAVATA3/ESR genes, including four new family members, correlate with tandem variations in the conserved CLAVATA3/ESR domain. Plant Physiol **140,** 1331-1344.

Sussman, M.R., Amasino, R.M., Young, J.C., Krysan, P.J., and Austin-Phillips, S. (2000). The Arabidopsis knockout facility at the University of Wisconsin-Madison. Plant Physiol **124,** 1465-1467.

Swarup, R., Kramer, E.M., Perry, P., Knox, K., Leyser, H.M., Haseloff, J., Beemster, G.T., Bhalerao, R., and Bennett, M.J. (2005). Root gravitropism requires lateral root cap and epidermal cells for transport and response to a mobile auxin signal. Nat Cell Biol **7,** 1057-1065.

Tamaki, T., Betsuyaku, S., Fujiwara, M., Fukao, Y., Fukuda, H., and Sawa, S. (2013). Suppressor of llp1 1-mediated c-terminal processing is critical for cle19 peptide activity. Plant J.

Torii, K. (2008). Transmembrane receptors in plants:receptor kinases and their ligands. In Annual Plant Reviews, Z. Yang, ed (www.interscience.wiley.com), pp. 1-29.

Truernit, E., Bauby, H., Dubreucq, B., Grandjean, O., Runions, J., Barthélémy, J., and Palauqui, J.C. (2008). High-resolution whole-mount imaging of three-dimensional tissue organization and gene expression enables the study of Phloem development and structure in Arabidopsis. Plant Cell **20,** 1494-1503.

Whitford, R., Fernandez, A., De Groodt, R., Ortega, E., and Hilson, P. (2008). Plant CLE peptides from two distinct functional classes synergistically induce division of vascular cells. Proc Natl Acad Sci U S A **105,** 18625-18630.

Wysocka-Diller, J.W., Helariutta, Y., Fukaki, H., Malamy, J.E., and Benfey, P.N. (2000). Molecular analysis of SCARECROW function reveals a radial patterning mechanism common to root and shoot. Development **127,** 595-603.

Yadav, R.K., Fulton, L., Batoux, M., and Schneitz, K. (2008). The Arabidopsis receptor-like kinase STRUBBELIG mediates inter-cell-layer signaling during floral development. Dev Biol **323,** 261-270.

Zhang, C., Gong, F.C., Lambert, G.M., and Galbraith, D.W. (2005). Cell type-specific characterization of nuclear DNA contents within complex tissues and organs. Plant Methods **1,** 7.

Figure legends

Figure 1. Root growth defects of rpk1, toad2 and rpk1; toad2/+ mutants.

A-D: Root phenotypic classes: S-short roots (less than 15% of wild type root length), M-medium roots (between 15 and 70% of wild type root length), L-long roots (average within wild type range, ±2 SD) **A.** Root phenotypic classes of *rpk1* and *toad2*

and *rpk1; toad2/+* mutants shown at five DAG. Arrowheads indicate seedlings with one cotyledon. **B.** Root length at two and six DAG is different for all phenotypic classes and genotypes ($p<0.001$) except the S phenotypic class marked by brackets (a) (*rpk1*, n=130; *toad2*, *rpk1; toad2/+* and wild type, n=45 for each, error bars are SD). **C.** Distribution of root phenotypic classes of single and double mutants (*rpk1*, n=130; *toad2*, *rpk1; toad2/+* and wild type, n=45). **D.** Morphological defects of RAM of roots in the S and M phenotypic class: representative pictures of longitudinal optical sections of five DAG roots stained using a modified pseudo Schiff propidium iodide (mPS-PI) method. Asterisks indicate the position of cortical endodermal initial cells and their daughters. Black arrows indicate regions of abnormal cell division. Red arrowheads point at specific cell files: stele (St), endodermis (En), cortex (Co), and epidermis (E) and red arrows indicate cell types: quiescent center (QC), columella stem cells (CSC), columella cells (CC), cortical endodermal initial (CEI), lateral root cap cells (LRC). Scale bars are 20 μm.

Figure 2. Marker expression analysis indicates abnormal morphology and patterning of root cells in rpk1; toad2/+ mutants.

Representative confocal images of *DR5rev::GFP* (A-C), *PIN1p::PIN1-GFP* (D-F, D´-F´), *SCRp::GFP-NLS* (G-I) and *WOX5p::GFP-NLS* (J-L) expression and *QC25::GUS* and *QC184::GUS* localization (M) in wild-type (wild type) and *rpk1-1; toad2/+* roots. D´-F´ represents a close-up view of the GFP channel in the region marked by boxes in D-F, the white arrowheads indicate the localization of PIN1 at the plasma membrane in the cortex (Co) and endodermis (En). Mutant roots of the short and medium phenotypic

classes are indicated. Seven-day old seedling roots were imaged in A-F and J-M, and five-day old roots were used in G-I. White arrowheads in G-I indicate endodermal cells lacking a green fluorescent signal. The red counterstain is propidium iodide (PI) and the green is GFP fluorescence (A-L). Roots in M are stained with X-Gluc for GUS activity (blue) and with Lugol's solution for starch granules (brown). Arrows in M mark the position of the QC. Scale bars are 20 μm.

Figure 3. *RPK1* and *TOAD2* are expressed in partially overlapping domains in the RAM

Representative confocal images of *RPK1p::RPK1-GFP* (A,B); *RPK1p::YFP-NLS* (C,D); *TOAD2p::TOAD2-GFP* (E,F); and *TOAD2p::YFP-NLS*, (G,H). Images represent median optical sections (B,F,D,H) and surface view s(A,C,E,G) of seven-day-old root tips counterstained with PI in. Scale bars are 20 μm.

Figure 4. Expression of RPK1 and TOAD2 in specific radial root layers has different effects on the short root phenotype.

A: Confocal images of 10 day-old roots of wild type (top panel) and *rpk1-1; toad2/+* (lower two panels) transgenic plants expressing translational fusion of GFP with *RPK1* and *TOAD2* under the control of various promoters (p): *AtmL1p, SCRp, PNHp, RPK1p*, and *TOAD2p* and no promoter control. Red staining is PI, green is GFP. **B:** Frequency of the short root phenotype in plants expressing the above transgenes expressed as number of short roots/ total number of *rpk1;toad2/+* plants. The number in parenthesis represents the number of independent lines analyzed.

Figure 5. *CLE17* and *CLE19* are expressed in the root apical meristem

Representative confocal pictures of roots counterstained with PI (red) expressing *CLE17p::YFP-NLS* (A-C) and *CLE19p::YFP-NLS* (D-F) (green) in three-day-old root tips of wild type *Arabidopsis*. Optical cross sections (A) and (E) show the region marked by arrowheads in B and F, respectively. Images represent root tips in median sections (A and D) and surface view of the root tip (B) and of differentiation zone (F). Scale bars equal 20µm.

Figure 6. Root growth sensitivity assay after treatment with CLE peptides.

A: Root phenotypes of *rpk1* and *toad2* and *rpk1; toad2/+* mutants and wild type, *crn-1* and *clv2-8* control plants shown after five days of treatment with exogenous CLE peptides. Progeny of *toad2/+* plants and *rpk1, toad2/+* heterozygote parents were used in the assays. Plants marked with white asterisks were genotyped as *rpk1* mutants only and with yellow asterisks were wild type or heterozygous for *toad2*. Scale bar is 2 mm. **B:** Distribution of root lengths five days after transfer to CLE treatment plates. Values represent average of root length measurements in three independent experiments. Error bars represent standard deviation (* $p < 0.001$; n=8 for *toad2/+;* n>16 for all other genotypes) **C:** Alignment of Arabidopsis CLV3 amino acid sequence with sequences of CLE peptides used in this study and the synthetic peptides (box) used for the root assay. Completely conserved amino acids are shaded in black; partially conserved or highly similar amino acids (groups of strongly similar properties scoring > 0.5 in the

Gonnet PAM 250 matrix ClustalW) are shaded in gray and the conserved CLE motif is framed.

Figure 7. Root apical meristem defects in roots treated with CLE peptides.

A: Longitudinal median optical sections of CLE treated roots stained using mPS-PI. Brackets indicate the size of the RAM of roots grown in the presence of CLE17 for five days. Enlarged image of boxed area shows cortical cells (outlined in red) and dividing cells (marked by arrowheads). Scale bars are 20 μm. **B:** Confocal image showing the organization of RAM cells with the stem cell niche area outlined by a dashed red line. **C-G:** The effect of CLE17 treatment on root morphology. RAM length of seedlings grown on CLE17 plates for five days (* $p<0.001$, $n>12$) **(C)**; the number of cells in the stem cell niche (**D**) (** $P<0.001$; * $0.005<P<0.05$) and the surface area occupied by the stem cell niche **(E)** (* $p< 0.001$) in roots treated with CLE17 peptide. The average number of epidermal and cortical cells in RAM files **(F)** and the frequency of cell divisions occurring in the cortical file **(G)** measured in median optical sections CLE17 treated and mPS-PI fixed samples (* $p< 0.001$).

Figure 8. The root apical meristem of roots treated with CLE peptides contains supernumerary CEI and CEI daughter cells.

A: Representative pictures of longitudinal median optical sections of CLE17 treated roots stained using mPS-PI. Areas of CEI cells and their undivided daughters are outlined in red. Scale bars are 20 μm. **B:** The number of vascular initials, the CSCs and QC cells in plants treated with CLE17 (no significant differences, $p> 0.05$).

Figure 9. *RPK1* and *TOAD2* transcriptional and translational reporter genes show regulation of RPK1 and TOAD2 after treatement with CLE17 peptide.

Representative confocal pictures of PI counterstained roots expressing the *RPK1p::YFP-NLS* (A), *TOAD2p::YFP-NLS (D)*, *RPK1p::RPK1-GFP (B, C)* *TOAD2p::TOAD2-GFP* (E,F); wild type (A,B,D,E), *toad2-1* mutant (C) and *rpk1-1* mutant plants (F) express the transgenes. Each panel contains images of surface and median views of the RAM and an image of an emerging lateral root from the same plant. Close-up view of B and C are marked by white boxes and labeled B´ and C´, respectively. Arrows indicate subcellular localization of GFP labeled protein in intracellular vesicular compartments.

Figure 10. *RPK1* overexpression induces TOAD2-dependent changes in root growth and distal meristem morphology.

A: Confocal images of eight-day-old root tips of wild type and mutant *rpk1-1* and *toad2-1* expressing *RPK1p::RPK1-GFP* or *TOAD2p::TOAD-GFP.* **B**: Root lengths of CLE17 treated and control plants overexpressing RPK1 or TOAD2. Letters indicate statistically significant differences ($p<0.001$) between the labeled pairs (a, b, and c).

Figure 11. Expression of SCR and WOX5 in CLE17 treated roots

Eight-day-old roots treated (CLE17) or untreated (control) imaged five days after transfer to treatment plates. *SCRp::GFP* (top panel), *SCRp::GFP-NLS* (middle) and *WOX5p::YFP-NLS* (bottom panel) expression (green) in roots counterstained with PI. Arrows indicate the position of the QC. Scale bars are 20 μm.

Figure 12. Model for *RPK1* and *TOAD2* interactions in controlling root growth

Diagram shows a proposed model of a regulatory network controlling root meristem growth by TOAD2, RPK1, CLV2, CRN and other unknown components. Dotted double arrows indicated potential direct interaction, solid double arrows indicate known interactions. Arrows symbolize a positive regulation and bars are negative regulation. Unknown components are likely to have both positive and negative regulatory roles.

Fig 1

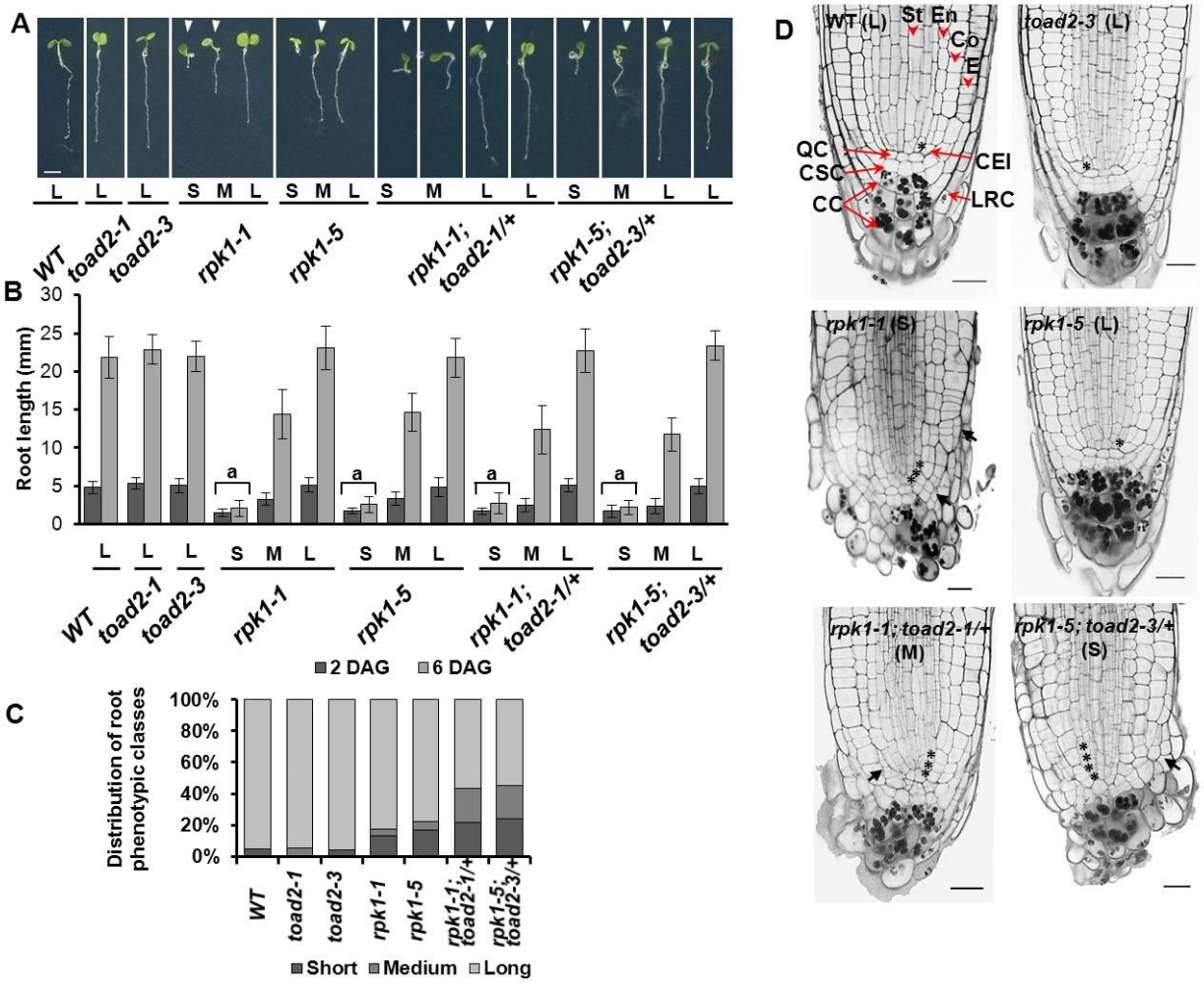
A
L L L S M L S M L S M L L S M L L
WT
toad2-1
toad2-3
rpk1-1
rpk1-5
rpk1-1; toad2-1/+
rpk1-5; toad2-3/+
B
Root length (mm)
30
25
20
15
10
5
0
a
L L L S M L S M L S M L S M L
WT
toad2-1
toad2-3
rpk1-1
rpk1-5
rpk1-1; toad2-1/+
rpk1-5; toad2-3/+
2 DAG
6 DAG
C
Distribution of root phenotypic classes
100%
80%
60%
40%
20%
0%
WT
toad2-1
toad2-3
rpk1-1
rpk1-5
rpk1-1; toad2-1/+
rpk1-5; toad2-3/+
Short
Medium
Long
D
WT (L)
St
En
Co
E
QC
CSC
CC
CEI
LRC
toad2-3 (L)
rpk1-1 (S)
rpk1-5 (L)
rpk1-1; toad2-1/+ (M)
rpk1-5; toad2-3/+ (S)

Fig 2

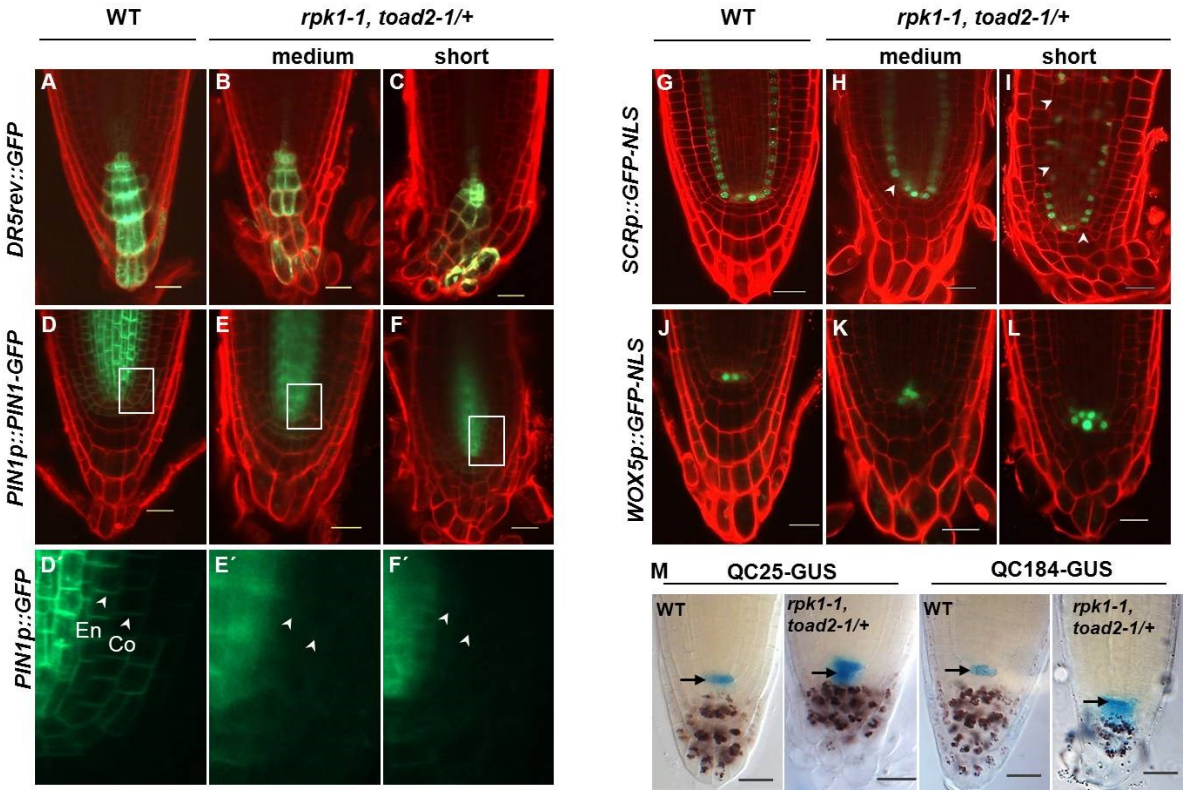
WT
rpk1-1, toad2-1/+
medium
short
DR5rev::GFP
PIN1p::PIN1-GFP
PIN1p::GFP
A
B
C
D
E
F
D´
E´
F´
En
Co
SCRp::GFP-NLS
WOX5p::GFP-NLS
G
H
I
J
K
L
M
QC25-GUS
QC184-GUS
WT
rpk1-1, toad2-1/+

Fig 3

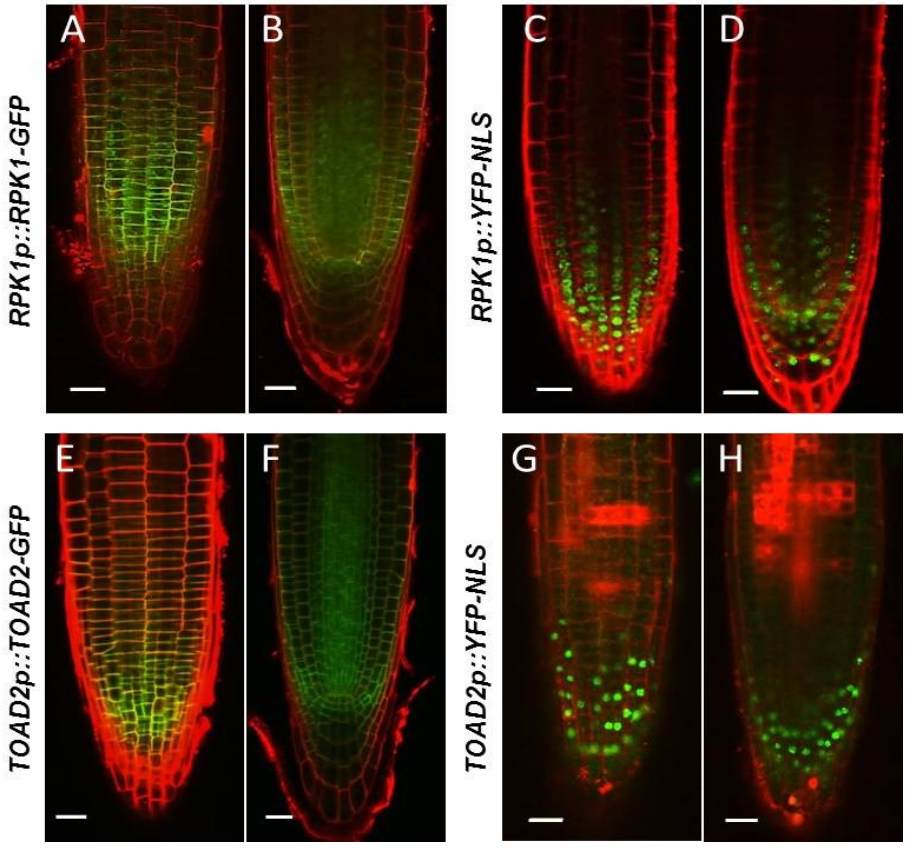
A
B
C
D
RPK1p::RPK1-GFP
RPK1p::YFP-NLS
E
F
G
H
TOAD2p::TOAD2-GFP
TOAD2p::YFP-NLS

Fig 4

A

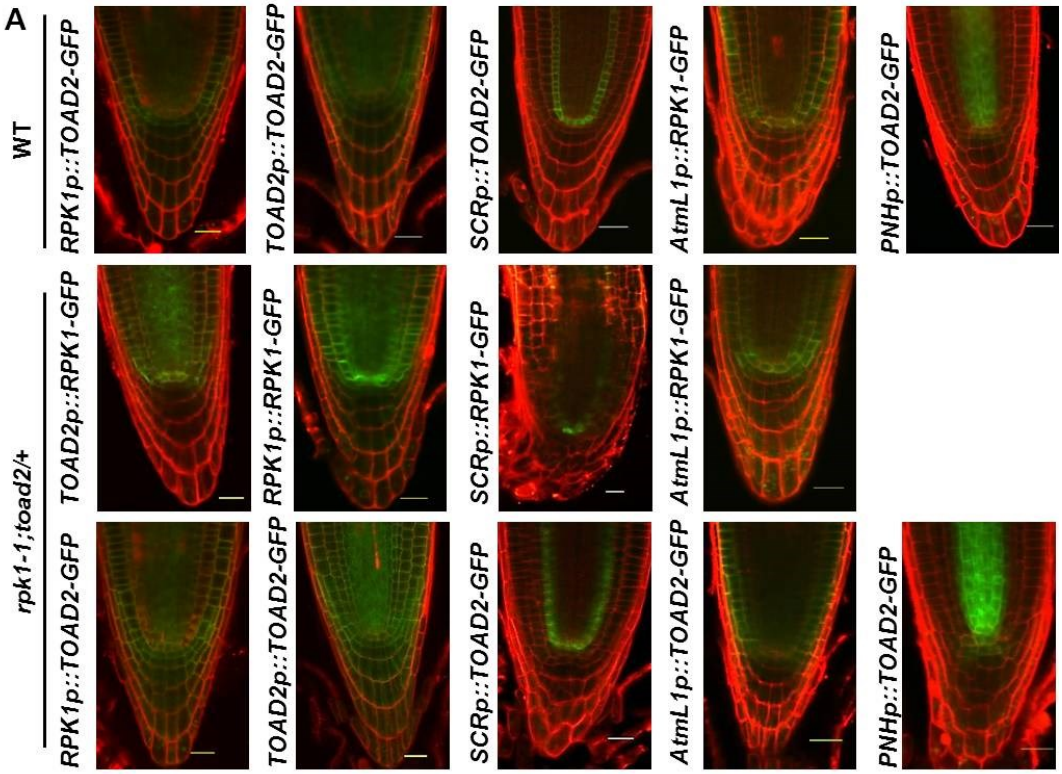

B

Promoter	Coding region	
	RPK1-GFP	*TOAD2-GFP*
AtmL1	0/58 (4)	4/70 (2)
SCR	6/38 (2)	8/36 (2)
PNH	7/47 (2)	4/36 (3)
TOAD2	0/68 (4)	3/56 (3)
RPK1	0/75 (4)	2/45 (4)
none	5/40 (1)	6/52 (1)

Fig 5

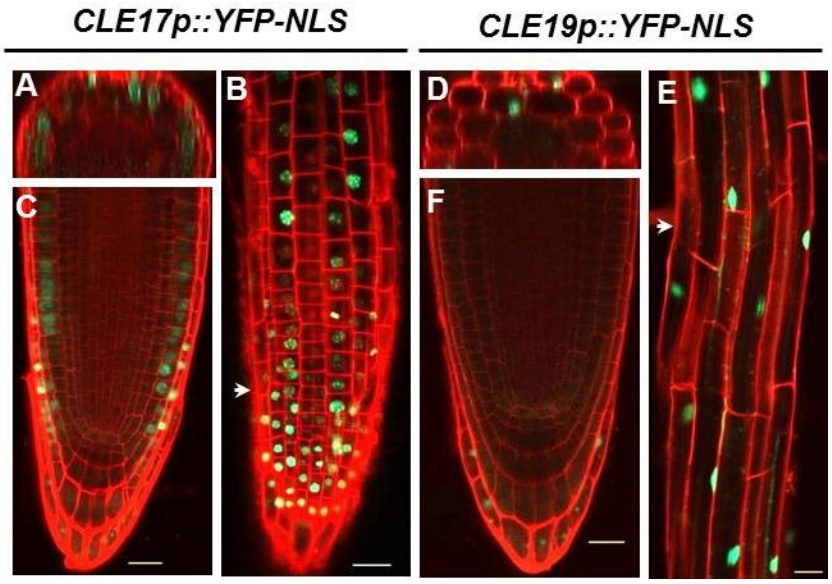

Fig 6

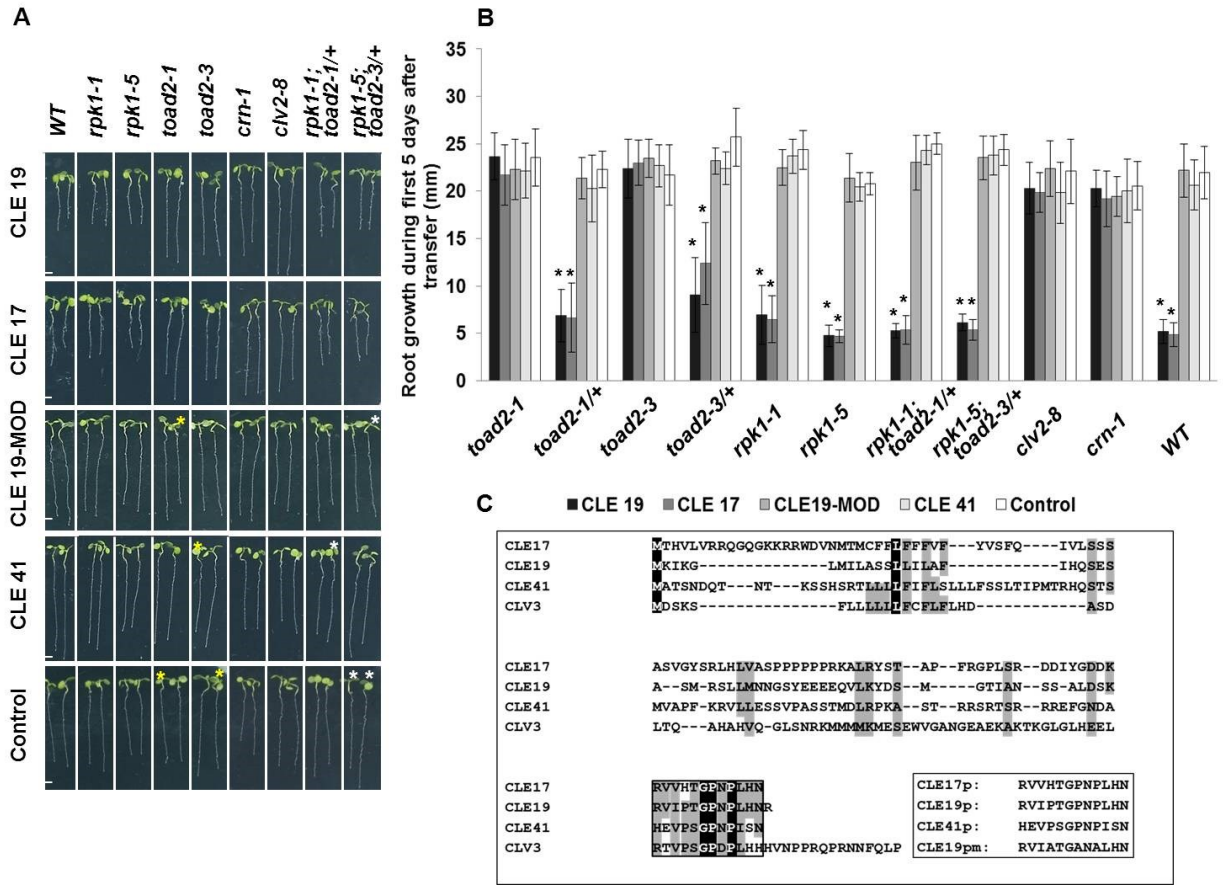
A
WT
rpk1-1
rpk1-5
toad2-1
toad2-3
crn-1
clv2-8
rpk1-1; toad2-1/+
rpk1-5; toad2-3/+
CLE 19
CLE 17
CLE 19-MOD
CLE 41
Control
B
Root growth during first 5 days after transfer (mm)
35
30
25
20
15
10
5
0
toad2-1
toad2-1/+
toad2-3
toad2-3/+
rpk1-1
rpk1-5
rpk1-1; toad2-1/+
rpk1-5; toad2-3/+
clv2-8
crn-1
WT
C
CLE 19
CLE 17
CLE19-MOD
CLE 41
Control
CLE17 MTHVLVRRQGQGKKRRWDVNMTMCFFLFFVF---YVSFQ----IVLSSS
CLE19 MKIKG----------LMILASSLLILAF----------IHQSES
CLE41 MATSNDQT---NT---KSSHSRTLLLLFIFLSLLLFSSLTIPMTRHQSTS
CLV3 MDSKS----------FLLLLLLFCFLFLHD----------ASD
CLE17 ASVGYSRLHLVASPPPPPPRKALRYST--AP--FRGPLSR--DDIYGDDK
CLE19 A--SM-RSLLMNNGSYEEEEQVLKYDS--M-----GTIAN--SS-ALDSK
CLE41 MVAPF-KRVLLESSVPASSTMDLRPKA--ST--RRSRTSR--RREFGNDA
CLV3 LTQ---AHAHVQ-GLSNRKMMMMKMESEWVGANGEAEKAKTKGLGLHEEL
CLE17 RVVHTGPNPLHN
CLE19 RVIPTGPNPLHNR
CLE41 HEVPSGPNPISN
CLV3 RTVPSGPDPLHHHVNPPRQPRNNFQLP
CLE17p: RVVHTGPNPLHN
CLE19p: RVIPTGPNPLHN
CLE41p: HEVPSGPNPISN
CLE19pm: RVIATGANALHN

Fig 7

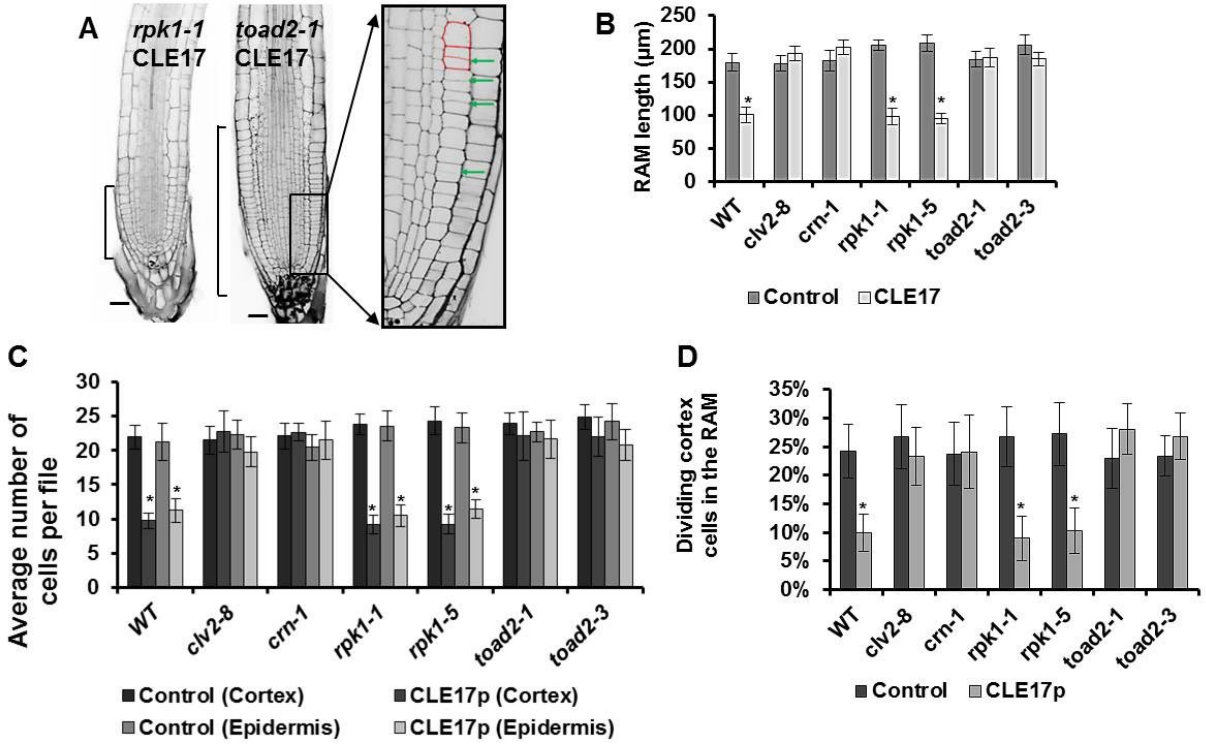
A
rpk1-1
CLE17
toad2-1
CLE17
B
RAM length (µm)
250
200
150
100
50
0
WT
clv2-8
crn-1
rpk1-1
rpk1-5
toad2-1
toad2-3
Control
CLE17
C
Average number of cells per file
30
25
20
15
10
5
0
WT
clv2-8
crn-1
rpk1-1
rpk1-5
toad2-1
toad2-3
Control (Cortex)
CLE17p (Cortex)
Control (Epidermis)
CLE17p (Epidermis)
D
Dividing cortex cells in the RAM
35%
30%
25%
20%
15%
10%
5%
0%
WT
clv2-8
crn-1
rpk1-1
rpk1-5
toad2-1
toad2-3
Control
CLE17p

Fig 8

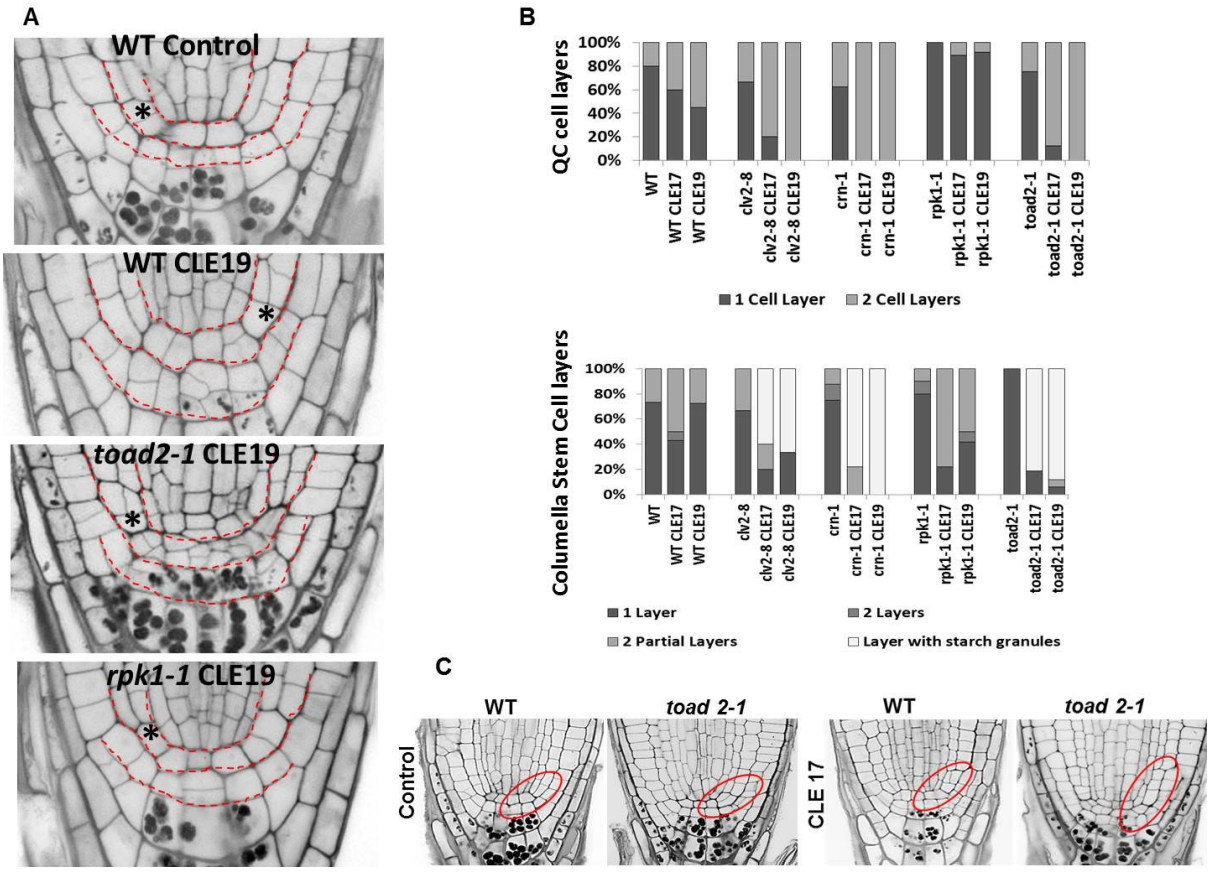
A
WT Control
WT CLE19
toad2-1 CLE19
rpk1-1 CLE19
B
QC cell layers
100%
80%
60%
40%
20%
0%
WT
WT CLE17
WT CLE19
clv2-8
clv2-8 CLE17
clv2-8 CLE19
crn-1
crn-1 CLE17
crn-1 CLE19
rpk1-1
rpk1-1 CLE17
rpk1-1 CLE19
toad2-1
toad2-1 CLE17
toad2-1 CLE19
1 Cell Layer
2 Cell Layers
Columella Stem Cell layers
1 Layer
2 Layers
2 Partial Layers
Layer with starch granules
C
WT
toad 2-1
WT
toad 2-1
Control
CLE 17

Fig 9

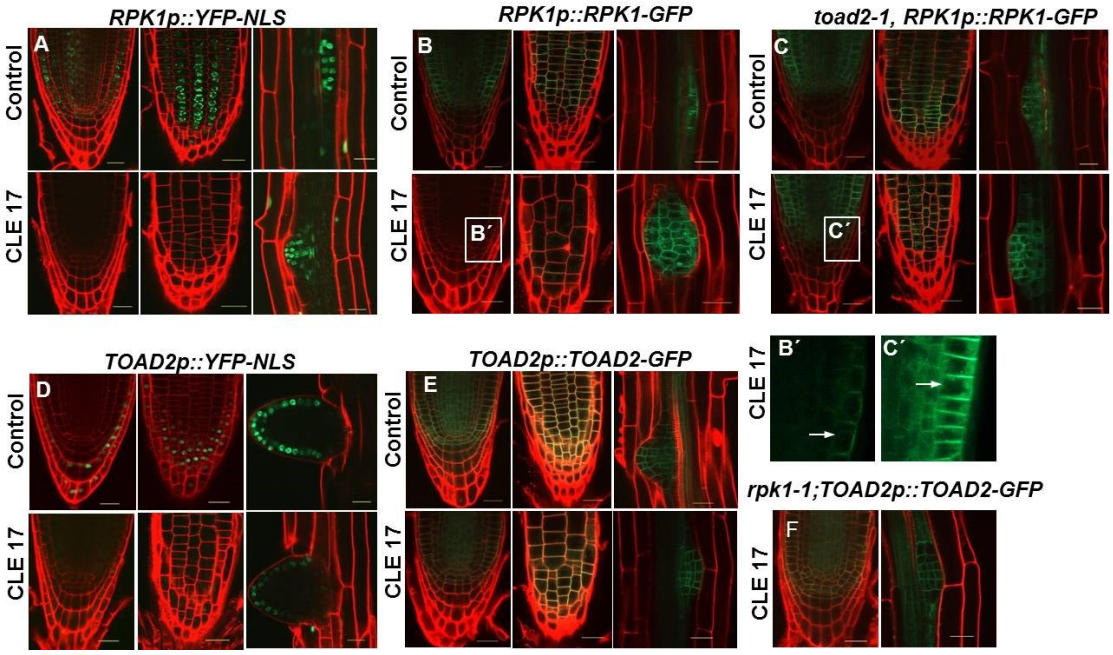
RPK1p::YFP-NLS
RPK1p::RPK1-GFP
toad2-1, RPK1p::RPK1-GFP
Control
CLE 17
A
B
C
B´
C´
TOAD2p::YFP-NLS
TOAD2p::TOAD2-GFP
rpk1-1;TOAD2p::TOAD2-GFP
D
E
F

Fig 10

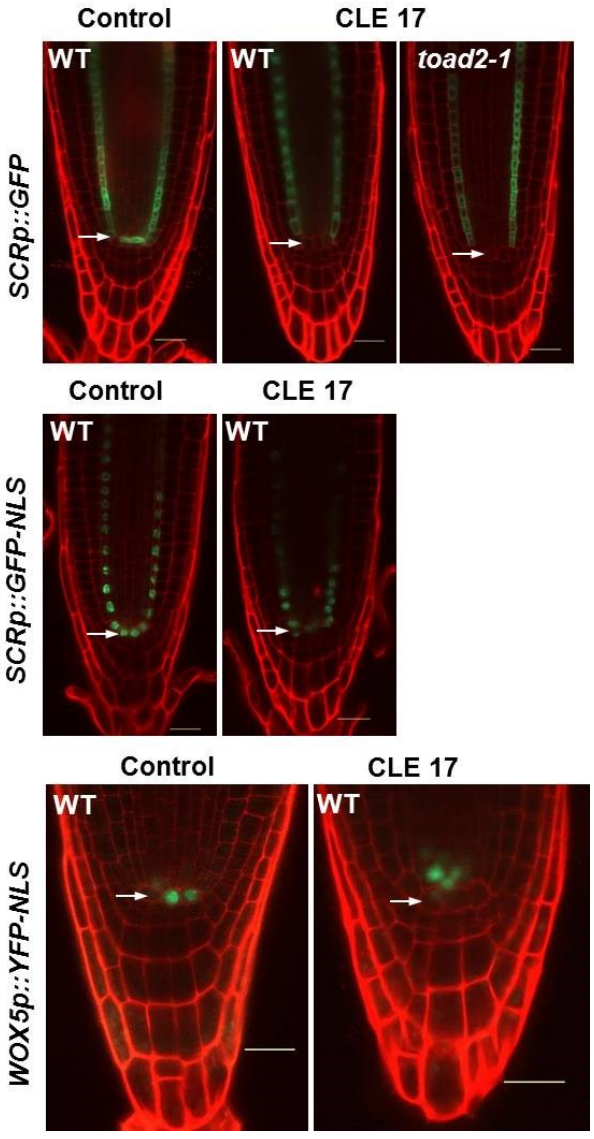
Control
CLE 17
WT
WT
toad2-1
SCRp::GFP
Control
CLE 17
WT
WT
SCRp::GFP-NLS
Control
CLE 17
WT
WT
WOX5p::YFP-NLS

Fig 11

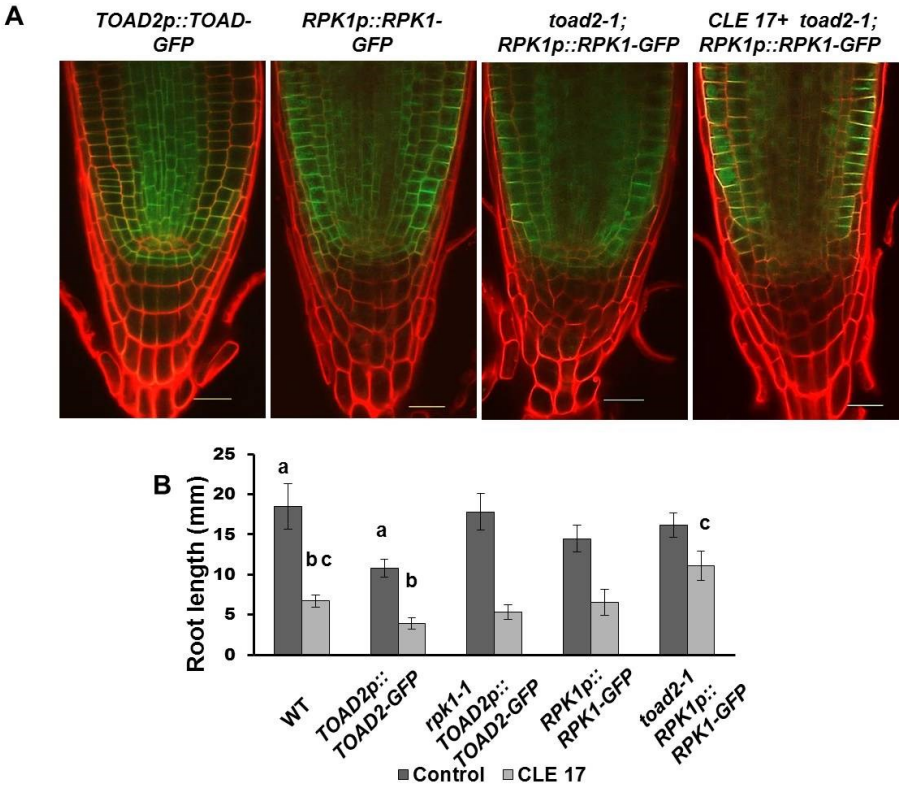
A
TOAD2p::TOAD-GFP
RPK1p::RPK1-GFP
toad2-1; RPK1p::RPK1-GFP
CLE 17+ toad2-1; RPK1p::RPK1-GFP
B
Root length (mm)
25
20
15
10
5
0
a
b c
a
b
a
c
WT
TOAD2p::TOAD2-GFP
rpk1-1 TOAD2p::TOAD2-GFP
RPK1p::RPK1-GFP
toad2-1 RPK1p::RPK1-GFP
Control
CLE 17

Fig 12

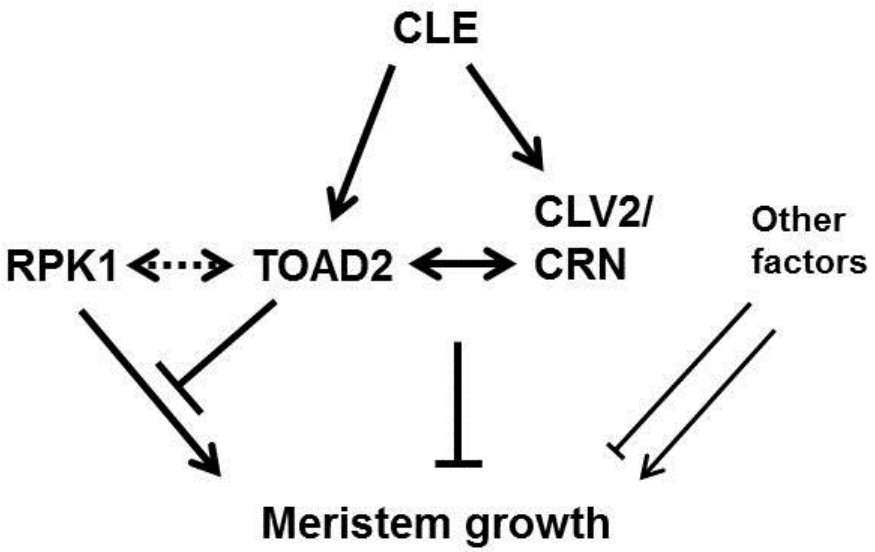

APPENDIX C: GLOBAL PERSPECTIVES ON RLK SIGNALING AND THE ROLES OF GSO1/2 AND RPK1/TOAD2 IN DEVELOPMENT

Global perspectives on RLK signaling and the roles of GSO1/2 and RPK1/TOAD2 in development

Structural and functional diversity of plant Receptor-Like Kinases

Studying the function of Receptor-Like Kinases (RLKs) in plants is a promising approach in plant biology to unravel basic signaling mechanisms that will advance our understanding of plant development. Of the over 600 identified RLKs in *Arabidopsis*, less than 10% are functionally characterized. The RLK family of *Arabidopsis* contains both transmembrane and cytoplasmic protein kinases. Phylogenetic analysis of transmembrane RLKs revealed a great diversity of their extracellular domains that lead to their classification into more than 21structural classes (Shiu and Bleecker, 2001b). The best studied transmembrane RLKs are those containing conserved Leucine-Rich Repeat (LRR) domains in their extracellular region. The LRR motifs, found in over 200 *Arabidopsis* LRR-RLKs (Shiu and Bleecker, 2001b, a) and also in 57 LRR receptor-like proteins (LRR-RPs) (Wang et al., 2008), contain 20-30 amino acids and form solenoid structures that are predicted to provide a scaffold for protein-protein interactions (Bella et al., 2008). However, despite the similar predicted structures of their receptor domains, recent functional analyses of a small number of LRR-RLKs and RPs revealed that they are involved in a variety of signal transduction pathways controlling cell proliferation, cell death and the response to pathogens and hormones. Even with recent advances in functional characterization of several LRR-RLKs, the function of the majority of these kinases is still unknown. Further research is needed to elucidate whether even more diverse cellular processes are regulated by LRR-RLK signaling or

whether a multitude of redundantly acting RLKs function in the already characterized pathways.

Diversity of ligands binding LRR-RLKs

What is the molecular basis for the diverse biological functions of RLKs with similar LRR domains? Identification of ligand molecules that bind to the extracellular domain as well as the exact structure of their binding sites within the receptor will advance our understanding about the diversity of LRR-RLKs signal transduction. A few example of how LRR domains could directly bind the ligands were recently described.

BRI1, the best characterized LRR-RLK, binds the plant brassinosteroid hormones that control cell elongation and cell division (Li and Chory, 1997). *Arabidopsis* CLV1 perceives the CLE peptide CLV3 and promotes stem cell differentiation (Clark et al., 1997; Ogawa et al., 2008). BAM1, 2 and 3 also act as receptors for CLE peptides and the LRR regions required for ligand binding were recently demonstrated in the case of CLE9 (Shinohara et al., 2012). PSKR binds the peptide hormone phytosulfokine to promote plant growth and differentiation (Matsubayashi et al., 2002). LRR regions required for binding of bacterial elicitor flagellin to the extracellular domain LRR-RLK FLS2 were also characterized (Dunning et al., 2007). Although LRR motifs were shown in several cases to be the sites of ligand binding, additional features of extracellular domains of LRR-RLKs might be important in diversification of signal recognition. The LRR sequences of some RLKs (such as BRI1, BRLs, PSKR and RPK2/TOAD2) and LRR RPs (CLV2) (Torii, 2004; Song et al., 2013) are interrupted by sequences of 30-70

residues (called island domains) that loop out of the solenoid structure and are also implicated in ligand binding. The vast majority of LRR RLKs (such as CLV1, ERECTA, FLS2, HAESA, etc) lack an island domain and the region of direct contact between their ligands and the LRR domains remains to be elucidated. The structural variability of extracellular LRR domains could represent a mechanism that provides considerable functional flexibility of this ligand binding receptor kinase family.

The known ligands of LRR-RLKs are very diverse, ranging from steroid hormones (BRs) to secreted proteins (TPD1, IDA) and processed peptides (PSK, CLV3/CLE). One class of putative ligands, the peptides from the CLE family, have been implicated in controlling various aspects of development, although the precise mechanism of action and the range of responses triggered by CLE peptides in the affected cells still remains to be clarified. Importantly, an initial screen of their general expression pattern in plants has elucidated some aspects of their spatiotemporal regulation (Jun et al., 2010).

Functional analysis of RLKs and their putative ligands is often challenging as a result of a high degree of structural homology, and therefore redundant activity. As we have seen with numerous examples in the case of RLKs, obvious phenotypes that allow for meaningful assessment of gene function often require analysis of double or triple mutants. An even greater challenge of using mutant analysis in CLE genes is posed by the genetic redundancy of these ligands, as often the 12 to 14 amino acid long peptides differ by only one or two amino acids. Due to the high sequence similarities of CLE peptides, signaling specificity is probably achieved by controls at levels different than

the sequence itself. From the few examples studied so far, we can infer that posttranslational modification of peptides, along with cell-type specific expression, as well as the localization and the rate of turnover of the receptors are likely mechanisms that control signaling specificity.

Coordinated function of multiple RLKs in root development

The research described here illustrates that studies of RLKs are often hindered by their functional redundancy. In the present study, the analysis of the pathways in which the LRR-RLKs GSO1/GSO2 and RPK1/TOAD2 function was conducted using mostly analysis of double mutants, when viable, due to the absence or low penetrance of phenotypes in single mutants. These studies reveal important mechanisms of signaling that maintain the integrity and function of the actively dividing root meristem and establish a basic function for signaling through these RLKs in organ patterning. Similarities in mutant root growth phenotypes and the particular cellular defects observed in *gso1/2* and *rpk1/toad2* pairs of double mutants, raise the intriguing possibility that crosstalk between these pathways might occur either at the level of extracellular signaling or in downstream signal transduction. Further research is needed to clarify the possible interaction between these pathways.

Root growth in *Arabidopsis* represents a valuable system for analysis of molecular mechanisms governing tissue patterning and the role of intercellular signaling during development. An important question to be addressed in elucidating intercellular communication relates to the role of RLKs in root patterning and growth. Considering

the large number of RLKs present in the plant genomes, one could ask how many of these genes are expressed and how do they function in the roots? An extensive study of 69 root-expressed LRR-RLKs recently indicated that analysis of single mutant phenotypes does not reveal the developmental role of these genes in the root (ten Hove et al., 2011). As illustrated by our findings with GSO1/2 and RPK1/TOAD2, root development is affected mostly in higher order mutants, indicating a redundant role of these RLKs or a requirement for multiple pathways to be affected in order to hinder development. In addition, the study by ten Hove et al, 2011 also reports that given mutants respond to various environmental and chemical treatments, indicating extensive cross-talk between various biochemical pathways involving RLKs. These findings strengthen not only the idea that a specific developmental response arises as a consequence of integrating multiple signaling pathways but also that RLKs might function together in molecular complexes to coordinate important developmental decisions.

RLKs affect various cellular and developmental programs

What are the basic cellular processes that are affected by disturbed signaling during organogenesis, in general, and root formation, in particular? In our studies on the role of GSO1/2 and RPK1/TOAD2 in root development we revealed that asymmetric cell division leading to correct patterning and proliferation of root meristematic cells are two plausible mechanisms that are interconnected and lead to normal root growth. What could be the direct consequences of impaired signaling through these RLKs and what are the secondary defects leading to arrested root development? Our studies indicate a

link between the behavior of cells in the stem cell niche in terms of the frequency and orientation of their cell division pattern, and subsequent proliferation of cells in the proximal meristem.

Root growth is largely dependent on generation of new cells in the root apical meristem. These cells will subsequently increase in size when displaced in the elongation and differentiation zones of the root, also contributing to normal root growth. Reduced meristem size was observed in *gso1/2* and *rpk1/toad2* double mutants and these phenotypes correlate with reduced/aberrant mitotic activity of cells in the proximal meristem. We can hypothesize that these root growth arrest phenotypes are a consequence of impairment of any or several of the following cellular activities: cytoplasmic growth (macromolecular synthesis), cell wall remodeling, cell cycle regulation and cell differentiation.

Cytoplasmic growth, the synthesis and accumulation of macromolecules in a cell is tightly linked to the nutrient availability of a cell. Inhibition of cellular growth in eukaryotes is generally thought to stall the cell cycle (Su and O'Farrell, 1998) and plant cells may possess a cell size checkpoint acting in the G1-S phase of the cell cycle (Schiessl et al., 2012). This could indicate that if signaling through RLKs converges on the energetics of the cell, impaired cytoplasmic growth could lead to decreased mitotic activity. Recently, the TOR pathway of *Arabidopsis* was linked to the control of growth related genes to sugar levels (Xiong et al., 2013). A link between the GSO1/2 signaling and sucrose-induced mitotic activity was suggested in our study by the effect of exogenous sucrose to rescue the *gso1/2* root arrest and proximal meristem

proliferation. This indicates that developmental mechanisms controlled by GSO1/2 pathway converge on signaling mechanisms controlling sucrose-dependent mitotic activity. A potential link between the TOR and GSO1/2 pathways awaits further testing.

A second mechanism that could hinder cell cycle progression resulting in short meristems is the control of cell wall expansion. In plants, cells are immobilized and attached to each other through their cell walls. Extensive cell wall remodeling has to occur to allow proper cell growth (Wolf et al., 2012) and several plant hormones (auxin, brasssinosteroids) are important in controlling the associated processes. It was proposed that regulation of cell wall components affects tissue elasticity and allows for cytoplasmic growth and cell division (Peaucelle et al., 2011). How does RLK signaling interfere with cell wall remodeling in cell growth? Several RLK types such as the wall-associated kinases (WAKs) and the *Catharanthus roseus-like* RLKs (CrRLKs) provide a link between cell expansion and the cell wall composition or provide a monitoring system for the integrity of the cell wall. In addition, downregulation of CrRLKs in mutants defective in BR signaling indicate a crosstalk between the BRI1 and CrRLKs pathways in mediating cellular processes required for cell elongation. In addition to these classes of RLKs, the function of several other LRR-RLKs interferes with the normal lignification of cell walls (RPK2, HAE, PXC1) (Mizuno et al., 2007; Stenvik et al., 2008; Wang et al., 2013). We speculate that downregulation of cell wall remodeling enzymes in *toad2/rpk2* mutants (Mizuno et al, 2007) also could interfere with cell wall expansion in the root meristem and in turn, affect cell proliferation, but experimental evidence is needed to validate these assumptions. In addition a root growth defect in which cells lose their

shape is only observed in *rpk1;toad2*/+ mutants and the role of RPK1 in putative lignin deposition defects of *toad2* needs to be further considered.

A third cellular mechanism, that we are only beginning to understand, links both cell division and patterning processes indicating that coordination of cell type with cell cycle control is essential. Although the current paradigm is that cell identity is controlled by master regulatory transcription factors also affecting cell division, a growing body of evidence indicates that some of these mechanisms could be under the direct control of LRR-RLK signaling. Several LRR- RLKs were shown to affect both cell proliferation and cell fate specification. Analyses of mutants defective in the BR signaling pathway indicate they have reduced mitotic rates that correlate with a reduction in expression levels of cell division related genes (Cheon et al., 2010; Gonzalez-Garcia et al., 2011; Zhiponova et al., 2013). The LRR-RLK ER functions to prolong the proliferative phase and inhibit the premature cell differentiation in the epidermis (Bundy et al., 2012). PXY controls cell proliferation and orientation of cell division in vascular cells (Etchells and Turner, 2010; Etchells et al., 2013) that is a prerequisite for cells to acquire a specific fate. Our studies on RPK1/TOAD2 and GSO1/2 also indicate that these LRR-RLKs might control orientation of cell division planes and subsequent cell fate specification in the root meristem. A very important question that still remains to be answered is whether the immediate effect of LRR-RLK signaling is to control the orientation of cell division that in turn allows for cell differentiation or alternatively, if the LRR-RLKs directly control the cell fate, which affects intrinsic genetic programs modulating cell division.

Answering these very important questions of which cellular processes are directly controlled by LRR-RLKs and what are the secondary, indirect effects of their function is essential in understanding how cell-cell signaling contributes to coordinated organ growth. In addition, the complexity of redundantly acting RLKs needs to be elucidated to validate specific interactions among the members of this important family of proteins in plant development.

Bella, J., Hindle, K.L., McEwan, P.A., and Lovell, S.C. (2008). The leucine-rich repeat structure. Cell Mol Life Sci **65,** 2307-2333.

Bundy, M.G., Thompson, O.A., Sieger, M.T., and Shpak, E.D. (2012). Patterns of cell division, cell differentiation and cell elongation in epidermis and cortex of Arabidopsis pedicels in the wild type and in erecta. PLoS One **7,** e46262.

Cheon, J., Park, S.Y., Schulz, B., and Choe, S. (2010). Arabidopsis brassinosteroid biosynthetic mutant dwarf7-1 exhibits slower rates of cell division and shoot induction. BMC Plant Biol **10,** 270.

Clark, S.E., Williams, R.W., and Meyerowitz, E.M. (1997). The CLAVATA1 gene encodes a putative receptor kinase that controls shoot and floral meristem size in Arabidopsis. Cell **89,** 575-585.

Dunning, F.M., Sun, W., Jansen, K.L., Helft, L., and Bent, A.F. (2007). Identification and mutational analysis of Arabidopsis FLS2 leucine-rich repeat domain residues that contribute to flagellin perception. Plant Cell **19,** 3297-3313.

Etchells, J.P., and Turner, S.R. (2010). The PXY-CLE41 receptor ligand pair defines a multifunctional pathway that controls the rate and orientation of vascular cell division. Development **137,** 767-774.

Etchells, J.P., Provost, C.M., Mishra, L., and Turner, S.R. (2013). WOX4 and WOX14 act downstream of the PXY receptor kinase to regulate plant vascular proliferation independently of any role in vascular organisation. Development **140,** 2224-2234.

Gonzalez-Garcia, M.P., Vilarrasa-Blasi, J., Zhiponova, M., Divol, F., Mora-Garcia, S., Russinova, E., and Cano-Delgado, A.I. (2011). Brassinosteroids control meristem size by promoting cell cycle progression in Arabidopsis roots. Development **138,** 849-859.

Jun, J., Fiume, E., Roeder, A.H., Meng, L., Sharma, V.K., Osmont, K.S., Baker, C., Ha, C.M., Meyerowitz, E.M., Feldman, L.J., and Fletcher, J.C. (2010). Comprehensive

analysis of CLE polypeptide signaling gene expression and overexpression activity in Arabidopsis. Plant Physiol **154,** 1721-1736.

Li, J., and Chory, J. (1997). A putative leucine-rich repeat receptor kinase involved in brassinosteroid signal transduction. Cell **90,** 929-938.

Matsubayashi, Y., Ogawa, M., Morita, A., and Sakagami, Y. (2002). An LRR receptor kinase involved in perception of a peptide plant hormone, phytosulfokine. In Science (United States), pp. 1470-1472.

Mizuno, S., Osakabe, Y., Maruyama, K., Ito, T., Osakabe, K., Sato, T., Shinozaki, K., and Yamaguchi-Shinozaki, K. (2007). Receptor-like protein kinase 2 (RPK 2) is a novel factor controlling anther development in Arabidopsis thaliana. Plant J **50,** 751-766.

Ogawa, M., Shinohara, H., Sakagami, Y., and Matsubayashi, Y. (2008). Arabidopsis CLV3 peptide directly binds CLV1 ectodomain. Science **319,** 294.

Peaucelle, A., Braybrook, S.A., Le Guillou, L., Bron, E., Kuhlemeier, C., and Höfte, H. (2011). Pectin-induced changes in cell wall mechanics underlie organ initiation in Arabidopsis. Curr Biol **21,** 1720-1726.

Schiessl, K., Kausika, S., Southam, P., Bush, M., and Sablowski, R. (2012). JAGGED controls growth anisotropyand coordination between cell sizeand cell cycle during plant organogenesis. Curr Biol **22,** 1739-1746.

Shinohara, H., Moriyama, Y., Ohyama, K., and Matsubayashi, Y. (2012). Biochemical mapping of a ligand-binding domain within Arabidopsis BAM1 reveals diversified ligand recognition mechanisms of plant LRR-RKs. Plant J **70,** 845-854.

Shiu, S.H., and Bleecker, A.B. (2001a). Receptor-like kinases from Arabidopsis form a monophyletic gene family related to animal receptor kinases. Proc Natl Acad Sci U S A **98,** 10763-10768.

Shiu, S.H., and Bleecker, A.B. (2001b). Plant receptor-like kinase gene family: diversity, function, and signaling. Sci STKE **2001,** re22.

Song, W., Han, Z., Sun, Y., and Chai, J. (2013). Crystal structure of a plant leucine rich repeat protein with two island domains. Sci China Life Sci.

Stenvik, G.E., Butenko, M.A., and Aalen, R.B. (2008). Identification of a putative receptor-ligand pair controlling cell separation in plants. Plant Signal Behav **3,** 1109-1110.

Su, T.T., and O'Farrell, P.H. (1998). Size control: cell proliferation does not equal growth. Curr Biol **8,** R687-689.

ten Hove, C.A., Bochdanovits, Z., Jansweijer, V.M., Koning, F.G., Berke, L., Sanchez-Perez, G.F., Scheres, B., and Heidstra, R. (2011). Probing the roles of LRR RLK genes in Arabidopsis thaliana roots using a custom T-DNA insertion set. Plant Mol Biol **76,** 69-83.

Torii, K.U. (2004). Leucine-rich repeat receptor kinases in plants: structure, function, and signal transduction pathways. Int Rev Cytol **234,** 1-46.

Wang, G., Ellendorff, U., Kemp, B., Mansfield, J.W., Forsyth, A., Mitchell, K., Bastas, K., Liu, C.M., Woods-Tör, A., Zipfel, C., de Wit, P.J., Jones, J.D., Tör, M., and Thomma, B.P. (2008). A genome-wide functional investigation into the roles of receptor-like proteins in Arabidopsis. Plant Physiol **147,** 503-517.

Wang, J., Kucukoglu, M., Zhang, L., Chen, P., Decker, D., Nilsson, O., Jones, B., Sandberg, G., and Zheng, B. (2013). The Arabidopsis LRR-RLK, PXC1, is a regulator of

secondary wall formation correlated with the TDIF-PXY/TDR-WOX4 signaling pathway. BMC Plant Biol **13,** 94.

Wolf, S., Hématy, K., and Höfte, H. (2012). Growth control and cell wall signaling in plants. Annu Rev Plant Biol **63,** 381-407.

Xiong, Y., McCormack, M., Li, L., Hall, Q., Xiang, C., and Sheen, J. (2013). Glucose-TOR signalling reprograms the transcriptome and activates meristems. Nature **496,** 181-186.

Zhiponova, M.K., Vanhoutte, I., Boudolf, V., Betti, C., Dhondt, S., Coppens, F., Mylle, E., Maes, S., González-García, M.P., Caño-Delgado, A.I., Inzé, D., Beemster, G.T., De Veylder, L., and Russinova, E. (2013). Brassinosteroid production and signaling differentially control cell division and expansion in the leaf. New Phytol **197,** 490-502.